3
2000

This is to certify that the

dissertation entitled

VARIABLE FREQUENCY MICROWAVE PROCESSING AND MICROWAVE PROCESS CONTROL FOR POLYMER COMPOSITES

presented by

Yunchang Qiu

has been accepted towards fulfillment
of the requirements for

Ph.D. degree in Chemical Engineering

Martin C Hawley
Major professor

Date August 21, 2000

VARIABLE FREQUENCY MICROWAVE PROCESSING AND MICROWAVE PROCESS CONTROL FOR POLYMER COMPOSITES

By

Yunchang Qiu

A DISSERTATION

Submitted to
Michigan State University
in partial fulfillment of the requirements
for the degree of

DOCTOR OF PHILOSOPHY

Department of Chemical Engineering

2000

ABSTRACT

VARIABLE FREQUENCY MICROWAVE PROCESSING AND MICROWAVE PROCESS CONTROL FOR POLYMER COMPOSITES

By

Yunchang Qiu

This dissertation presents the research work on the development of a variable frequency microwave processing system for polymer and composite materials, with an emphasis on achieving uniform temperature distribution using intelligent process control. A variable frequency microwave material processing system was constructed based on the existing fixed frequency microwave processing technology with the use of a variable-frequency microwave power source. Data acquisition and control hardware was implemented for process monitoring, measurement, and control. Software programs were developed in LabVIEW for data acquisition, system characterization, and process control. The control objective is to achieve efficient, uniform, and controlled heating, which was realized by mode tuning, intelligent mode switching, on-line mode characterization, and effective power control.

Two uniform processing techniques were developed and evaluated. They are mode sweeping heating, and intelligent mode switching heating. Mode sweeping heating proved to be very effective for small size samples. Intelligent mode switching heating optimizes the sequence of the modes used for heating, by comparing the mode heating characteristics with measured temperature distributions and selecting the mode that will alleviate the temperature gradients the most. Using intelligent mode switching heating,

great improvement of temperature uniformity was achieved over single mode heating and mode sweeping heating. An on-line mode characterization technique was developed to enable the process control system to adjust to process condition changes. With the addition of on-line mode characterization capability, consistent and good performance was ensured for the variable frequency microwave processing system, as demonstrated by the uniform and stable processing of composite parts with complex geometry.

During the mode selection process in the intelligent mode switching heating, modes were compared by their ability to decrease the temperature gradients and generate the most uniform temperature distribution within a desired period of time. Temperature uniformity was measured by the standard deviation of the temperatures. Therefore, the optimal mode would decrease the temperature standard deviation the most within the specified period of time. Two power control algorithms were designed to achieve the objectives of providing fast heating, reducing temperature overshoot, and maintaining constant curing temperature. Consequently, a simple parabolic power controller and a multi-staged PID controller were designed for microwave power control. The former needed no controller tuning, while the latter required proper tuning of the control parameters but provided more stable and accurate control performance.

The experimental results proved the variable frequency microwave processing system successful in achieving uniform processing with consistent performance. A viable variable frequency microwave processing system for industrial applications can be developed based on this newly developed system. The full automation of the hardware and the flexibility of the software ensure easy implementation and make the system adaptable to different types of applications.

To my wife Fang,

my parents, ZhaoLong and FuZhao,

and my brothers, Bao, Yu, and Hong,

for the unconditional love and everlasting inspiration.

ACKNOWLEDGMENTS

I wish to thank Dr. Martin C. Hawley for his invaluable guidance and tremendous support throughout the research work and editorial process for this dissertation. Thanks are also extended to Professor Jes Asmussen, Professor Kun-mu Chen, Professor Larry Drzal, Dr. Jianghua Wei, and Dr. Valerie Adegbite for many enlightening discussions and their insightful advice and suggestions.

This research was funded by the NSF I/UCRC Polymer Processing Center at Michigan State University.

TABLE OF CONTENTS

LIST OF TABLES

LIST OF FIGURES

Some images in this dissertation are presented in color.

INTRODUCTION

Microwaves are electromagnetic waves in the frequency range from 300 MHz to 300 GHz. Since the discovery of electromagnetic waves, it has been widely used in communications. The earliest reported commercial use of microwaves in polymer processing was in 1940 in an attempt to cure plywood cement [1]. Over the decades, microwaves have been applied in polymer and composite materials processing, adhesive and repair, ceramic materials processing, food processing, wood drying, waste treatment, and in medical use as well. In the 1960s, microwave processing was successfully applied in the vulcanization of the rubber in the tire industry [2]. By now, the vulcanization of extruded rubber weather-stripping for the automotive and construction industries has been one of the most successful applications of microwave heating in industry [3]. Since the mid-1980s, there has been a resurgence of interest in the microwave processing of polymers and composites [4-9].

Compared with conventional means, microwave heating has the advantages of being volumetric, direct, selective and instantaneously controllable. Microwaves can penetrate the material placed inside its fields. All the molecules of the material are subject to the electromagnetic field, although the field strength decreases as it gets deeper into the material. The interaction between materials and microwaves is direct and occurs as soon as the electromagnetic field is established. The ability of the material to absorb microwave energy and convert it to thermal energy depends largely on the dielectric properties of the material. Microwave heating is, therefore, selective. Material with higher dielectric loss factor can dissipate more electromagnetic energy into thermal energy than a material with a lower dielectric loss factor. The amount of microwave energy absorbed by the material also depends on the magnitude of the electric field strength. Higher field strength results in faster heating, provided other conditions are the same. A desired temperature distribution can be obtained if one can find ways to control the electric field as desired inside the material. As a comparison, in conventional heating the difference between surface temperature and inside temperature is the driving force. In a sense, the microwave heating process can be viewed as having three degrees of freedom, while conventional heating as having one degree of freedom.

The application of microwave heating in polymer and composite processing has been shown very promising. Significant advantages over conventional heating have been demonstrated. Examples are: increased polymerization rate for epoxy curing (DGEBA/DDM) [10]; reduced drying time for pelletized polycarbonate and polypropylene [11]; increased T_g for cured epoxy (DGEBA/DDS) [9]; enhanced fiber/matrix adhesion in carbon composites [12], and increased mechanical strength of graphite/epoxy composite [13]. Microwave energy also offers the potential for processing of materials that are difficult to process by conventional thermal conduction methods, such as polymeric materials that have poor thermal conductivity.

To utilize the heating effects of microwaves, a device termed a microwave applicator is needed to effectively couple the microwave energy into the material to be processed. There are three kinds of microwave applicators that are commonly used in microwave processing of materials: single-mode, multi-mode, and waveguide applicators. The single mode resonant applicator is designed to support only one resonant mode, while results in highly localized heating. A mode has defined electromagnetic patterns.

Therefore, strong fields at desired regions can be established with single mode applicators. In a multi-mode oven, several electromagnetic modes are randomly excited simultaneously for a given applicator volume [14]. The features of a multi-mode applicator are such that it is versatile in heating a wide range of materials, but it is not efficient in energy use and is limited in heating uniformity resulting in unpredictable hot spots. A waveguide is a hollow conducting pipe with either a rectangular or a circular cross-section. The wave inside a waveguide is fundamentally different from that inside a multi-mode or a single-mode applicator. The former is a travelling wave and the latter is a standing wave. Energy from the microwave generator travels through the waveguide and is partially absorbed by the process material. The remainder of the energy is directed to a terminating load. Travelling wave applicators are primarily used for continuous processing of high-loss materials. Low-loss materials require an excessively long waveguide or a slow processing speed to absorb the necessary energy.

The temperature distribution inside the material heated by microwave energy is dictated by the electromagnetic field distribution inside the material and the material properties. Uneven heating results from an uneven electromagnetic field distribution, inhomogeneous material properties, and the difference between material temperature and ambient temperature. The common techniques to achieve uniform heating inside multi-mode cavities include the use of a mode-stirrer and a turntable, as in home microwave ovens, and frequency sweeping. The shortcomings of these techniques are unpredictable temperature distribution and poor energy efficiency. For a given multi-mode applicator, the various modes that can be excited may be known, however, the type of modes that are excited at any time are unknown and cannot be controlled. Similarly for waveguides, the type and number of modes that can be excited are fixed. Therefore multi-mode applicators and waveguides are not controllable to compensate for varying material changes such as size, shape, and especially material property changes during processing. Since most materials have dielectric properties that change with temperature and chemical composition, the tuning mechanism of single-mode cavities provides an advantage over other applicators to compensate for the change. Due to its design and mechanism, single-mode cavities are also much more efficient in energy use. Another advantage of single-mode cavities is that the electromagnetic field distribution inside the cavity is more predictable and process modeling with a single-mode cavity is computationally less complex also. To achieve uniform heating inside a single-mode cavity, a mode switching technique can be used to improve temperature uniformity. Modes with complementary electromagnetic patterns can be excited selectively by adjusting the frequency or the cavity volume.

Research efforts have been carried out to use the single-mode resonant cylindrical cavity to achieve efficient, fast, and highly controllable processing for polymers and composites. Chen and Lee [15] studied the cure of graphite/epoxy and graphite/PEEK (polyether ether ketone) with TE112 mode at 2.45 GHz. They concluded that the coupling of interactions between microwave energy and composites depended on the fiber orientation and sample geometry in a complex manner. Vogel et al. [16] demonstrated that a 3-inch square, 24-ply graphite/epoxy composite could be processed in a single-mode cavity with low input power. The heating rate and uniformity were dependent upon the electromagnetic processing modes. Wei et al. showed [13] that both unidirectional and cross-ply, thin and thick section graphite/epoxy composite materials could be successfully processed using hybrid modes. Also using the single-mode resonant cavity, Fellows et al. [17] successfully processed polyimide graphite composite panels and planar and complex shaped polyester glass composite materials using a fixed frequency mode switching technique. Reported benefits of microwave processing of polymeric composites in a single-mode cavity include enhanced mechanical properties, such as enhanced glass transition temperature of the cured epoxy [13], enhanced conductive fiber/matrix adhesion [12], faster processing times [18], and capability to control temperature excursions [7][19].

In spite of the demonstrated advantages of microwave heating in composite processing, current research has focused on laboratory-scale, exploratory efforts. Failure to realize expected benefits from microwave processing is a result of inadequate methodology for system integration, including system design, process control, and rapid equipment prototyping. In many cases, the inability to provide steady temperature control and uniform heating hindered the microwave processing systems from moving toward production scale.

Typical microwave research at the lab scale involves intensive and cumbersome manual operations. The microwave processing system was usually operated as an open-loop system. Modes were selected by manually adjusting the cavity length and the coupling probe depth. Automatic on/off control or manual rotation of dial knobs was used to control the microwave power such that the temperature can be maintained as desired. In most cases, computer data acquisition was not involved in the control decision making. As a result, processing results varied for different microwave processing research groups.

Other problems encountered in microwave processing are temperature fluctuations, instability of curing temperature, and large temperature gradients inside the material.

In order to realize the potential of microwave processing and develop a viable microwave technology, work is needed to integrate microwave processing system design with robust process control system development. The generation and transmission of microwave energy is essentially an electronic process, an advantage that can be taken of when designing control instrumentation. For the single-mode resonant cavity, while controllability is one of the attractive attributes, it is yet to be fully utilized for the advancement of the technology.

In the first comprehensive effort to build a process control system for microwave processing in single-mode cavity, Adegbite et al. [20] automated the control of the fixed frequency microwave power source and the adjustment of the resonant cavity. The operation of the microwave processing system was significantly eased. Two different control software programs were developed; one included all necessary control system components to meet the process control objectives, and the other included only data acquisition, hardware and interface instructions to facilitate an interface with a knowledge-based system planner. Using a fixed frequency microwave power source, a mode switching technique was employed to obtain uniform heating by adjusting cavity length and coupling probe depth. Relatively uniform processing was achieved for 3-inch 24-ply graphite/epoxy composite parts. However, the mechanical tuning of the cavity proved to be a roadblock to more precise and consistent temperature control.

The scope of this research work is the development of a variable frequency microwave processing system and the process control system for optimal processing performance. A single-mode microwave cavity was used as the microwave applicator. The variable frequency microwave processing system was developed based on the configuration of the fixed frequency microwave processing system. The variable frequency microwave power source was composed of a microwave signal generator, with a frequency range from 1.7 GHz to 4.3 GHz, and a microwave amplifier. Microwave circuit components were selected to be operational in the frequency range of 2 to 4 GHz. A computer data acquisition and control system was designed and implemented. Measured parameters included temperature and microwave power. Microwave frequency and power are the two controlled parameters. The microwave frequency was controlled through the GPIB interface between the computer and the microwave signal generator. Two techniques were designed to control the microwave power. One was by electronically adjusting the dial knob on the microwave amplifier through a stepper motor, and the other used a voltage-controlled variable attenuator to attenuate the output of the microwave signal generator.

Two types of uniform processing techniques were designed to attain uniform processing temperature and the corresponding control software programs were developed. One is variable frequency mode sweeping and the other is variable frequency intelligent mode switching. Mode sweeping heating uses the modes in a cyclic fashion, while intelligent mode switching heating selects the mode that is optimal for improving heating uniformity. A mode tuning subprogram was utilized to ensure that microwave energy was optimally coupled into the microwave cavity. An on-line mode characterization algorithm was also designed to acquire accurate and up-to-date mode heating characteristics for mode selection in intelligent mode switching heating. The input microwave power was the processing variable regulated to control the processing temperature level. Both a PID control algorithm and a parabolic equation based relational control algorithm were designed and succeeded in maintaining a constant processing temperature and minimizing reaction excursion. The performance of the variable frequency microwave processing system was demonstrated and evaluated by curing simple- and complex-shaped graphite/epoxy composite materials.

The significance of this work is in the development of a variable frequency microwave processing technology that provides uniform and stable processing with consistent performance and great flexibility and applicability. The advantages of using variable frequency microwave technology have been explored and demonstrated. A systematic processing procedure was established, including selection of sample loading positions, location of the mode frequencies, characterization of the heating modes, and finally computer controlled variable frequency microwave processing of the materials. A complete set of variable frequency techniques has been created to optimize microwave processing. The process control system that included optimal mode selection and robust temperature control has been designed and developed. Specifically, this work made the following contributions to the microwave material processing technology development:

1. The design and implementation of hardware and software for the automation of a variable frequency microwave processing system to achieve fast and precise control.
2. The development and implementation of a process control system using innovative control methodologies, to achieve uniform and controlled heating by mode sweeping or switching, mode tuning, and power control.

3. A microwave cavity characterization program that would determine the frequencies of the heating modes and the optimal loading position of the samples.
4. A predictive mode selection algorithm that would select an optimal heating mode to alleviate the temperature gradients by matching the sample temperature distribution with the heating characteristics of the modes.
5. Power control execution programs that provided fast and precise tuning of the power control devices, stepper motor and variable attenuator.
6. An on-line mode heating preference characterization program that would update the mode heating characteristics database so as to improve the robustness of temperature uniformity control.
7. A variable frequency mode tuning program that provides fast and timely tuning of the mode frequency so as to minimize reflected microwave power.
8. Analysis and characterization of the performance of microwave circuit components, such as power meters, in variable frequency processing.
9. Automatic data acquisition for fast, reliable and convenient data collection, tracking, and maintenance.
10. Demonstration of the ability of the variable frequency microwave processing system to provide uniform and controlled processing of complex-shaped graphite/epoxy composite parts.
11. A robust procedure for variable frequency microwave processing of polymer composites, including: optimization of sample loading position, location and

characterization of the modes, mode sweeping heating or intelligent mode switching heating with the option of on-line mode characterization.

12. An intuitive graphical user interface for the operation and control of the variable frequency microwave processing system.

The dissertation layout is as follows:

In chapter 1, related concepts and equations in electromagnetic theory are discussed and wave equations are solved for an empty cylindrical single-mode resonant cavity. The fundamentals of the interaction between microwave and materials are discussed, along with previous research efforts and results in microwave processing of polymers and composites. Process modeling of microwave material processing is also discussed to present a general picture of the microwave environment that should be carefully considered during control system design.

In Chapter 2, the configuration and components of the variable frequency microwave processing system are presented. The variable frequency microwave processing system with a variable frequency power source was developed based on the fixed frequency system configuration. The specifications of the power source, microwave applicator, and other microwave circuit components are provided. The computer-based measurement and control instrumentation for the processing system is discussed in detail.

In Chapter 3, the characterization results of the variable frequency microwave processing system are presented and discussed. The cylindrical cavity was characterized to make sure that it met the requirements for a single mode resonant cavity. A procedure for characterizing sample-loaded cavity was developed to locate empirical modes and determine the heating characteristics of the modes. Power meters were tested for the speed of response to power step changes. The characteristics of the stepper motor and the variable attenuator were also determined. The experimental results on the effects of frequency on dielectric properties are also presented and discussed.

In Chapter 4, a variable frequency mode sweeping heating technique and its software program are presented. The concept of complementary heating is illustrated. Experimental results for square graphite/epoxy composite samples are presented, which demonstrate that the variable frequency mode sweeping technique provided uniform and fast heating for composite parts of small size.

In Chapter 5, an intelligent variable frequency mode switching technique and the corresponding control software (VFMPCSI) are presented. The control system including mode tuning algorithm, mode selection algorithm, and the parabolic power control algorithm are discussed. The performances of the variable attenuator and the stepper motor in microwave power control were tested and compared. Intelligent variable frequency mode switching heating results of both 3-inch square 24-ply and 3-inch V-shaped 24-ply graphite/epoxy composite parts are also presented. The results are discussed and compared with those of single mode heating and mode sweeping heating.

In Chapter 6, an on-line mode characterization technique and the correspondingly upgraded variable frequency mode switching control system (VFMPCSII) are presented. The necessity and benefits of on-line mode characterization are discussed. A multi-staged PID control algorithm was developed for microwave power control, the objective of which was to provide more stable and accurate curing temperature while reducing temperature overshoot. Experimental results of processing complexly shaped composite parts using the process control system with on-line mode characterization (VFMPCSII) are presented. The results are discussed and compared with those of single mode heating and mode sweeping heating. The performance of the process control system is evaluated in terms of processing temperature uniformity, and curing temperature control stability and accuracy.

Research results are summarized and conclusions are made in Chapter 7. Recommendations for future research work are presented in Chapter 8. Finally, Hardware instrumentation and LabVIEW programs are documented in the Appendices. Appendix A provides the hardware specifications. LabVIEW subprograms used in the characterization and control programs are documented in Appendix B. LabVIEW programs for system characterization are documented in Appendix C. LabVIEW programs for process control systems are documented in Appendix D.

CHAPTER 1

MICROWAVE PROCESSING FUNDAMENTALS AND LITERATURE REVIEW

Microwaves are electromagnetic waves with wavelengths measured from 30 cm to 0.3 mm, which correspond to the frequency range $10^9 - 10^{12}$ Hz. The heating effects of microwaves result from the interactions between material molecules and the electromagnetic fields. To better understand microwave heating, one needs to know how electromagnetic fields are established inside the materials, and how they interact with the material at the molecular level. In this chapter, fundamental electromagnetic theory related to microwave processing is presented. The interactions between microwaves and the materials are discussed. Research efforts in microwave processing are reviewed, including the recent development in variable frequency microwave processing. Process modeling and process control issues are also discussed for a better understanding of the microwave environment for control system development. Throughout this chapter, vectors are denoted in bold face, and scalar quantities are denoted in italic face.

1.1 Electromagnetic Theory

1.1.1 Electric Field and Magnetic Field

According to Coulomb's law, the force between two electric charges in free space separated by a distance r is given by:

$$\mathbf{F} = \frac{q_1 q_2}{4\pi\varepsilon_0 r^2}\mathbf{u}_r \tag{1.1}$$

where **F** is in newtons, r is in meters, q_1 and q_2 are in coulombs, $\mathbf{u}_r$ is the unit vector along r, and ε_0 is the permittivity of free space ($=8.854\times10^{-12}\approx\frac{1}{36\pi}\times10^{-9}$ farad/meter). A repulsive force results if the charges are of the same sign; whereas an attractive force results if the charges have opposite signs.

The electric field intensity **E** at a point in free space is defined as the Coulomb force acting on a test unit positive charge placed at that location, assuming a distance r from the charge q:

$$\mathbf{E}=\frac{q}{4\pi\varepsilon r^2}\mathbf{u}_r \tag{1.2}$$

In general, the electric field **E** at any point in an electrostatic field due to a sum of charges distributed throughout space can be obtained by summation or integration of the effects exerted by each charge. The charge distribution can be represented by charge density $\rho(\mathbf{r})$ ([=]coulomb/meter^3), which is time invariant in electrostatics.

The electric displacement density or electric flux density **D** ([=] coulomb/meter^2) is defined as:

$$\mathbf{D}=\varepsilon_0\mathbf{E}+\mathbf{P} \tag{1.3}$$

where **P** is the volume density of polarization ([=]coulombs/meter^2), the measure of the density of electric dipoles.

A static electric charge produces a static electric field, whereas a steady electric current generates a static magnetic field, which can be detected with a magnetic compass. A current-carrying wire produces a magnetic field whose direction is related to that of the current by the right-hand rule. This magnetic field creates a force on moving charges in the field.

The magnetic force acting between two charges moving slowly with constant velocities is termed the Lorentz force, and in free space can be expressed as:

$$\mathbf{F}_{1,2} = \frac{\mu_0}{4\pi} \cdot q_1 \mathbf{v}_1 \times \frac{q_2 \mathbf{v}_2 \times \mathbf{u}_{1,2}}{r^2} \tag{1.4}$$

where $\mathbf{F}_{1,2}$ is the force exerted on charge 1 by charge 2, $\mathbf{v}_1$ and $\mathbf{v}_2$ are velocities of the two charges respectively, r is the distance between the two charges, $\mathbf{u}_{1,2}$ is the unit vector along r with a direction pointing to charge 1, and μ_0 is the permeability of free space (=$4\pi \times 10^{-7}$ henry/meter).

The magnetic flux density **B** at a point in free space has the magnitude of the Lorentz force acting on a test unit moving charge (1 coulomb moving at 1m/second) at that location, assuming a distance r from the charge q moving with a velocity **v**, but with a direction perpendicular to both the Lorentz force and the moving charge q:

$$\mathbf{B} = \frac{\mu_0}{4\pi} \cdot \frac{q\mathbf{v} \times \mathbf{u}_r}{r^2} \tag{1.5}$$

Therefore, for a charge q_t moving with a velocity $\mathbf{v}_t$ the Lorentz force is:

$$\mathbf{F} = q_t \mathbf{v}_t \times \mathbf{B} \tag{1.6}$$

In general, the magnetic flux density at any point due to a sum of moving charges distributed throughout space can be obtained by summation or integration of the effects exerted by each moving charge. The distribution of moving charges can be represented by the electric current density **J** ([=]ampere/meter^2), which is time invariant in magnetostatics.

The magnetic flux density can also be expressed as:

$$\mathbf{B} = \mu_0(\mathbf{H} + \mathbf{M}) \tag{1.7}$$

where **H** is the magnetic field intensity ([=]ampere/meter), and **M** is the volume density of magnetization ([=]ampere/meter), the measure of the density of magnetic dipoles in the material.

A material is called a simple matter if:

$$\begin{cases} \mathbf{D} = \varepsilon \mathbf{E} \\ \mathbf{B} = \mu \mathbf{H} \\ \mathbf{J} = \sigma \mathbf{E} \end{cases} \tag{1.8}$$

where σ (mhos/meter) is the conductivity. $\varepsilon = \varepsilon_r \varepsilon_0$, and $\mu = \mu_r \mu_0$. ε_r is called the relative permittivity or dielectric constant, and μ_r is called the relative permeability. In an isotropic medium, ε is a scalar having only magnitude. However, in an anisotropic medium, such as plasma and conductive fiber reinforced composites, ε is a tensor of rank two with nine components.

Materials having large σ are called conductors and those having small σ are called insulators or dielectrics. Conductors have many "free" electrons, easily detachable from atoms. A perfect dielectric material like vacuum has zero conductivity, i.e. no detachable electrons. All other dielectric materials have finite conductivity. For most linear matter, the permeability μ is approximately that of free space μ_0. There is a class of materials, called diamagnetic, for which μ is slightly less than μ_0 (of the order of 0.01 percent). There is a class of materials, called paramagnetic, for which μ is slightly greater than μ_0 (again of the order of 0.01 percent). A third class of materials, called ferromagnetic, has values of μ much larger than μ_0, but these materials are often nonlinear. Therefore, all materials except ferromagnetic can be called nonmagnetic and $\mu = \mu_0$ can be taken for them.

A material is called a linear matter if [21]:

$$\begin{cases} \mathbf{D} = \varepsilon\mathbf{E} + \varepsilon_1 \dfrac{\partial \mathbf{E}}{\partial t} + \varepsilon_2 \dfrac{\partial^2 \mathbf{E}}{\partial t^2} + \cdots \\ \mathbf{B} = \mu\mathbf{H} + \mu_1 \dfrac{\partial \mathbf{H}}{\partial t} + \mu_2 \dfrac{\partial^2 \mathbf{H}}{\partial t^2} + \cdots \\ \mathbf{J} = \sigma\mathbf{E} + \sigma_1 \dfrac{\partial \mathbf{E}}{\partial t} + \sigma_2 \dfrac{\partial^2 \mathbf{E}}{\partial t^2} + \cdots \end{cases} \tag{1.9}$$

The physical significance of this extended definition arrives from the consideration of the mass. The atomic particles of matter have mass as well as charge, so when the field changes rapidly the particles cannot "follow" the field because of momentum. For example, there will be a time lag before an electron accelerated by the field can change direction, when the direction of **E** changes.

1.1.2 Fundamental Electromagnetic Theory

As discussed in electrostatics and magnetostatics, a charge distribution $\rho(\mathbf{r})$ produces an **E** field, while a current distribution **J**(**r**) produces a **B** field. In a time-varying case, where there are charge $\rho(\mathbf{r},t)$ and current **J**(**r**,t) in a source region, the Equation of Continuity holds due to the conservation of electric charge:

$$\nabla \cdot \mathbf{J}(\mathbf{r},t) + \frac{\partial}{\partial t}\rho(\mathbf{r},t) = 0 \tag{1.10}$$

Since $\rho(\mathbf{r},t)$ and **J**(**r**,t) are coupled through the Equation of Continuity, it is reasonable to think that **E**(**r**,t) and **B**(**r**,t) are coupled in the time-varying situation.

The relations between the field vectors and the source current and charge are captured by a set of equations called Maxwell's Equations:

$$\nabla \times \mathbf{E} = -\frac{\partial \mathbf{B}}{\partial t} \quad \text{(Faraday's law)} \tag{1.11}$$

$$\nabla \times \mathbf{H} = \mathbf{J} + \frac{\partial \mathbf{D}}{\partial t} \quad \text{(Maxwell – Ampere law)} \tag{1.12}$$

$$\nabla \cdot \mathbf{D} = \rho \quad \text{(Gauss law)} \tag{1.13}$$

$$\nabla \cdot \mathbf{B} = 0 \quad \text{(Gauss law - magnetic)} \tag{1.14}$$

where **D** is defined by Equation 1.3 and **H** is defined through Equation 1.7:

$$\mathbf{H} = \frac{\mathbf{B}}{\mu} - \mathbf{M} \tag{1.15}$$

Equations 1.11 and 1.12, along with Equation 1.10, constitute the three independent equations in Maxwell's theory of electromagnetism. Equation 1.13 can be derived by taking the divergence of Equation 1.12 and eliminating **J** between the resultant equation and Equation 1.10. Equation 1.14 can be derived by taking the divergence of Equation 1.11 and setting the constant of integration with respect to time equal to zero. Therefore, Equations 1.13 and 1.14 are dependent equations.

In order to make the Maxwell's equations definite, we need additional information provided by the constitutive relations between the field quantities. As aforementioned, in a simple isotropic medium, the field quantities are related as follows:

$$\mathbf{D} = \varepsilon \mathbf{E} \tag{1.16}$$

$$\mathbf{H} = \frac{\mathbf{B}}{\mu} \tag{1.17}$$

$$\mathbf{J} = \sigma\mathbf{E} \tag{1.18}$$

Now the system of Equations 1.10 through 1.12 and Equations 1.16 through 1.18 becomes definite. There are 16 unknowns and 16 equations. In many boundary-value problems, the constitutive relations between **D**, **B**, **E**, and **H** are usually known while the current density **J** is treated as a source term. In that case, **E** and **H** are solved in terms of **J** and satisfy certain boundary conditions.

Maxwell's equations and the Equation of Continuity can also be expressed in integral form, if the fields and their derivatives are continuous throughout the region of integration. By integrating the equations through a volume V with an enclosing surface S, and applying the curl theorem and the divergence theorem, the following equations can be obtained:

$$\oiint (\mathbf{n} \times \mathbf{E}) dS = -\iiint \frac{\partial \mathbf{B}}{\partial t} dV \tag{1.19}$$

$$\oiint (\mathbf{n} \times \mathbf{H}) dS = \iiint (\mathbf{J} + \frac{\partial \mathbf{D}}{\partial t}) dV \tag{1.20}$$

$$\oiint (\mathbf{n} \cdot \mathbf{J}) dS = -\iiint \frac{\partial \rho}{\partial t} dV \tag{1.21}$$

$$\oiint (\mathbf{n} \cdot \mathbf{B}) dS = 0 \tag{1.22}$$

$$\oiint (\mathbf{n} \cdot \mathbf{D}) dS = \iiint \rho dV \tag{1.23}$$

In the Maxwell's equations, equations for **E** and **B** are coupled. They can be decoupled to simplify the solving process of the equations. Through mathematical manipulations of the Maxwell's equations, the following equations are obtained [22]:

$$[\nabla^2 - \mu\sigma\frac{\partial}{\partial t} - \mu\varepsilon\frac{\partial^2}{\partial t^2}]\begin{Bmatrix}\mathbf{E}\\ \mathbf{B}\end{Bmatrix} = \begin{Bmatrix}\nabla(\frac{\rho}{\varepsilon}) + \mu\frac{\partial \mathbf{J}^s}{\partial t}\\ -\mu\nabla\times\mathbf{J}^s\end{Bmatrix} \tag{1.24}$$

where $\mathbf{J}^s$ is the source current term. In a source free region, Equations 1.24 become:

$$[\nabla^2 - \mu\sigma\frac{\partial}{\partial t} - \mu\varepsilon\frac{\partial^2}{\partial t^2}]\begin{Bmatrix}\mathbf{E}\\ \mathbf{B}\end{Bmatrix} = 0 \tag{1.25}$$

When the source functions, $\mathbf{J}(\mathbf{r},t)$ and $\rho(\mathbf{r},t)$, oscillate with a constant angular frequency of ω in the system, all the fields will oscillate with the same frequency. The Maxwell's equations can be written in time-harmonic form:

$$\begin{cases}\nabla\times\mathbf{E}(\mathbf{r}) = -i\omega\mathbf{B}(\mathbf{r})\\ \nabla\times\mathbf{H}(\mathbf{r}) = \mathbf{J}(\mathbf{r}) + i\omega\mathbf{D}(\mathbf{r})\\ \nabla\cdot\mathbf{D}(\mathbf{r}) = \rho(\mathbf{r})\\ \nabla\cdot\mathbf{B}(\mathbf{r}) = 0\end{cases} \tag{1.26}$$

In time-harmonic case, Equations 1.24 become Helmholtz Equations and Equations 1.25 become Helmholtz equations in source-free region:

$$[\nabla^2 + \omega^2\mu\varepsilon^*]\begin{Bmatrix}\mathbf{E}\\ \mathbf{B}\end{Bmatrix} = 0 \tag{1.27}$$

where

$$\varepsilon^* = \varepsilon(1 - i\frac{\sigma}{\omega\varepsilon}) \tag{1.28}$$

ε^* is called the complex permittivity.

1.1.3 Boundary Conditions

In the Maxwell's equations, boundary conditions must be specified at the interface of two media. For ideal conductors, they can not sustain a field inside. Table 1.1 lists the boundary conditions associated with the corresponding differential equations [23].

Table 1.1 Boundary Conditions

Differential Equations	Boundary Conditions
$\nabla \times \mathbf{E} = -\dfrac{\partial \mathbf{B}}{\partial t}$	1. $\mathbf{n}_1 \times (\mathbf{E}_1 - \mathbf{E}_2) = 0$ 2. $\mathbf{n}_1 \times (\mathbf{E}_1 - \mathbf{E}_2) = 0$ 3. $\mathbf{n}_1 \times \mathbf{E}_1 = 0$
$\nabla \times \mathbf{H} = \mathbf{J} + \dfrac{\partial \mathbf{D}}{\partial t}$	1. $\mathbf{n}_1 \times (\mathbf{H}_1 - \mathbf{H}_2) = \mathbf{K}$ 2. $\mathbf{n}_1 \times (\mathbf{H}_1 - \mathbf{H}_2) = 0$ 3. $\mathbf{n}_1 \times \mathbf{H}_1 = \mathbf{K}$
$\nabla \cdot \mathbf{J} = \dfrac{\partial}{\partial t}\rho = 0$	1. $\nabla_s \cdot \mathbf{K} = -\mathbf{n}_1 \cdot (\mathbf{J}_1 - \mathbf{J}_2) - \dfrac{\partial \rho_s}{\partial t}$ 2. $\mathbf{n}_1 \cdot (\mathbf{J}_1 - \mathbf{J}_2) = -\dfrac{\partial \rho_s}{\partial t}$ 3. $\nabla_s \cdot \mathbf{K} = -\mathbf{n}_1 \cdot \mathbf{J}_1 - \dfrac{\partial \rho_s}{\partial t}$
$\nabla \cdot \mathbf{D} = \rho$	1. $\mathbf{n}_1 \times (\mathbf{D}_1 - \mathbf{D}_2) = \rho_s$ 2. $\mathbf{n}_1 \times (\mathbf{D}_1 - \mathbf{D}_2) = \rho_s$ 3. $\mathbf{n}_1 \times \mathbf{D}_1 = \rho_s$
$\nabla \cdot \mathbf{B} = 0$	1. $\mathbf{n}_1 \times (\mathbf{B}_1 - \mathbf{B}_2) = 0$ 2. $\mathbf{n}_1 \times (\mathbf{B}_1 - \mathbf{B}_2) = 0$ 3. $\mathbf{n}_1 \times \mathbf{B}_1 = 0$

Case 1. General boundary condition

Case 2. Neither of the two adjacent media being a perfect conductor

Case 3. Medium 2 being a perfect conductor

Notes: 1. The unit vector $\mathbf{n}_1$ is pointed from the interface to medium 1.

2. $\mathbf{K}$ is the surface current density.

3. ρ_s is the surface charge density.

4. ∇_s is the surface divergence.

1.1.4 Electromagnetic Fields in a Cylindrical Cavity

Consider an empty cylindrical cavity (cavity length = h, radius = a) with metal walls in a time-harmonic situation. The electromagnetic fields can be solved as a function of position using the Helmhotz Equations 1.27. Since the medium air is virtually vacuum, $\varepsilon^* = \varepsilon$. The equations can be conveniently solved in cylindrical coordinates through transformation to eigenvalue problems.

The corresponding boundary conditions and assumptions are:

1. Tangential component of the electric field is equal to zero at the cavity walls, and the top and base of the cavity, i.e. E_ρ (z = 0, z = h) = 0, E_ϕ (r = a, z = 0, z = h) = 0, and E_z (r = a) = 0.

2. Fields must be finite everywhere, which means the Bessel's function of the second kind cannot be a solution since it can go to infinite when the argument goes to zero.

3. Fields must repeat every 2π in ϕ.

With the above boundary conditions, the Helmholtz equation can be transformed into an eigenvalue problem whose eigenfunctions are Bessel's functions and harmonic functions. These eigenfunctions describe the electric and magnetic field components of a mode while the eigenvalues index the modes and describe the propagation characteristics of the mode. There are two different types of modes that can propagate in a cylindrical cavity, TE (transverse electric) or TM (transverse magnetic). TM modes are solutions to the Maxwell's equations with the boundary condition that there are no longitudinal magnetic field components while the TE modes are the solutions with the boundary condition that there are no longitudinal electric field composites. Therefore, in TE modes the electric field is aligned perpendicular to the direction of wave propagation and in TM modes the electric field is aligned in the direction of wave propagation.

1.1.4.1 TE Modes

For TE modes the electric field components are transverse and the magnetic field components are parallel to the direction of wave propagation, which is the z-axis and thus $E_z = 0$. The TE mode field components in the form of a vector potential is given as [21]:

$$\psi(\rho,\phi,z) = B_{mnp} J_m(\frac{X_{mn}}{a}\rho)\sin(m\phi)\sin(\frac{P\pi}{h}z)$$

$$m=0,1,2,3,\ldots$$

$$p,n=1,2,3,\ldots \tag{1.29}$$

The field components are solved as follows [21]:

$$E_\rho = E_1 J_m(\frac{X_{mn}}{a}\rho)\sin(m\phi)\sin(\frac{p\pi}{h}z)$$

$$E_\phi = E_2 J_m'(\frac{X_{mn}}{a}\rho)\cos(m\phi)\sin(\frac{p\pi}{h}z)$$

$$E_z = 0$$

$$H_\rho = H_1 J_m'(\frac{X_{mn}}{a}\rho)\cos(m\phi)\cos(\frac{p\pi}{h}z)$$

$$H_\phi = H_2 J_m(\frac{X_{mn}}{a}\rho)\sin(m\phi)\cos(\frac{p\pi}{h}z)$$

$$H_z = H_3 J_m(\frac{X_{mn}}{a}\rho)\cos(m\phi)\sin(\frac{p\pi}{h}z) \tag{1.30}$$

where,

$$E_1 = j\frac{\omega\mu H_3 am}{X_{mn}\rho},\ E_2 = j\frac{\omega\mu H_3 a}{X_{mn}},\ H_1 = \frac{H_3 am}{X_{mn}}\left(\frac{p\pi}{h}\right),$$

$$\text{and } H_2 = \frac{H_3 a^2}{X_{mn}^2}\left(\frac{m}{r}\right)\left(\frac{p\pi}{h}\right) \qquad (1.31)$$

1.1.4.2 TM Modes

For TM modes the electric field components are parallel and the magnetic field components are transverse to the direction of wave propagation which is the z-axis, and thus H_z=0. The TM mode field components in the form of a vector potential is given as [21]:

$$\psi(\rho,\phi,z) = A_{mnp}J_m(\frac{X_{mn}}{a}\rho)\cos(m\phi)\cos(\frac{P\pi}{h}z)$$

$$m=0,1,2,3,\ldots$$

$$p,n=1,2,3,\ldots \qquad (1.32)$$

The field components are solved as follows [21]:

$$E_\rho = E_1 J_m^{'}(\frac{X_{mn}}{a}\rho)\cos(m\phi)\sin(\frac{p\pi}{h}z)$$

$$E_\phi = E_2 J_m(\frac{X_{mn}}{a}\rho)\sin(m\phi)\sin(\frac{p\pi}{h}z)$$

$$E_z = E_3 J_m(\frac{X_{mn}}{a}\rho)\cos(m\phi)\cos(\frac{p\pi}{h}z)$$

$$H_\rho = H_1 J_m(\frac{X_{mn}}{a}\rho)\sin(m\phi)\cos(\frac{p\pi}{h}z)$$

$$H_\phi = H_2 J_m^{'}(\frac{X_{mn}}{a}\rho)\cos(m\phi)\cos(\frac{p\pi}{h}z)$$

$$H_z = 0 \qquad (1.33)$$

where $E_1 = \dfrac{E_3 a}{X_{mn}}\left(\dfrac{p\pi}{h}\right)$, $E_2 = \dfrac{E_3 a^2}{X_{mn}^2}\left(\dfrac{m}{\rho}\right)\left(\dfrac{p\pi}{h}\right)$, $H_1 = -j\dfrac{\omega\varepsilon E_3 a^2}{X_{mn}^2}\left(\dfrac{m}{\rho}\right)$,

$$\text{and } H_2 = -j\frac{\omega\varepsilon E_3 a}{X_{mn}} \tag{1.34}$$

1.1.4.3 Mode Designation

The field component solutions, i.e. Equation 1.30 and Equation 1.33, determine the characteristic field patterns associated with these modes. These field patterns indicate the variations and amplitude of the field components as a function of the cavity axis. In the cylindrical cavity the field indices (***m***, ***n***, ***p***) correspond to the components (ϕ, ***r***, ***z***). Where ***r*** is the radial direction, ϕ is the circumferential direction, and ***z*** is the vertical direction. The index ***m*** is the periodicity in the radial direction, ***n*** is the number of half wavelengths in the circumferential direction, and ***p*** is the number of circular wavelengths along the vertical axis. For an example, TM_{010} designates a transverse magnetic mode with (0) wave variations along the radial direction, (1) wave variation in the circumferential direction, and (0) wave variations in the vertical direction.

1.1.4.4 Electric Field Pattern

The field patterns for different modes can be determined by plotting the magnitude of the electric or magnetic field components. It is only necessary to plot these patterns for one plane since similar patterns are repeated in all the repeating planes along the z-axis. Several plots of the electric field patterns were generated and are shown in Figure 1.1 and Figure 1.2. These plots are shown as density plots where the white regions represent high field strength regions and the dark areas represent low field intensity regions.

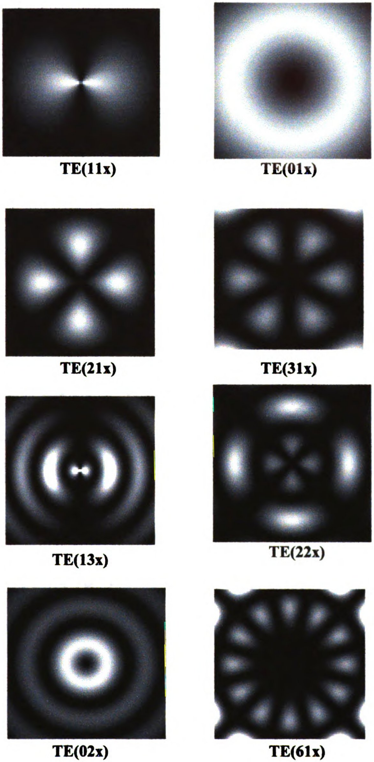

Figure 1.1 Electric Field Patterns for TE Modes

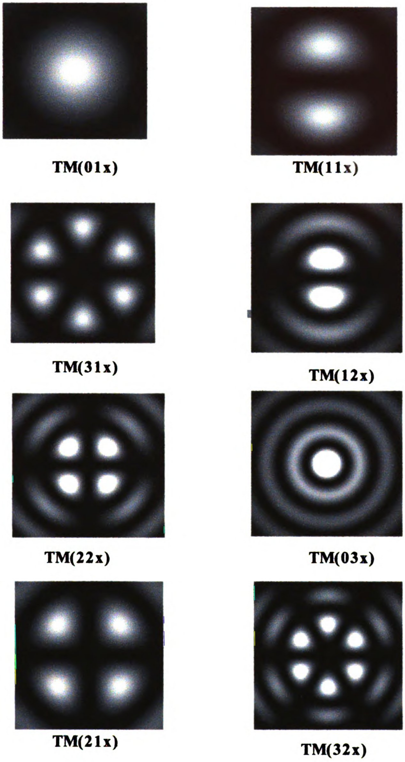

Figure 1.2 Electric Field Patterns for TM Modes

1.1.4.5 Cut-off Frequency

With the eigenvalues of the solutions to the Helmholtz Equation 1.27, the wave propagation characteristics can be derived in a form of what is known as the cut-off frequency equations. The cutoff frequency defines the minimum frequency for a given cavity diameter that modes can propagate. The cut-off frequency equations for the TE and TM modes are shown in Equations 1.35 and 1.36. They show a relationship of frequency as a function of cavity length, ***h***, cavity radius, ***a***, permittivity and permeability, and the tabulated zeros of the Bessel's function or its derivative.

Waves of frequencies below the cut-off frequency of a particular mode cannot propagate, and power and signal transmission at that mode is possible only for frequencies higher than the cut-off frequency. At frequencies below the cut-off frequency of a given mode the propagation constant is purely imaginary, corresponding to a rapid exponential decay of the field and the generation of evanescent modes [24].

$$(f)_{mnp}^{TE} = \frac{1}{2\pi\sqrt{\mu\varepsilon}}\sqrt{\left(\frac{x'_{mn}}{a}\right)^2 + \left(\frac{p\pi}{h}\right)^2} \tag{1.35}$$

where, x'_{mn} =tabulated zeros of the derivative of the Bessel's function.

$$(f)_{mnp}^{TM} = \frac{1}{2\pi\sqrt{\mu\varepsilon}}\sqrt{\left(\frac{x_{mn}}{a}\right)^2 + \left(\frac{p\pi}{h}\right)^2} \tag{1.36}$$

where, x_{mn} = tabulated zeros of the Bessel's function.

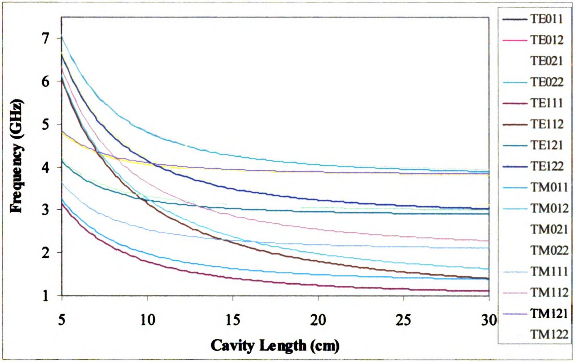

Figure 1.3 Mode Chart for a 7 Inch Diameter Empty Cavity

The significance of the cut-off frequency equations is that they indicate the frequencies and cavity lengths where a single mode can resonate in a cavity of a known radius. Another useful form of these equations is a plot of the frequency versus the cavity length for a fixed cavity radius, to generate what is know as the mode chart (see Figure 1.3). The mode chart shows the locations of modes with respect to other modes as a function of frequency and cavity radius. It is important to note that these equations can be used in two forms: by fixing the frequency at a constant value and varying the cavity length to excite different modes or by fixing the cavity length at a constant value and varying the frequency to excite different modes. The previous method is the fixed frequency method and the latter is the variable frequency method, which is used in this

work. In the variable frequency method more modes can be theoretically excited than in the fixed frequency method. This is evident by the number of modal lines that a vertical line intersects for the variable frequency method and the number of modal lines that a horizontal line intersects for the fixed frequency method.

By intersecting the mode chart, it is apparent that, as the order of modes increase (increase in the indices) the modes become close together in frequency. Thus, suggesting that it may be difficult to excite higher order single modes. The mode chart also indicates that the modes that can be excited at a fixed frequency.

1.1.4.6 Cavity Quality Factor

The cavity quality factor, or Q-factor, is a measure of how well the cavity stores microwave energy. The definition of Q-factor of a resonant cavity is defined as the ratio of the energy stored inside the cavity volume to the energy lost to the cavity surface area per unit time, as formulated in Equation 1.37 [21].

$$Q = 2\pi f_0 \left(\frac{energy \quad stored}{energy \quad lost} \right) = 2\pi f_0 \left(\frac{\varepsilon \int\limits_V |E|^2 d\tau}{R \oint\limits_S |H|^2 ds} \right) \tag{1.37}$$

where R is the intrinsic wave resistance of the metal walls.

The Q-factor is a function of the resonant mode. For an empty cylindrical in microwave frequency range, it is usually very high with a range from 10,000 to above 40,000 [25]. The theoretical Q value increases as the order of modes increases at a given frequency. The reason is that for high order modes, the cavity volume becomes relatively larger, which results in a greater volume-to-surface ratio. Since energy is stored in the volume and lost on the imperfectly conducting surface, the Q factor increases due to the increased volume-to-surface ratio. In practice, the Q-factor can be lowered by the introduction of a feed system (coupling system), a large impedance, imperfections in the construction, and imperfect conductivity at the cavity surface [26].

An experimental method called half power point method is used to measure the Q factor using an oscilloscope. The power reflectance (input power over reflected power ratio) curve is generated versus the frequency on the oscilloscope screen. The Q factor is calculated as follows:

$$Q = 2\pi f_0 \left(\frac{energy \;\; stored}{energy \;\; lost} \right) = 2 \frac{f_0}{\Delta f} \tag{1.38}$$

The method is illustrated in Figure 1.4.

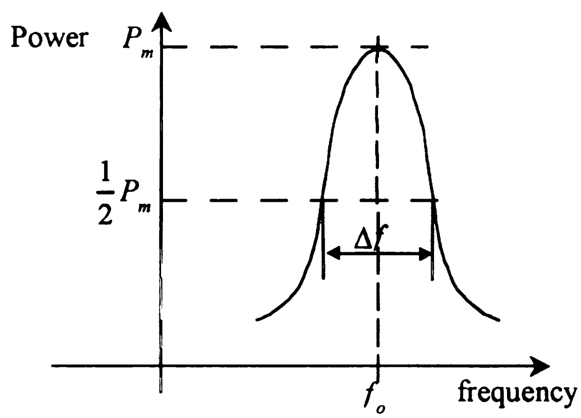

Figure 1.4 Q Factor Calculation using Half Power Point Method

1.2 Interactions Between Microwaves and Materials

Typical frequencies used in material processing are 915 MHz, 2.45 GHz, 5.8 GHz and 24.124 GHz. However, if the microwave leakage can be controlled within safety limits, any frequency can be used in industrial applications. When introduced into microwave field, the materials will interact with the alternating electromagnetic field at the molecular level. Different materials will have different responses to the microwave irradiation.

If the material is conductive, the electrons move freely. When exposed to the electric field, an electric current results. The current in the conductor will heat the material through resistive heating. However, for conductors with high conductivity, the incident microwaves will be largely reflected and therefore they can not be effectively heated by microwave. The fields attenuate towards the interior of the material due to skin effect, which involves the magnetic properties of the material. The conducting electrons are limited in the skin area to some extent, which is called the skin depth, d_s. Defined as the distance into the sample, at which the electric field strength is reduced to $1/e$, the skin depth is given by [21]:

$$d_s = \frac{1}{\left(1/2\omega\mu_o\mu'\sigma\right)^{1/2}} \tag{1.39}$$

where ω is the frequency of the EM waves in rad/sec, μ_o is the permeability of the free space, $4\pi \times 10^{-7}$ H/m, μ' is the relative permeability, and σ is the conductivity of the conductor in mhos/m. For graphite, $\sigma = 7\times10^4$ mhos/m, and $d_s = 38.4$ μm at 2.45 GHz in free space. Therefore, the skin depth for AS4 graphite fiber at 2.45 GHz is about four times the fiber diameter. As frequency increases, the skin depth decreases.

When a dielectric material is exposed to electromagnetic waves, four polarization mechanisms may take place [13]. They are electron (or optical), atomic, dipolar (or orientational), and interfacial or space-charge polarization. The electron or optical polarization is due to the shift of the orbit center of electron cloud caused by the applied electric field. No dielectric losses will result since the induced dipole moment is always in phase with the electric field. The relaxation time for electron polarization is 10^{-15} seconds [27]. Atomic polarization results when the molecules placed in the electric field consist of two different kinds of atoms. The magnitudes of atomic polarization of non-ionic, or non-partially ionic polymers are much less than those of ionic or partially ionic polymers. The typical relaxation time of atomic polarization is 10^{-13} seconds. Orientation or dipole polarization is observed for dipolar or polar molecules placed in the electric field. The dipolar molecules will rotate until they are aligned in the direction of the external electric field. The dielectric loss of orientation polarization is mainly due to the friction force that the dipoles rotate against. The typical relaxation time for this type of polarization is 10^{-9} seconds. The interfacial or surface-charge polarization is caused by the migration of charges inside and at the interface of dielectrics in a large scale field. Microwave heating is mainly contributed by the dipolar polarization, because it occurs in the microwave frequency range.

The measure of the ability of a dielectric material to absorb and to store electric potential energy is the complex permitivity,

$$\varepsilon = \varepsilon^{'} - j\varepsilon^{''} \quad (1.40)$$

where the real permitivity $\varepsilon^{'}$ is also called the dielectric constant, which characterizes the penetration of microwaves into the material. The dielectric loss $\varepsilon^{''}$ indicates the ability of the dielectrics to store the energy. The average microwave power per unit volume converted into heat is given as follows,

$$P_{ave} = 1/2\omega\varepsilon_o\varepsilon^{'}\tan\delta E^2 \text{ (W/m}^2\text{)} \tag{1.41}$$

where,

$$\tan\delta = \frac{(\sigma_e + \sigma_i)/\omega\varepsilon_0 + \varepsilon^{"}}{\varepsilon^{'}} \tag{1.42}$$

is the loss tangent, characterizing the ability of the material to convert the absorbed microwave energy into heat.

The skin depth for dielectric material is defined as before and given by,

$$d_s = \frac{2}{\omega\varepsilon^{"}\left(\mu_0/\varepsilon^{'}\right)^{1/2}} \tag{1.43}$$

For fully cured DGEBA/DDS epoxy, $\varepsilon = \varepsilon_0(3.5 - j0.1)$, so the skin depth is $d_s = 0.729$ m at 2.45 GHz. In general, the skin depth can be calculated for the homogeneous materials by [28],

$$d_s = \frac{1}{2\omega}\left(\frac{2}{\mu_0\mu^{'}\varepsilon_0\varepsilon^{'}}\right)^{1/2}\left[\left(1+\left(\frac{\varepsilon^{"}}{\varepsilon^{'}}\right)^2\right)^{1/2} - 1\right]^{-1/2} \tag{1.44}$$

The dielectric properties of composite materials are anisotropic. The skin depth can be calculated in the principal directions using Equation 1.44. For AS4/3501-6 graphite/epoxy composite, the effective complex permitivity is $\varepsilon^* = \varepsilon_0(1\text{-}j2500)$ along the fiber direction, and $\varepsilon^* = \varepsilon_0(14.5\text{-}j75.8)$ perpendicular to the fiber direction [29]. Taking the fiber direction as the principal direction, the skin depth of this composite is 9.8 mm and 3.2 mm for electric fields along and perpendicular to the fiber direction, respectively.

The power absorption rate inside the composite can be calculated by Poynting's theorem as [21],

$$P = \frac{1}{2}\omega\varepsilon_0 \vec{E} \bullet \overset{\leftrightarrow}{\varepsilon}_{eff}{}^{*} \bullet \vec{E}^{*} \tag{1.45}$$

where $\overset{\leftrightarrow}{\varepsilon}_{eff}{}^{*} = \overset{\leftrightarrow}{\varepsilon}_{d}{}^{*} + \frac{\overset{\leftrightarrow}{\sigma}}{\varepsilon_0 \omega}$, $\overset{\leftrightarrow}{\varepsilon}_{eff}{}^{*}$ and $\overset{\leftrightarrow}{\varepsilon}{}^{*}_{d}$ are relative effective dyadic factor and relative dyadic loss factor due to dipolar distribution, $\overset{\leftrightarrow}{\sigma}$ is the dyadic conductivity in S/m and $\vec{E}^{*}$ is the conjugate electric field vector in V/m.

Microwave heating is unique in that it is rapid, instantaneous, volumetric and selective. Whether a material can be effectively heated by microwave depends on its dielectric loss factor. High dielectric loss factor results in better heating. Microwaves offer self-limiting heating in the processing of thermosets. As the crosslinking proceeds, the mobility of dipoles decreases due to the "trapping" or reaction. Therefore, the dielectric loss factor diminishes with the extent of cure. However, in practical applications, if the dielectric loss factor of the material increases with the temperature, such as in the rubber processing, thermal runaway will usually be observed. This problem can be solved by regulating the input microwave power, since microwave heating is instantaneous. The non-uniformity of microwave heating can also be alleviated by controlling the electric field exerted onto the material.

Whether there is a "microwave effect" in chemical reactions has been a rather controversial topic. A proposed mechanism for the "microwave effect" in polymers suggests a non-equilibrium, non-uniform energy distribution at the molecular level (or a non-equilibrated temperature), resulting in certain dipoles having a greater energy than the "average" energy of adjacent groups [30][31][32]. This increased energy corresponds to an increase in an effective temperature of the reacting groups. The energy couples directly with a reactive polar group in the system and dissipates through adjacent groups by the usual mechanisms. It is impossible to determine the effect that microwave processing has on reaction kinetics based on the available data, because of the range of materials studied, differences in temperature and control and measurement methods, lack of knowledge on microwave energy absorbed, and variations in microwave applicators. However, two general observations can be made [33]: (1) slower-reacting systems tend to show a greater effect under microwave radiation than faster-reacting systems and (2) the magnitude of the observed effect decreases as the temperature of the reaction is increased.

1.3 Microwave Processing of Materials

1.3.1 Microwave Processing of Polymers

Microwaves have been used to process both thermosets and thermoplastics. The heating characteristics for these two types of polymers are different due to the different dielectric behavior during heating. George et al. used microwave energy to dry various thermoplastics, including powdered poly(vinyl chloride), pelletized polycarbonate, pelletized polypropylene and acrylonitrile-butadiene-styrene polymer [11]. The microwave drying time was about 4-20 times less as compared with the conventional tray dryer at 104°C. All the microwave-dried polymers have equivalent or higher tensile strength and impact resistance as compared to the hot-air-dried polymers. Microwaves have also been used to cure many thermosets, including polyesters [4][34], polyurethanes [35][36], polyimides [37][38] and epoxies [4][5][7][9][39][40][41]. Most of the results showed that the cure speed is faster for microwave cure than for thermal cure. Epoxies are the most widely studied thermosets. Both pulsed and continuous microwave curing of epoxies have been studied [13][42]. A systematic study was performed to elucidate the effects of microwaves on the crosslinking of epoxies using two epoxy systems, stoichiometric mixtures of DGEBA epoxides with a high-loss curing agent, diamino-diphenyl sulfone (DDS), and a low-loss curing agent, *meta*-phemylene diamine (*m*PDA) [9]. Experimental results showed that increased reaction rates were observed in microwave cure as compared with those in thermal cure at the same temperature. At low conversion, the T_g's were similar for both microwave and thermally cured samples. But high T_g's were observed for the microwave cured samples at high conversion. This effect is more significant with DDS as cure agent than with *m*PDA, which may be due to the higher dipole moment of DDS. Bush et al. suggested that the reaction rate enhancement be the result of a non-equilibrated temperature effect where the local temperature is higher than that of the bulk, especially for high-loss species such as DDS [32].

1.3.2 Microwave Processing of Composites

In composite material processing, both conducting and non-conducting fiber-reinforced composites have been processed by microwave energy. Lee et. al. processed continuous graphite-fiber-epoxy laminates up to 32 plies using a waveguide and multimode applicators [29]. However, the attempt to process multi-directional graphite-epoxy composites was not successful. Wei et al. used a cylindrical, tunable single-mode cavity and successfully processed both cross-ply and unidirectional 24-ply 7.62 X 7.62 cm Hercules AS4/3501-6 graphite/epoxy prepreg laminates with 2.45 GHz microwaves [18].

In comparison, mcirowave processed parts in an unpressurized system after 90 minutes of heating had similar strength to that of autoclave processed parts with a five hour heating cycle under a pressure of 690 kPa. Continuous processing has also been studied and developed for composites with conducting and non-conducting fibers [43-47]. The control of microwave leakage at the entrance and exit ports is the critical issue in continuous microwave processing. Usually an anti-leakage structure called a choke is used at the entries. However, for conducting fiber-reinforced composites, a specially designed microwave leakage jacket should be used [48]. In recently developed microwave-assisted pultrusion processes, the length of the process chamber, the processing time and the pulling forces were reduced significantly [47][49][50]. Single-mode applicators proved to be more efficient than waveguide in the microwave assisted pultrusion [47].

1.3.3 Kinetics of Microwave Curing of Epoxies and Epoxy Composites

Microwave processing of polymers and composites has been demonstrated to have advantages over thermal processing, including enhanced polymerization rates [32], increased glass transition temperatures of cured epoxies [9], improved interfacial bonding between graphite fiber and matrix [12], and increased mechanical properties of some composites. Thermoset epoxy resins are the most widely used matrix materials for advanced composites. Epoxy resins are processed or cured by conversion of liquid monomers into a three dimensional thermoset network via chemical reactions. A large amount of work has been performed in the microwave curing of the general class of epoxy resins.

Thermal cure kinetics models can be used in modeling the reaction kinetics of microwave cured epoxy resins [13]. There are mainly two types of kinetics models for the thermal cure of epoxy. One is the n^{th} order reaction kinetics model [56][57] and the other is the autocatalytic reaction model [58-61]. The n^{th} order reaction kinetics model assumes that the kinetics can be expressed as:

$$\frac{d\alpha}{dt} = k(T)f(\alpha) \tag{1.46}$$

where α is the extent of cure, t is the time, the function $f(\alpha)$ is expressed as $(1-\alpha)^n$, and k(T) is the overall reaction rate constant which obeys the Arrhenius relation:

$$k(T) = A\exp(-\frac{E/R}{T}) \tag{1.47}$$

From Equations 1.46 and 1.47, one can derive that:

$$\ln(t) - \frac{E/R}{T} = [\text{constant}] \qquad \text{for fixed } \alpha \text{ or } T_g \tag{1.48}$$

A master curve can be obtained by plotting α or T_g versus $\ln(t)$ at a reference temperature[62]. The activation energy E can be determined by comparing an experimental curve with the master curve, where the shift should be $(E/R)(1/T-1/T_{ref})$. A and n can be calculated by fitting the data to the equation:

$$\ln(\frac{d\alpha}{dt}) + \frac{E/R}{T} = \ln(A) + n\ln(1-\alpha) \tag{1.49}$$

The autocatalytic kinetics model is more commonly used, in which the phenomenological cure kinetics expression for a stoichiometric epoxy resin is given by[58][60][61]:

$$\frac{d\alpha}{dt} = (k_1 + k_2\alpha^m)(1-\alpha)^n \tag{1.50}$$

where k_1 is the non-catalytic polymerization reaction rate constant, k_2 is the autocatalytic polymerization reaction rate constant, m is the autocatalyzed polymerization reaction order, and n is the non-catalyzed polymerization reaction order. When there is no etherification reaction or OH impurity, a general cure kinetics expression can be derived as follows, provided that the reaction rate constants for primary and secondary amine-epoxies are the same [63]:

$$\frac{d\alpha}{dt} = (k_1 + k_2)(1-\alpha)(B-\alpha)\text{, when } \alpha < \alpha_{gel} \qquad (1.51)$$

where B is the ratio of the initial hardener equivalents to epoxide equivalents. Equation 1.51 works well before the gelation point. However, after the gelation point, the reaction kinetics is better represented by [64]:

$$\frac{d\alpha}{dt} = k_3(1-\alpha)\text{, when } \alpha > \alpha_{gel} \qquad (1.52)$$

The n^{th} order reaction kinetics is computationally simple. According to this model, the maximum reaction rate should occur at the beginning of the reaction. However, in real cases, α =0.3 ~ 0.4 at maximum reaction rate, which is better explained by the autocatalyzed reaction mechanism. It was demonstrated that the cure kinetics of DGEBA/*m*PDA and DGEBA/DDS systems could be described by the autocatalytic kinetic model up to vitrification in both microwave cure and thermal cure [13].

In microwave processing, the dielectric property change of materials being processed becomes an important issue. Comprehensive knowledge of epoxy dielectric properties during processing is necessary to properly interpret the cure mechanism induced electromagnetic radiation. Like most thermosets, the permitivity and dielectric loss factor of epoxy resins increase with temperature and decrease with extent of cure[65][66]. Epoxy is an efficient absorber of microwave radiation at the beginning of heating, with ε'' increasing as the resin is heated. As the cure reaction progresses, the heat input will be mainly from the exothermic reaction. The pure compounds of an epoxy system (epoxy resin and hardeners before mixing) have different dielectric behavior with respect to temperature. DGEBA (diglycidylether of bisphenol-A) exhibits an ε'' maximum around 50 °C [67]. The dielectric constant variations of the hardeners with temperature is presented in Figure 1.5 [66].

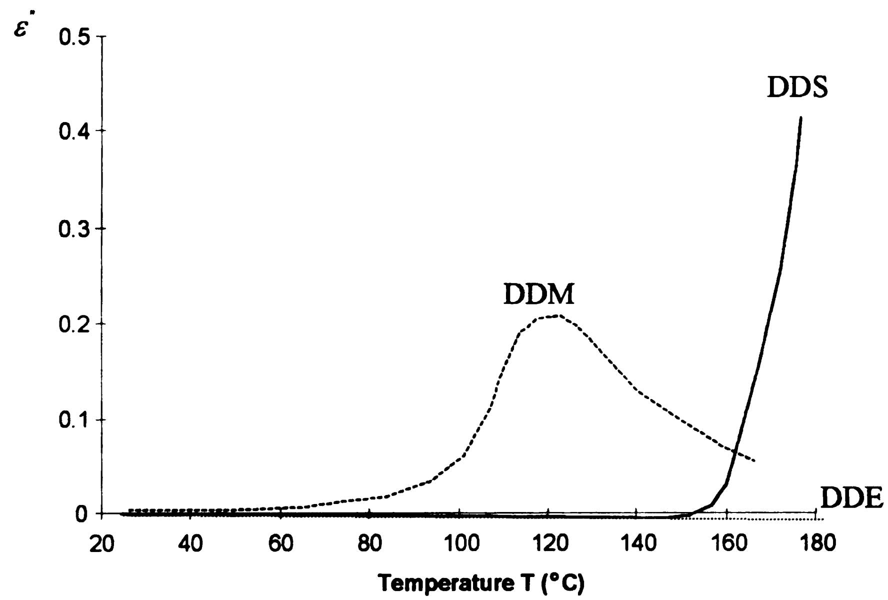

Figure 1.5 Dissipation Factor ε^{*} vs Temperature for DDS, DDM and DDE

There is a sharp ε'' increase beyond 150 °C for DDS(4,4'-diaminodiphenylsulphone) and at about 100 °C for DDM (4,4'-diaminodiphenylmethane) while no such variation is observed for DDE (4,4'-diaminodiphenylether). One of the recent studies suggested that the decrease in the microwave dielectric properties of the DGEBA/DDS epoxy system undergoing cure is predominantly dictated by the nature of the polymer superstructure, and not as much by the changes in the polar end group concentrations [68]. It was further concluded that the use of microwave energy for driving reactions may be useful in systems where the network morphology is not rigid and the dipoles are free to move, giving rise to a relatively high dielectric loss. However, in another study on dielectric behavior of an epoxy resin during crosslinking at microwave frequencies, it was found that both the real and imaginary part of the dielectric constant were mainly affected by the disappearance of specific dipolar species, whose relaxation times did not change significantly [69].

Microwave processing of epoxy resin composites has been under intensive investigation among other composites because of their widespread application. Unidirectional graphite/epoxy composites were first processed up to 32 plies using microwave energy, while the attempt to process multidirectional samples was not successful [29]. In later studies, the microwave processing of both crossply and unidirectional graphite/epoxy was achieved using a cylindrical single-mode cavity [18]. The unpressurized microwave processed composites showed higher modulus with shorter cure time compared with thermal autoclave process. Part of the reason is that microwave heating environment can substantially increase the amount of chemical interaction between the fiber surface and the epoxy resin and amine components of the matrix [12]. As a result, the composite performance can be improved. Thick section graphite/epoxy composites were also successfully processed or heated using single-mode cylindrical cavity [18][70]. Continuous microwave processing of graphite/epoxy prepregs was also studied and the processing time was shorter as compared with thermal pultrusion process [47][71]. Microwaves have also been used to process non-conducting fiber reinforced epoxy composites. A 457 mm long, 127 mm OD epoxy/glass filament wound tube with a wall thickness of 9.5 mm was processed in one minute using a rectangular multi-mode cavity at a power level of 20 KW [72]. Different applicators were used to process planar glass fiber/epoxy laminates [29][73][74]. However, there was no evidence of improved fiber/matrix bonding by microwaves for glass reinforced composites [12].

1.3.4 Other Microwave Heating Applications

Commercial exploitation of microwave heating in the food, rubber, textile and wood products industries has been successful. Modern microwave rubber processing offers significant advantages over conventional rubber processing, including improved product uniformity, reduced extrusion-line length, reduced scrap, improved cleanliness, enhanced process control and automation, and the capability of continuous vulcanization [2][3][51]. In general, microwave energy enables operating cost reduction, energy saving, higher quality and reliable products and a greatly improved environment both internally and externally [2]. Studies have been conducted in using microwave energy to attain the high temperature required for processing ceramic materials [52]. A combination of microwave energy with conventional heating has been used to elevate the temperature of the entire sample rapidly [53]. More uniform microstructures were obtained as examined as a function of cross-sectional position in the sample. Improved microstructural uniformity and performance for microwave processed Si_3N_4 tool bits have been reported as compared to those processed by conventional methods [54][55]. There has also been growing interest in application areas such as pollution control, medical sterilization, medical waste treatment, etc.

1.4 Variable Frequency Microwave Material Processing

Single-mode cavities and multi-mode cavities are commonly used in microwave heating studies. A familiar example of the multi-mode applicator is the domestic microwave oven, in which several modes are excited at the same time [14]. Multi-mode cavities provide somewhat more uniform heating than single-mode cavities if single-mode cavities use only one mode. However, only single-mode cavities can efficiently couple the microwave energy into the load, which has been shown in the processing of crossply and thick-section graphite fiber reinforced composites [75][76]. Single-mode cavities can provide uniform heating using mode-switching method, in which several modes with complementary heating patterns are alternatively excited [17]. For a fixed frequency system mode switching can be only achieved by mechanically change the volume of the cavity. This eventually affects the rapidity of the process. The other approach is to vary the frequency to change modes. The adjustment of frequency is an electronic process. As a result of the instantaneous switching between modes, not only the speed of the process but also the controllability of the process can be increased by using variable frequency switching.

Variable frequency microwave processing is an innovative method to achieve uniform heating. The current approach of variable frequency heating is frequency sweeping. Continuous frequency sweeping method has been demonstrated to be able to improve the uniformity of heating in multi-mode microwave ovens [77]. By selectively or continuously sweeping through a certain frequency range within a short time, time-averaged uniformity of heating can be obtained [78][79]. However, this method has poor power efficiency and not suitable for processing high lossy and anisotropic materials, in which heating modes usually have common hot spots due to the selective heating of microwave. By selectively switching through resonant modes, the energy efficiency can be highly improved. To ensure uniform heating pattern, the heating cycle can be programmed such that the heating times of different modes are weighted by the corresponding heating characteristics.

1.5 Process Modeling and Processing Control in Microwave Processing

1.5.1 Microwave Process Modeling

The study of microwave processing of materials is interdisciplinary in that it calls upon the expertise in electrical engineering, material science, process engineering and design. To enhance its potential industrial applications, a large amount of effort has been expended in the studies to better understand and design the process. Successful models always help the design and control of real processes. Microwave process modeling involves the prediction of the electromagnetic field and the temperature distribution inside the material with the occurrence of chemical reactions and rheological changes. Usually, the extent of cure as a function of time and space is desired so as to predict the properties of the final product.

In general, a microwave material processing model should include mass balance, energy balance, and kinetic equations. Mass balance takes resin flow in the composite into consideration. Energy balance involves heat transfer, reaction heat, and microwave energy absorption. The kinetic equations are used to compute reaction rates and predict the curing time. These equations are coupled and therefore present a very complex system of equations. An example of the coupled system of equations are given as follows:

(1) Mass Balance:

$$\frac{dM_c}{dt} = -\rho_c A v_c \tag{1.53}$$

where $\frac{dM_c}{dt}$ is the rate of change of mass M_c in the composite, ρ_c is the resin density, and A is the cross-sectional area. v_c is the velocity of the resin flow in the composite and can be represented by Darcy's Law[80]:

$$v = \frac{-S}{\mu}\frac{dp}{dx} \tag{1.54}$$

where S is the apparent permeability, μ is the viscosity, and $\frac{dp}{dx}$ is the pressure gradient.

(2) Energy Balance

$$\frac{\partial}{\partial t}(\rho C_p T) = \frac{\partial}{\partial x}(K\frac{\partial T}{\partial x}) + \rho \dot{H} + P_m \tag{1.55}$$

where ρ, C_p, and K are the density, the specific heat, and the thermal conductivity of the composite respectively. $\dot{H}$ is the rate of heat generation per unit weight by the chemical reaction, which needs to be calculated with the aid of the kinetic equations. P_m is the rate of heat generation per unit volume by the absorbed microwave energy. To compute P_m, the Maxwell's Equations need to be solved for the field distribution inside the composite material.

(3) Kinetic Equations

The kinetic equations for Hercules 3501-6 resin are given as an example [81]:

$$\frac{d\alpha}{dt} = \begin{cases} (k_1 + k_2\alpha)(1-\alpha)(B-\alpha) & \alpha < \alpha_{gel} \\ k_3(1-\alpha) & \alpha > \alpha_{gel} \end{cases} \tag{1.55}$$

where α is the extent of cure, k_1, k_2, and k_3 are the reaction rate constants, B is the ratio of initial hardener equivalent to epoxide equivalents, and α_{gel} is the extent of cure at the gelation point.

Various models for computing the electric field inside a material placed in a microwave cavity have been proposed. To calculate the electric fields inside a microwave cavity, Maxwell's equations need to be solved with appropriate boundary conditions. Either an integral or differential formulation of Maxwell's equations can be used to start with. Analytical approaches have been used in simple cases of loaded rectangular applicators, such as the equivalent circuit [82], the moment method [83], and the matching method [84]. A cavity perturbation technique is usually applied when the cavity is loaded with a small object, which only perturbs the resonant frequency by a few percent [21]. This approach has been used in the measurement of dielectric properties of polymers in TM_{012} mode [42]. For a cylindrical cavity coaxially loaded with a homogeneous, isotropic lossy rod, the electric field inside the cavity was calculated using the mode-matching technique [85][86].

In general cases where the loaded samples have arbitrary geometry and anisotropic dielectric properties, one can only resort to numerical methods. A three dimensional finite element method (FEM) was used to calculate the power dissipated in lossy materials in a short-circuited rectangular waveguide [87]. Also developed was a three dimensional FEM to simulate the microwave field structure and the associated power distribution in the dielectric material in a multi-mode rectangular cavity excited by waveguides [88]. The numerical results were in good agreement with the analytical solutions. This method is applicable to microwave heating with arbitrary geometry of the cavity, load and varying dielectric properties of the load. However, the three dimensional finite element methods solving for electric fields require large computer storage and long computing time, especially when small FEM mesh sizes are needed to ensure desired accuracy. For example, the higher the permittivity of the material, the smaller the mesh size because of the decrease of the wavelength inside the material.

Composite materials usually are highly anisotropic. Various studies have been conducted on the interaction between traveling TEM waves and graphite fiber/epoxy composites [29][89][90][91]. In order to approximate the microwave absorption rate during the processing of anisotropic composite plates inside a cylindrical cavity, a simplified five-parameter model was developed by Wei et al. [13][92]. The incident wave on composite surface is assumed to be a linearly polarized transverse electromagnetic (TEM) wave. The power dissipated in the composite is decomposed into two components, P_1 and P_2. P_1 is the dissipated power due to the incident TEM waves from the sides. And P_2 is the power due to the incident TEM waves on the top and the bottom. P_1 is further assumed to be constant through the thickness of the composite. For a composite lamina, E in each laminate is composed of the electric fields propagating in opposite directions:

$$E=1/2(E^{+}_{n}+E^{+}_{n+1})+1/2(E^{-}_{n}+E^{-}_{n+1}) \tag{1.56}$$

where the TEM wave in each direction is obtained by averaging the waves at the two interfaces.

For TEM waves in the composite material, the electric field can be decomposed into its two principal directions, parallel and perpendicular to the fiber. The attenuation of the electric field in each direction can be computed separately. Therefore, the TEM waves propagating in two opposite directions can both be expressed in terms of the waves in the two neighbor laminates.

A system of equations can be obtained by combining the equation for each laminate. The system can be solved if the incident TEM waves form the top and the bottom are known, as well as the power dissipated due to these two incident waves. Therefore, the total power dissipation can be calculated by summing the power dissipated in each laminate due to the top and bottom incident waves and the power dissipated due to the side incident waves. A five parameter expression for the total power dissipation can be obtained and the five parameters can be optimized by minimizing the error function for temperature measurements [13]. A FORTRAN code combining the energy balance equation, the microwave power absorption model, and the least squares optimization was developed to generate the five parameters based on the temperature/time/position profiles obtained during microwave heating of a fully cured composite. With the relationship of the five parameters as functions of input power for the given mode, the temperature profiles during the microwave cure can be readily simulated [13].

1.5.2 Microwave Process Control

Thermal cure profile during material processing is the major factor in consistent and high quality manufacturing [93]. The main goal of the microwave process control system is to achieve an optimal thermal cure profile. Different composite materials require different temperature cycles. However, there are two invariant requirements for all optimal thermal cure cycles. They are uniformity of processing temperature and the accuracy of temperature control so that the desired thermal cycle can be realized. Therefore, these are the main objectives of a microwave process control system.

Since microwave processing of polymer composites is still in its developing stage, the concept of control is novel. The first published automated single-mode resonant cavity was that developed by Alliouat et al. [94] for sintering ceramic materials. The control system was based upon elements of intelligent control for regulating the input power and for tuning the cavity. A gradient search method was used for tuning the cavity where only sensed information about the cavity length and reflected power were required. Components of this processing include an infrared pyrometer for measuring the surface temperature, detectors for sensing the input, reflected and absorbed power. Controlled parameters were the microwave power supply by analog output, and stepper motors for adjusting the cavity volume.

Jow et al. [7] developed a controlled pulsed microwave processing and diagnostic system to cure expoy/amine resins at 2.45 GHz. Temperature excursion resulting from the exothermic reaction was effectively eliminated and the epoxy/amine resins were cured at a higher cure temperature without degradation. This system was also capable of measuring dielectric loss factor during the controlled pulsed power cycle. However, the accuracy and precision of the temperature control needed to be improved.

Adegbite et al. [20] developed an automated single-mode cavity in order to advance it as a viable process. In the automation, a control system was designed and built in addition to the development and implementation of a set of sophisticated and comprehensive control software programs for controlling the curing process in the cavity. These control programs combine traditional and non-traditional control methodologies. The control software programs were developed for mode tuning, mode selection and power control which were constructed independently and then integrated to form the overall closed-loop feedback control system. A mathematical 2-dimensional simplex method was used to construct the tuning control software. Both coupling probe depth and cavity length were adjusted simultaneously to tune the cavity. A traditional PID (proportional-integral-derivative) methodology was used for the power controller. The diagnostics system was also automated to provide for automatic empty cavity characterization and for automatic dielectric analysis of materials inside the cavity.

Beale et al. [95] designed and simulated a temperature control system for the process of microwave joining of ceramics in a single mode cavity. A microwave heating model was used in the control system design with the dielectric located at the maximum electric field position of a rectangular TE_{103} mode. The heating model equation was linearized and a closed control loop with a compensator was designed. The control algorithm was designed with the complete nonlinear model representation of temperatures at the surface and material center and the temperature dependence of the loss factor and cavity quality factor. The computer simulation yielded good results for the desired values in the material temperature, giving a zero steady-state error, closed-loop stability, and on overshoot of the desired temperature. The simulation results showed that the control system was able to overcome the thermal runaway problem associated with microwave joining of ceramics. Since no experimental results were presented in the paper, the applicability of the control system remains to be proved. The modeling of microwave joining given in this paper appears to be less complicated than the modeling of polymer composite processing in a microwave cavity.

Research efforts have also been made in developing a knowledge-based system for the control of microwave composite curing [20][96][97][98]. The problem-solving architecture addresses the entire life cycle of composite-materials fabrication from a generic-task viewpoint. The prototype systems capture the experience-based static design of fabrication plans, and the process-control knowledge of cavity tuning for the microwave curing of composites. The knowledge-based system for designing microwave composite fabrication plans will be beneficial when the application of microwave processing in industry becomes common. In order to achieve wide application of microwave processing technology in composite industry, process control systems at the material processing level need to be first developed with consistent and good performance.

The implementation of control strategy is limited by the sensing technology in microwave processing. For material processing in a single-mode cavity, the input and reflected power are measured using the power meters, which are used to tune the cavity and regulate the input power respectively. The temperatures are usually measured by the fiber optic thermometry. The desired process parameters such as the electric field strength inside the material and the dielectric properties of the material can not be measured on-line.

CHAPTER 2

VARIABLE FREQUENCY MICROWAVE PROCESSING SYSTEM AND COMPUTER CONTROL INSTRUMENTATION

In this Chapter, the components and configuration of the variable frequency microwave processing system are presented. The hardware instrumentation of the computer control system is also discussed. The variable frequency system has a power source with adjustable frequency, thus requires microwave components that operate in the corresponding frequency range. Microwave frequency and power are the two control parameters used to achieve optimized and uniform processing.

2.1 Variable Frequency Microwave Processing (VFMP) System

The configuration of the VFMP system is shown in Figure 2.1. It has the same configuration as the fixed frequency microwave processing system. However, the microwave circuit components now have an operating frequency range instead of a single operating frequency.

2.1.1 Variable Frequency Microwave Power Source

The variable frequency microwave power source consists of an HP8350B Sweep Oscillator, an HP™ 86235A RF plug-in and a Lambda™ VariWave® microwave power source. The Lambda™ VariWave® microwave power source was used as a TWT (Traveling Wave Tube) amplifier. The oscillator and RF plug-in function as the low power signal generator. The frequency can be manually or automatically adjusted from 1.7 GHz to 4.3 GHz. The power output from the RF plug-in was adjustable from 6 to 16 dBm. The amplification ratio of the TWT amplifier was high enough to generate a microwave output of 150 watts. Both the power output of the RF plug-in and the amplification ratio of TWT change with frequency.

2.1.2 *Cylindrical Single-Mode Resonant Cavity*

The cylindrical single-mode resonant cavity was made of brass. A schematic of the cavity is presented in Figure 2.2. The cavity has a diameter of 7 inches with cavity length adjustable from 10 cm to 30 cm. The coupling probe is side mounted 1.2 inches above the base of the cavity, with probe depth adjustable from 0 cm to 50 cm. The cavity length was adjusted by moving the top plate. The bottom plate of the cavity was removable so that sample could be loaded. Both the top and the bottom plates were shorted with the cavity wall by metallic finger stocks.

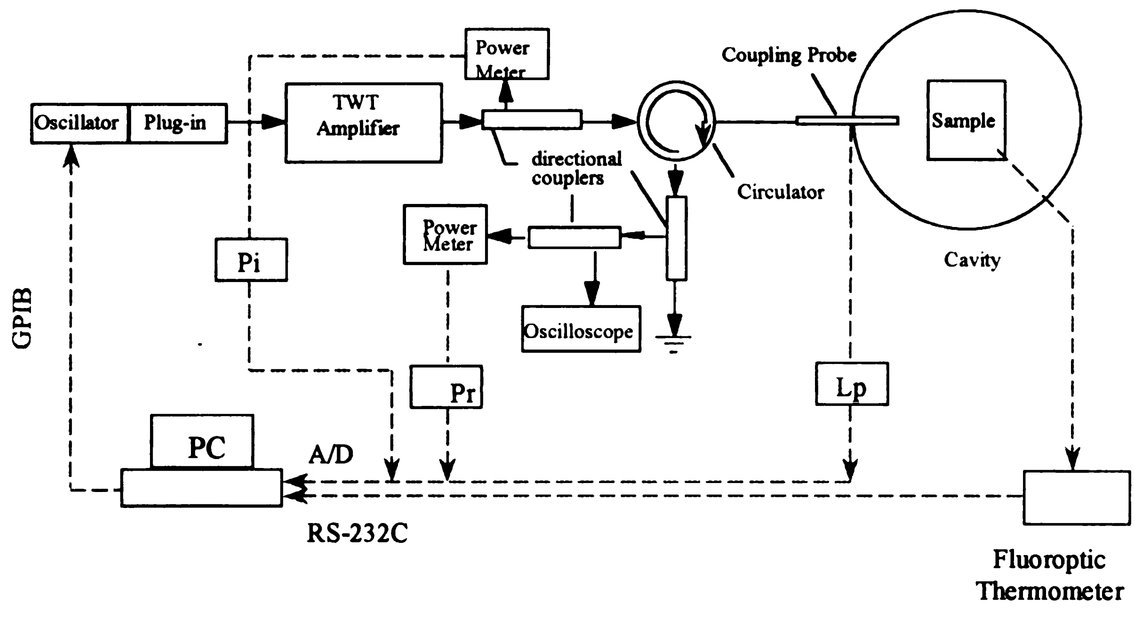

Figure 2.1 Variable Frequency Microwave Processing System

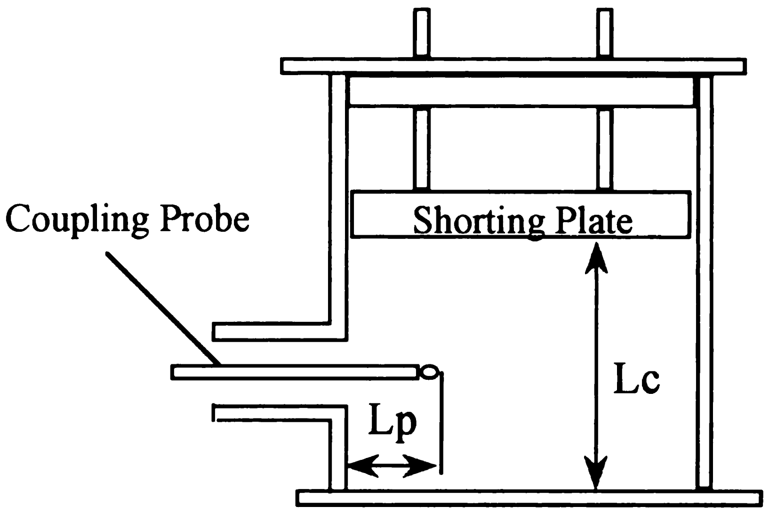

Figure 2.2 Cylindrical Single-Mode Resonant Cavity

2.1.3 Other Microwave Circuit Components

Other microwave circuit components included the circulator, directional couplers, power meters, the oscilloscope, and the dummy load. The circulator was used to protect the microwave power source from the microwave power reflected back from the microwave applicator. It redirected the reflected power to the dummy load. Power meters were used for both input and reflected power measurement. Directional couplers were used to obtain microwave signal in the measuring range of the power meters. Oscilloscope was used for low power diagnostics of the resonant cavity, which will be discussed in Chapter 3.

2.2 Automation of the Variable Frequency Microwave Power Source

The automation of the variable frequency microwave power source was essential to the development of the process control system, because microwave frequency and power were the only controlled parameters. Instrumentation details are presented in the next section.

2.3 Computer Data Acquisition and Control Implementation

The goal of the process control system is to achieve optimal product quality, which is greatly dependent on the temperature history of the materials being processed. Therefore, temperature control is essential in polymer composite processing. If temperature is too low, the polymerization reactions may not happen or proceeds very slowly. On the other hand, if the temperature is too high, undesired chemical reactions will occur and result in defective products. In addition, uneven temperature distribution inside the material leads to residual stress and affects the strength and other properties of the product. The temperature distribution can be controlled by changing the microwave frequency, while the temperature level can be varied by adjusting the microwave power. There are different approaches to achieving uniform processing temperature at a desired level, as will be discussed in details in the chapters to follow.

2.3.1 Measurement Instrumentation

2.3.1.1 Temperature Measurement

Since the samples were placed in the microwave field when being processed, the measurement of temperatures requires sensors that were transparent to microwave. Two temperature measurements systems that used optical fibers were used in the studies. One is the Luxtron™ Fluoroptic Thermometer, the other is the Nortech™ Fiberoptic Temperature Measurements Unit. The sensors of both systems are probes consisted of optic fibers at the core coated with low dielectric loss polymeric material. At the tip of the probes was a phosphor sensor with a fluorescent decay time that changes with temperature. The temperature change was detected by monitoring the percentage of infrared light reflected back through the optic fibers. The probe tips of the thermometry were inserted through the mold and placed on the top of the sample. Therefore, only surface temperatures were measured.

2.3.1.2 Power Measurement

Input and reflected microwave powers were measured using directional couplers and microwave power meters. Directional couplers are used to scale down the microwave power signal to within the power meter measurement range. Through the power meter, microwave power level was converted to analog voltage signal. The voltage signal value was converted back to microwave power level by the computer program.

2.3.2 Control Instrumentation

2.3.2.1 Frequency Control

The variable frequency microwave power source was consisted of an HP Oscillator with RF Plug-in, and the Lambda™ VariWave® microwave furnace as an amplifier. Since the HP™ Oscillator was the signal generator, frequency control was achieved by controlling the Oscillator output frequency. The GPIB interface of the HP 8350B Sweep Oscillator provided the communication interface with the computer. Any frequency change can be carried out digitally through GPIB. Either single frequency mode or frequency sweeping mode could be selected. The instruction string to set the frequency started with "CW" followed by the frequency. For example, if the desired frequency was 2.45 GHz, the computer would write "CW2.45" to the GPIB port.

2.3.2.2 Power Control

The control of the microwave power was a little more complicated issue. There was only a manual dial knob that could be used to adjust microwave power. One was installed on the RF plug-in, and the other was installed on the Lambda™ VariWave® power source. Two different approaches were used to achieve computer control of the microwave power. The first one was using a stepper motor to adjust the manual knob on the Lambda™ VariWave® to change the amplification. The pin configuration of the cable connector for the stepper motor is presented in Appendix A.

The other approach was using a variable attenuator with voltage-controlled attenuation rate. The variable attenuator would be connected between the signal generator and the amplifier since it has a survival input power of only 30 dBm (1 watt). The connection configuration of the variable attenuator is also presented in Appendix A. The characteristics of these two control units are examined and discussed in Chapter 2.

2.3.3 Computer Data Acquisition

The configuration of the connector board is given in Appendix 1 along with the configuration of the National Instruments™ PCI-MIO-16XE-50 data acquisition board. Inputs were the analog signals from the Luxtron™ and the Nortech™ temperature measurement units, and the power meters. The outputs are the control voltages to the variable attenuator and the stepper motor. The A/D and D/A conversions were accomplished through the National Instruments™ PCI-MIO-16XE-50 data acquisition board.

CHAPTER 3

CHARACTERIZATION OF VARIABLE FREQUENCY MICROWAVE PROCESSING SYSTEM

In this chapter, characterization results for the variable frequency microwave processing system are presented. Mode curves were measured for the empty microwave cavity and compared with theoretical calculations. The technique of characterizing the microwave cavity loaded with composite samples was also discussed. Mode frequencies, at which there was effective heating, were located. The heating patterns of the modes were obtained. This characterization technique is essential to all the processing experiments. The response time of the power meters was tested and the characteristics of the variable attenuator was also determined.

3.1 Variable Frequency Method

The theoretical characteristics of the electromagnetic field in a cavity can be determined by solving the Maxwell's equations with appropriate boundary conditions [21]. The cut-off frequencies corresponding to resonant modes can also be calculated for a fixed cavity volume. Theoretically there are two factors that determine a resonant mode in a cylindrical cavity: the frequency and the cavity length. Consequently, two approaches can be used to select a particular mode, as seen in Figure 3.1. Variable frequency method changes the mode electronically, thus is much faster than the fixed frequency method.

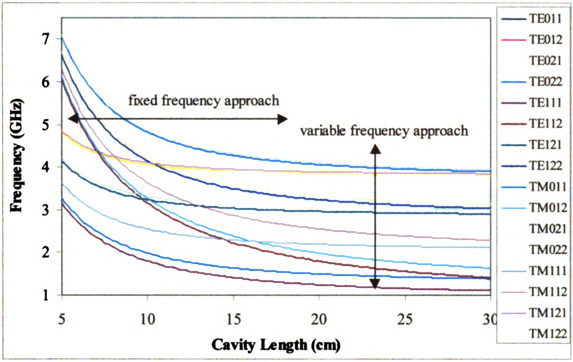

Figure 3.1 Mode Chart of the Empty Cavity

As frequency changes, not only the field pattern changes, the coupling efficiency of microwave energy into the load changes too. For a homogeneous, non-magnetic material, the microwave power absorption rate, P, (in W/m^3) can be modeled as following [21]:

$$P = \frac{1}{2}\varepsilon_o \varepsilon'' \omega \left|\bar{E}\right|^2 \tag{3.1}$$

where $\bar{E}$ is the electric field strength inside the material, V/m,

ω is the radian frequency, rad/sec, $\omega = 2\pi f$, f is the frequency in Hz,

ε_o is the free space permittivity, $\varepsilon_o = 1/(36\pi)\times10^{-9}$ F/m,

ε'' is the effective relative loss factor, $\varepsilon'' = \varepsilon''_d + \sigma/(\varepsilon_o \omega)$,

ε''_d is the relative loss factor due to dipolar contributions,

and σ is the material conductivity.

Qualitatively, assuming ε''_d and σ are constant, as frequency increases the power adsorption rate P increases for the same $\bar{E}$. Therefore, if the cavity is fully loaded with homogeneous non-magnetic material the coupling efficiency increases with frequency.

However, this model is not applicable when the material is anisotropic, which is almost always the case. From the mode chart in Figure 3.1, we can see that as frequency increases the order of resonant modes are getting higher. Since the E-fields of higher order modes are not as concentrated as lower order ones, the coupling of microwave energy is getting less efficient as the frequency increases when the cavity is partly loaded. Computation intensive model should be used to relate the frequency to microwave energy coupling. As for a fiber-reinforced composite, a five-parameter microwave power adsorption model is available in literature [13].

3.2 Variable Frequency Microwave Power Source Characteristics

As aforementioned, the variable frequency microwave power source consisted of a signal generator and a TWT amplifier. The frequency of the microwave output could only be controlled through the signal generator. However, the microwave power level could be controlled either through the signal generator by adjusting the attenuation level, or through the TWT amplifier by tuning the dial knob. In computer control implementation, the power could be controlled through variable attenuator connected to the signal generator, or the stepper motor attached to the dial knob of the TWT amplifier.

It was observed that the microwave power level changed when the frequency changed, even though the position of the dial knob for power level adjustment remained unchanged. As discovered by experimental tests, when the frequency changed, the power level of signal generator output changed. Moreover, the amplification rate of the TWT amplifier changed with frequency. Therefore, if the microwave power were to be maintained at constant when frequency was changed, a power control action would be needed. The microwave power level versus frequency curve is presented in Figure 3.2. The power level was about 25 watts at 2.45 GHz. The curve would change if power level changed. Generally, microwave power increased as frequency increased. Microwave frequency and power also shifts slightly with time.

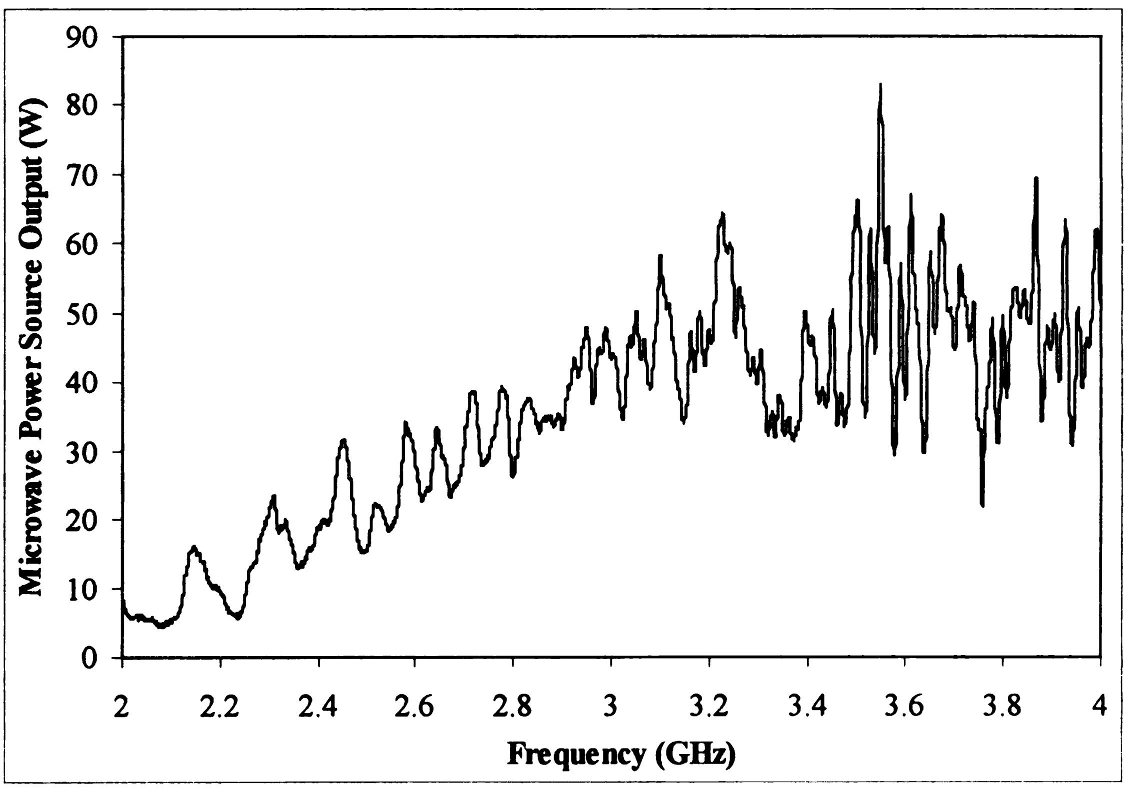

Figure 3.2 Microwave Power Source Output Versus Frequency Curve

The frequency of the variable frequency power source was controlled through the GPIB interface between the HP Oscillator and the computer. The speed of frequency control, i.e. the maximum frequency change rate, was very important to the variable frequency microwave processing studies. For example during the variable frequency microwave processing experiments, mode tuning, in which the power reflectance was measured while the frequency was swept in a certain range, needed to be carried out as fast as possible. Given sweeping time and interval, the size of the frequency sweeping range depends on the speed of frequency control. In order to measure the speed of frequency control, a program was written to write a number of frequencies to the Oscillator continually, and the total time used was measured. The time used to write a single frequency was obtained by dividing the total time by the number of frequencies written. Table 3.1 shows the test data. The result was that it took approximately 0.1 seconds for each frequency write.

Table 3.1 Time for the Computer to Write Frequency to the Oscillator

Tests	Sweeping Range	Sweeping Step (GHz)	Number of Writes	Total Time Used (sec)	Time for Each Write (sec)
1	2 GHz to 4 GHz	0.001	2001	196.80	0.09835
2	2 GHz to 4 GHz	0.01	201	19.81	0.09856
3	2 GHz to 4 GHz	0.1	21	2.13	0.10143

3.3 Characterization of the Empty Cavity

To test the theoretical predictability of the cavity, mode measurements were done using swept frequency diagnostic method. Mode frequencies were determined by identifying the valley of the power reflectance versus frequency curve. Mode curves were obtained experimentally by changing the cavity length while recording the mode frequency. Linear regression was carried out using the linear relationship between p^2 and χ^2, obtained by manipulation of the cut-off frequency equations (Equation 1.35 and Equation 1.36). Therefore p and χ were obtained and the mode was identified. A comparison of theoretical and measured mode curves for TM012 mode is presented in Figure 3.3. Measurement results are shown in Table 3.2. The experiment data were consistent with the theoretical results. The electromagnetic behavior of the cavity is theoretically predictable. Therefore the cavity satisfied the requirements for a single mode resonant cavity.

Table 3.2 Experimental Measurement of Resonant Modes in an Empty Cavity

Measured modes	TM012	TM211	TM111 /TE011	TM112 /TE012	TE211	TE311
% error of p	2.3%	0.2%	4.3%	1.7%	3.4%	6.1%
% error of χ^*	3.0%	0.4%	0.4%	0.3%	0.0%	0.1%

* χ is the corresponding root of Bessel's function (TM modes), or the derivative of Bessel's function (TE modes).

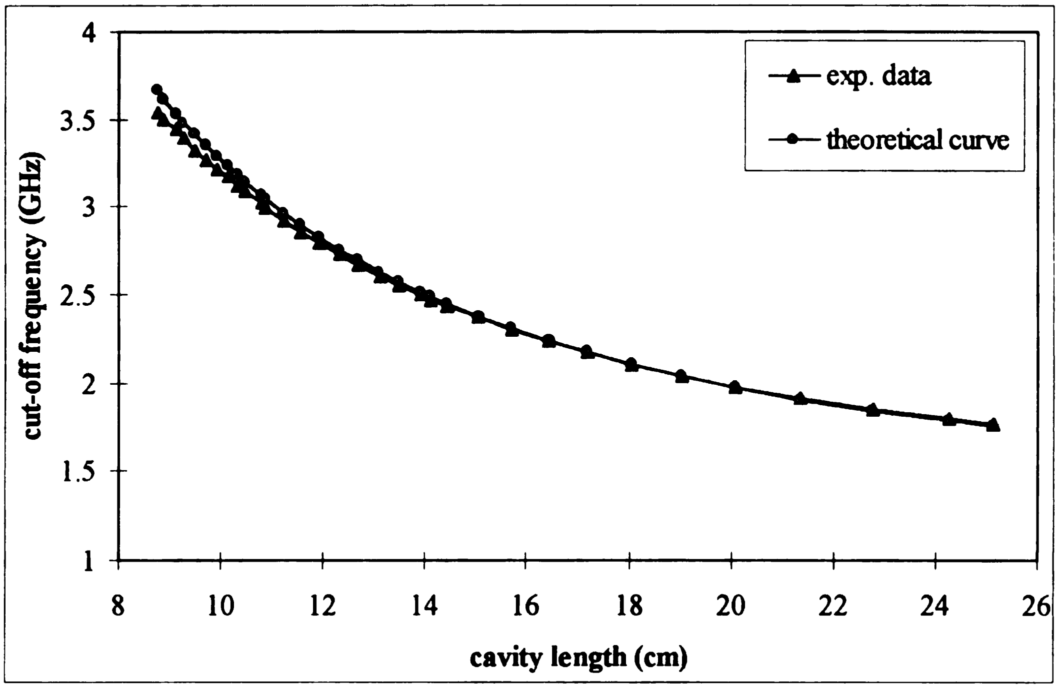

Figure 3.3 Comparison of Theoretical and Experimental TM012 Mode Curves

3.4 Characterization of the Loaded Microwave Cavity

The characterization of the loaded microwave cavity included locating the empirical mode frequencies and obtaining the heating pattern of each empirical mode. Empirical modes were determined by locating the local minimums of the power reflectance versus frequency curve for the loaded cavity with fixed cavity length and probe depth. A LabVIEW program was developed to acquire the power reflectance versus frequency curve and the details of the program (characterization&temp.vi) can be found in Appendix C.

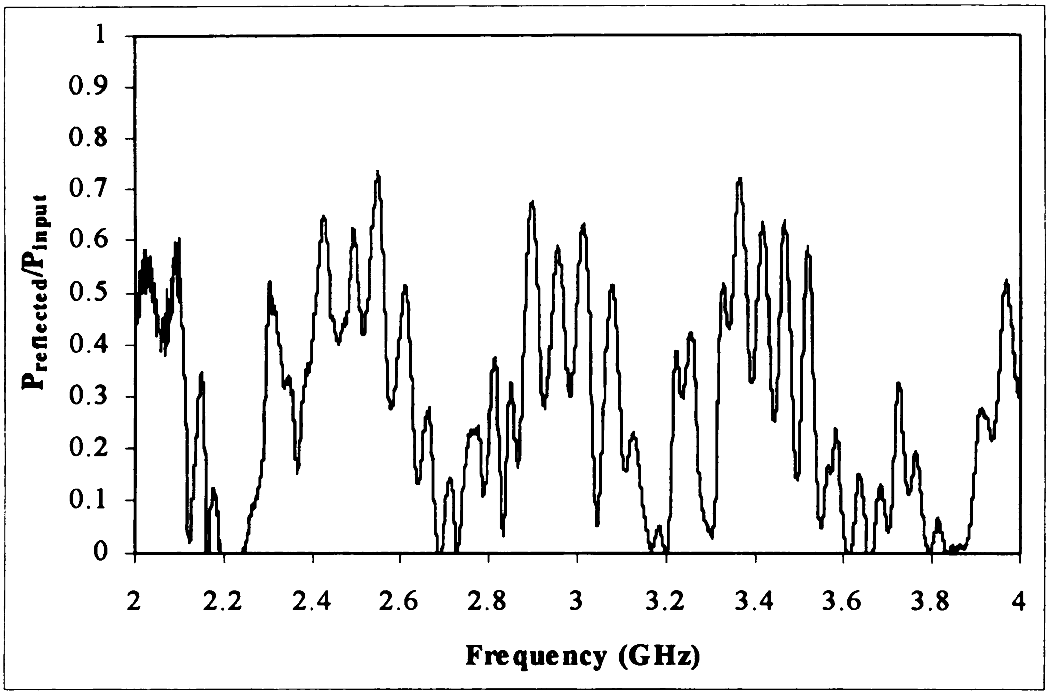

Figure 3.4 Power Reflectance versus Frequency During Frequency Scan

The characterization procedure for loaded cavity consisted of the measurement of input microwave power, reflected microwave power, and temperatures while sweeping the frequency from 2 GHz to 4 GHz. This frequency range was used instead of the available range from 1.7 GHz to 4.3 GHz, because the maximum microwave power output outside of the range from 2 GHz to 4 GHz was not high enough for composite processing.

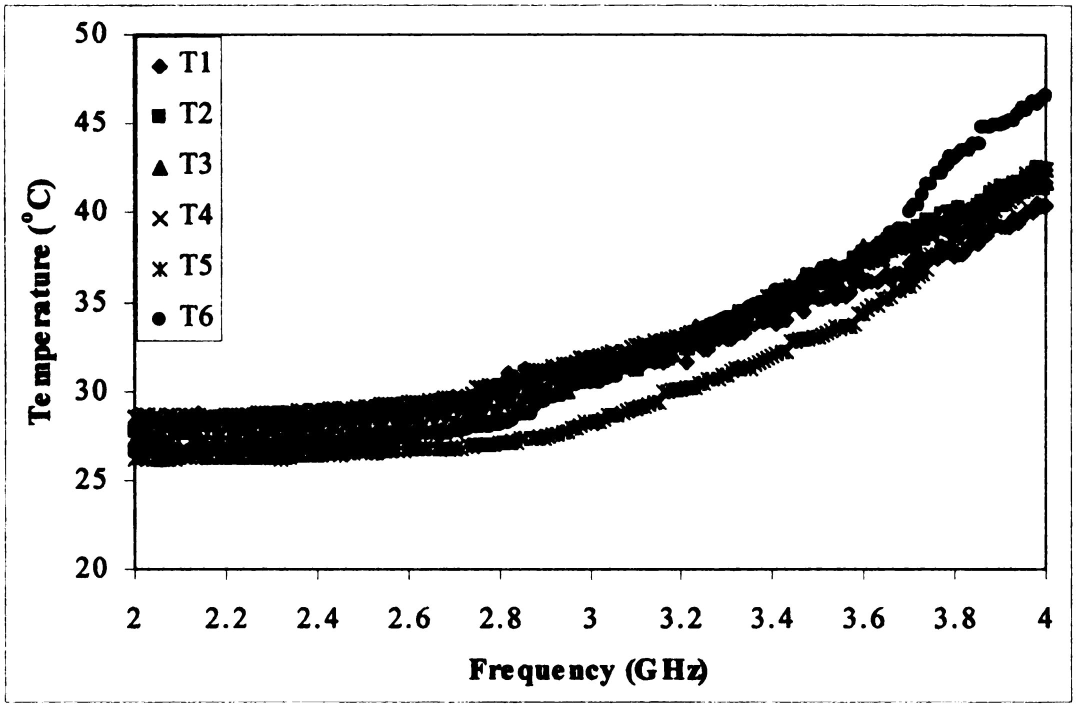

Figure 3.5 Temperature Change versus Frequency During Frequency Scan

Examples of the characterization results are given in Figure 3.4 and Figure 3.5. Due to the input microwave power, the temperature of the sample would rise during the frequency sweep. Figure 3.5 shows the temperature profiles versus frequency. As seen from the figure, the heating rates were changing as frequency changed. The reason was that at different frequencies, the electromagnetic fields inside the sample were different. As a result, the heating preference inside the sample differed. From Figure 3.5, important information can be obtained - how the heating preference changed at different frequencies. The sample could be loaded at different positions inside the cavity and the heating preference change with frequency would be different. An optimal loading position could be determined by measuring the temperature versus frequency profile and choosing the

position that would have the most diverse heating preference. This means that if different frequencies were excited for heating, the sample would have the most uniform time-averaged temperature distribution when loaded at the optimal position.

Figure 3.4 presents the power reflectance versus frequency curve. The frequencies at which the power reflectance is locally minimal and close to zero were considered the frequencies of empirical modes. Like the theoretical modes, these empirical modes had very small reflected power versus input power ratio. Some of these empirical modes correspond to theoretical modes, although the frequencies are different. Some others may be the result of two or more modes merging together due to the disturbance of the sample to the electromagnetic field. The power reflectance curve is not exactly reproducible due to the slight variation of microwave frequency and power versus time. However, the variation is usually less than 1%.

No attempts were made to correlate empirical modes to theoretical modes because the fields have been altered dramatically due to the lossy sample. An empirical mode would usually have a drastically different E-field distribution that its corresponding theoretical mode, if there is a corresponding theoretical mode. Therefore, any information regarding mode heating characteristics needed to be determined experimentally for it to be utilized during the processing. From here on, empirical modes will be just mentioned as modes. Therefore, the modes in a processing context are different from the modes mentioned in a theoretical context.

After the frequencies of the modes were determined, samples would be heated at these frequencies and temperatures were measured. The heating patterns of the modes were thus obtained. The control system then will use this information during the processing to select which mode to heat. There are different approaches to applying the heating characteristics in the mode selection process. They will be further discussed in the next few chapters.

3.5 Variable Attenuator Characteristics

Variable attenuator is an attenuator with adjustable attenuation by voltage control. It was used in the microwave circuitry in order to provide a means for the computer to control the microwave power level. The computer sent out an appropriate control voltage to attenuate the power of microwave signal from HP oscillator to a certain level before being amplified by the Traveling Wave Tube applifier. The specifications of the variable attenuator provided by the manufacturer is given in Appendix A.

The specifications of the Variable Attenuator indicate that the attenuation of the attenuator is proportional to the control voltage. The attenuation range is 0 to 60 dB, and the corresponding control voltage irange is 0 to 6 volts. In order to verify this relationship, attenuation measurements were made while changing the control voltage. The LabVIEW program (vatest.vi) for the characterization of the variable attenuator is documented in Appendix C. The test procedure was as follows:

1. Set control voltage = 0;
2. Measure the initial microwave power output from the power source (after the amplifier) = P_0;
3. Set control voltage = v;
4. Measure microwave power output = P;

According to the specifications (see Appendix A), the plots of 10Log(P/P_0) versus v should be straight lines with a slope of – 1. The results at five different frequencies (2 GHz, 2.5 GHz, 3 GHz, 3.5 GHz, and 4 GHz) are presented in Figure 3.6. Linear regression was used to fit the curves to linear equations. Overall, the linear fit was a close representation of the attenuation vs. control voltage relationship. For example, at f = 3 GHz, the slope of the linear fit was –1.0082 with an R^2 value of 0.9937. However, when the control voltage gets close to zero, the curve is not linear anymore. The linear relationship between the attenuation and the control voltage holds when the control voltage is greater than 0.2 volts. When the control voltage is smaller than 0.2 volts, the attenuation is very close to 0 dB.

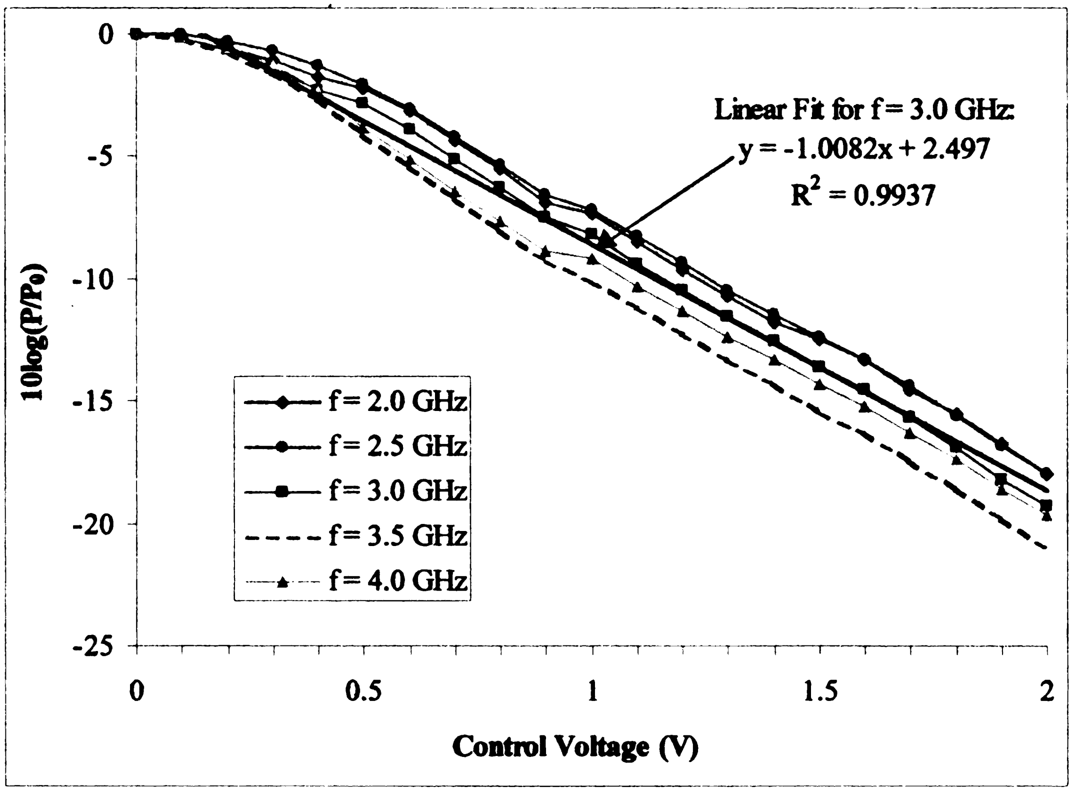

Figure 3.6 Relationship between Control Voltage and Power Attenuation

3.6 Power Meter Response Time

In the processing experiments of this research, step power changes were very common. They were mostly due to one two actions, frequency change or attenuation change. Because the microwave power output from the power source varied with frequency, if there was a frequency change, a microwave power change would follow. In microwave power control, the attenuation of the variable attenuator was changed to adjust the microwave power. The discontinuous change of the attenuation also would result in step power changes.

Since the power meters featured a dial attached to a spring, the dial movement could not precisely follow sudden power changes because of inertia. Therefore, the power reading immediately after the power change was inaccurate. A finite amount of time was needed for the mechanical dial to settle after power changes. In order to obtain accurate power measurement, the response time of the power meters needed to be determined.

Experiments were carried out to test the power meter response by changing the attenuation of the variable attenuator. The frequency was fixed at 2.5 GHz. Power changes of different step size were used to characterize the power meter response. The LabVIEW program (p-response-test.vi) is documented in Appendix C. The test was carried out as such:

1. A step change of microwave power was made by changing the control voltage of the variable attenuator.
2. The computer measured the microwave power by acquiring the analog output from the power meter at discrete times with an interval of 20 ms.

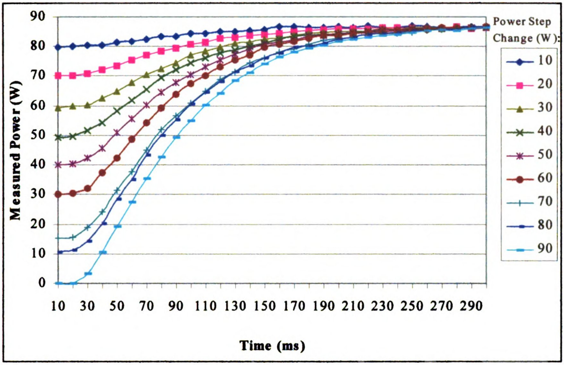

Figure 3.7 Measured Microwave Power versus Time after Power Step Change

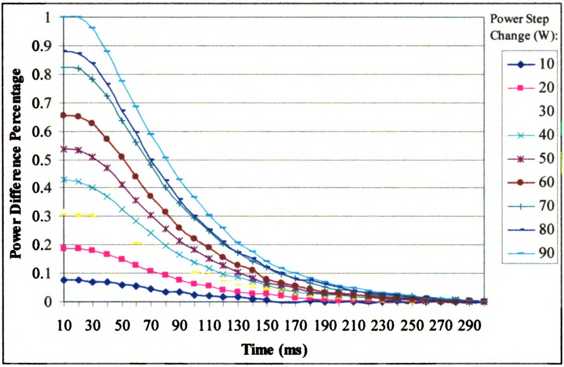

Figure 3.8 Difference Percentage versus Time after Power Step Change

The results are presented in Figure 3.7 and Figure 3.8. As we can see in Figure 3.7, the analog output of the power meter did not reflect the steady power level until some time after the control voltage change. Therefore, during microwave power adjustment, the computer should wait for a certain amount of time after attenuation change in order to assure accurate power readings. The percentage of power difference between measured power and steady power was plotted versus time in Figure 3.7. About 170 ms after the attenuation change, the measured microwave power was within 10% of the steady power even for power step change of 90 watts. The power difference percentages at different power step changes after 170 ms are listed in Table 3.3. The power difference percentage was calculated as follows:

$$\text{Power Difference Percentage} = \frac{|P_{steady} - P_{measured}|}{P_{steady}} \times 100\% \qquad (3.2)$$

Usually, the power change during processing would be less than 30 watts. In those cases, the measured power would be within 5% of the steady power 170 ms after the attenuation change.

Table 3.3 Power Difference Percentage after 170ms.

Power Change Step (W)	10	20	30	40	50	60	70	80	90
Power Difference Percentage	0.3%	1.3%	3.5%	3.5%	4.9%	5.5%	8.4%	8.1%	9.9%

3.7 Frequency Effects on Material Properties

3.7.1 Dielectric Measurements of Uncured DGEBA/DDS

In order to investigate the effects of frequency on dielectric properties of epoxy resins, experiments were conducted to measure the dielectric properties of uncured DGEBA/DDS resin with different frequencies at room temperature. DGEBA used in the study was EPON 828 supplied by Shell Chemical Company. DGEGBA and DDS were mixed with stoichiometric weight ratio 1 : 0.33. The resin was loaded in a Teflon holder and the dielectric properties were measured using single mode cavity perturbation method. An empty Teflon holder was loaded in the cylindrical single mode cavity as a reference state. Due to the limitation of the experimental setup, measurements were only possible to be made in the frequency range from 2.2 GHz to 2.7 GHz. The maximum cavity length prohibits the measurement for frequencies below 2.2 GHz. When frequency goes above 2.7 GHz, resonance peaks of different modes overlap one another to make it impossible to identify single mode resonance peak. In other words, the Q factor is too low to make dielectric measurement.

The results are presented in Table 3.4 and in Figures 3.9 and 3.10. No obvious trends were observed in the experimental data of dielectric constant, neither for dielectric loss factor. The average of the complex dielectric constants is 3.439 - *j*0.1328. Since the frequency range was not broad enough, the fluctuation of the data due to experimental errors concealed the trends, if any, of the dielectric property change with respect to frequency.

One important factor that affected the accuracy of the dielectric measurement is the Q factor of the cavity. As indicated by the mode chart, at higher frequencies the resonance peaks are closer to each other, which leads to lower Q factor of the cavity for a single mode. The Q factors of the cavity loaded with Teflon holder both with and without sample are shown in Figure 3.11. The data showed a decrease of the Q factor with the increase of frequency when the cavity was loaded with empty Teflon holder. However, there were no apparent trends of Q factor change with frequency when the sample was loaded.

Table 3.4 Dielectric Properties of Uncured DGEBA/DDS

f (GHz)	2.2563	2.3005	2.3502	2.3995	2.4502	2.4999	2.5500	2.6000	2.6498	2.6999
ε'	3.220	3.647	3.396	3.426	3.460	3.605	3.534	3.680	3.189	3.234
ε''	0.1384	0.1313	0.1383	0.1286	0.1343	0.1470	0.1352	0.1358	0.1004	0.1387

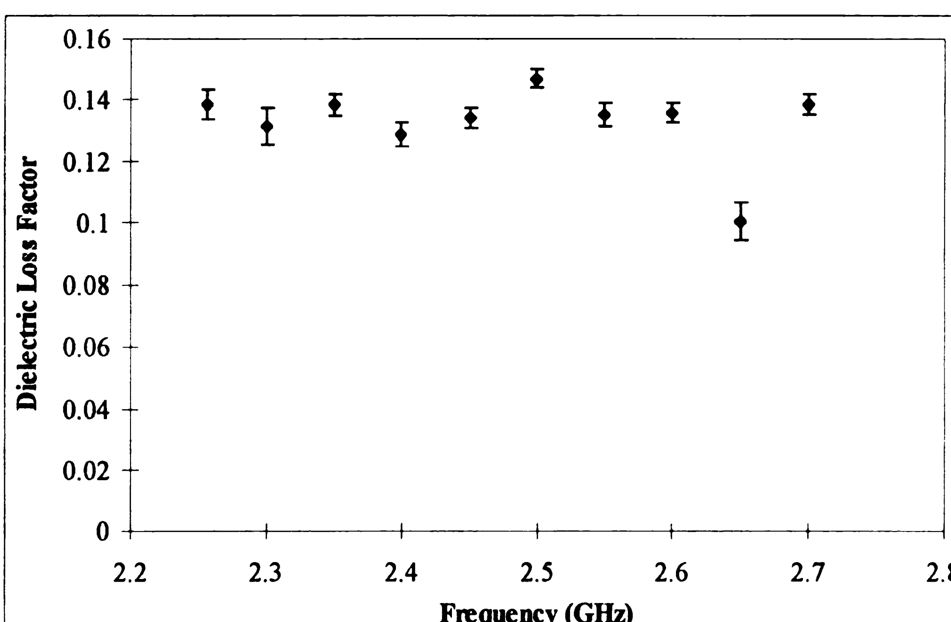

Figure 3.9 Dielectric Constant versus Frequency for DGEBA/DDS

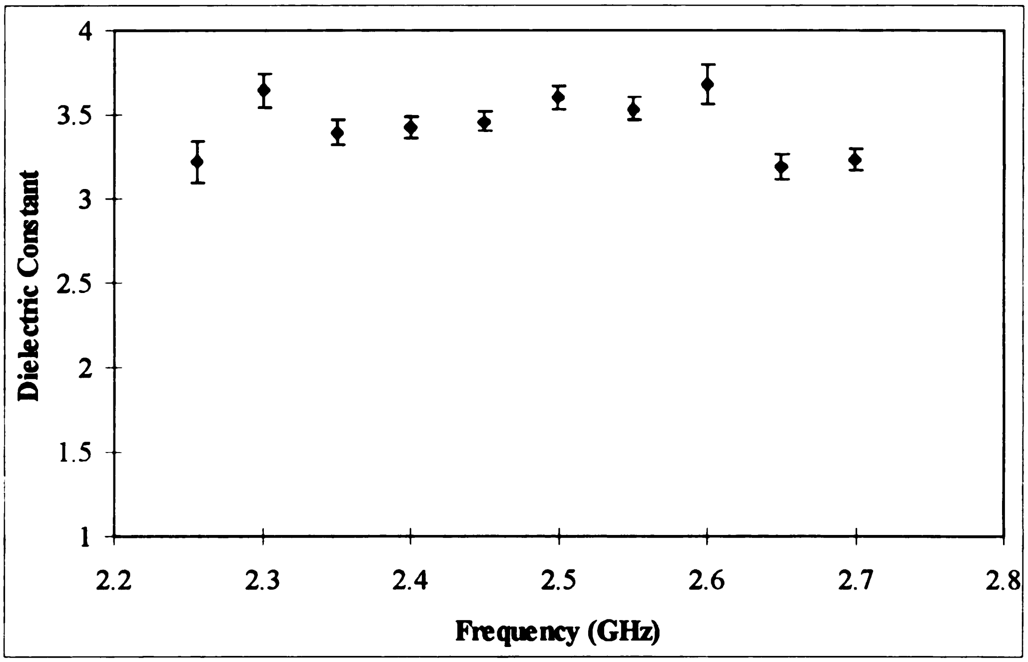

Figure 3.10 Dielectric Loss Factor versus Frequency for DGEBA/DDS

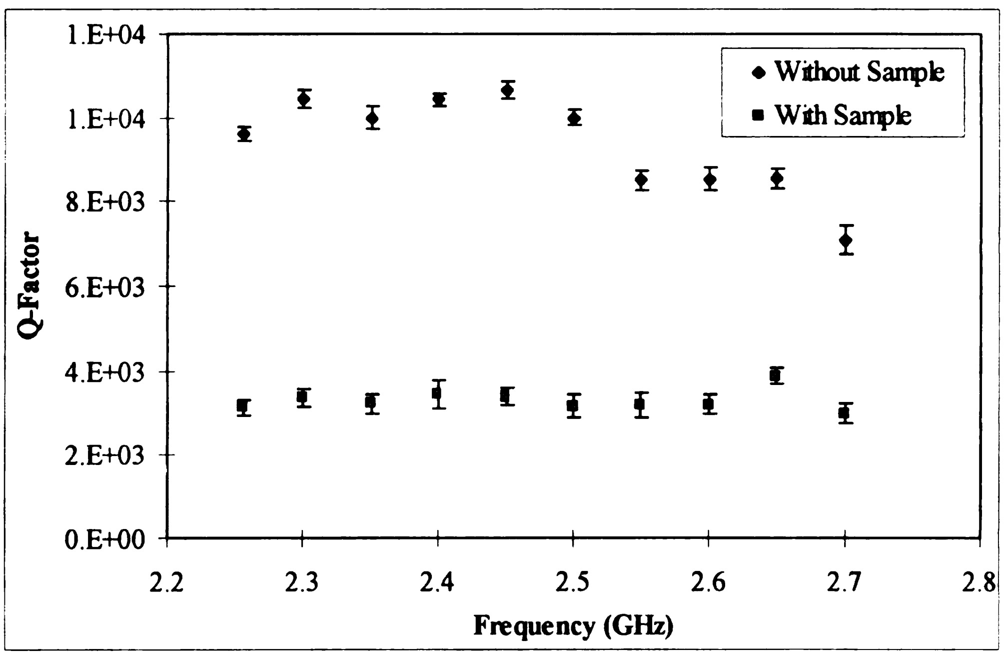

Figure 3.11 Q-Factor versus Frequency

CHAPTER 4

VARIABLE FREQUENCY MODE SWEEPING HEATING

In this chapter, a variable frequency mode sweeping technique is presented, which was used to uniformly heat graphite/epoxy composite parts of small size. The concept of complementary heating is demonstrated using thermal paper images. The cavity loaded with a unidirectional 2 inch 48-ply square graphite/epoxy composite sample was characterized. The frequencies and the heating characteristics of the empirical modes were determined. Four modes with complementary heating preferences were selected for the mode sweeping heating. The concept of process cycle design is presented for uniform and fast heating. Both thermal images and temperature profiles were obtained to show the success of the heating technique.

4.1 Experimental Preparation

Graphite/epoxy prepreg material (Hexel® AS4/3501-6) was used in the heating experiments. The prepreg laminates were cut into 2 inch by 2 inch squares and laid up uni-directionally to 48-ply parts. The lay-up procedure for the composite material is given in Figure 4.1. The weight of each part was about 30 g.

During the experiments, the microwave cavity length was fixed at 15 cm and coupling probe depth at 20 mm. The composite sample was placed inside a Teflon mold, the configuration of which is shown in Figure 4.2. The Teflon mold with the sample inside was placed on the center bottom of the cylindrical single-mode resonant cavity. The cavity system was not pressurized. The sample was loaded such that the fiber direction of the sample was perpendicular to the microwave coupling probe (Figure 4.3). Since Teflon is transparent to microwave, the microwave energy only heats the composite material.

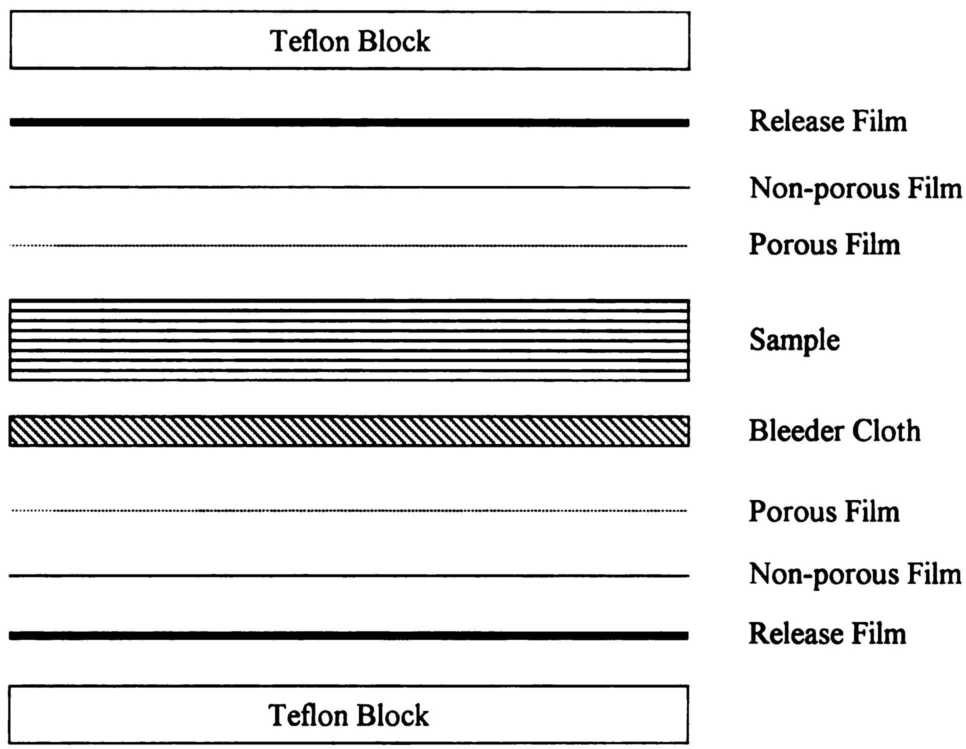

Figure 4.1 Composite Material Lay-up Procedure

Thermal paper was used for mapping the heating patterns. The thermal paper was placed under the sample between the sample and the Teflon material. It changes color from white to blue at about 85 °C. The dark areas on the thermal paper image indicate high temperature, and the bright areas indicate lower temperature.

Temperatures were also measured using the measurement probes of a Luxtron™ Fluoroptic Thermometer at four different sites on the sample surface. The temperature probes were inserted into the microwave cavity and through the top of the Teflon mold. The probe tips were protected using small glass tubes, which were in direct contact with the sample surface. These temperature probes were composed of optic fibers shielded with very low loss polymeric materials. Therefore, they do not interfere with the electromagnetic fields or absorb microwave energy, which assured the accuracy of the temperature measurement in microwave environment. The dimensions of Teflon molds used in the microwave heating experiments are given respectively in Appendix A.

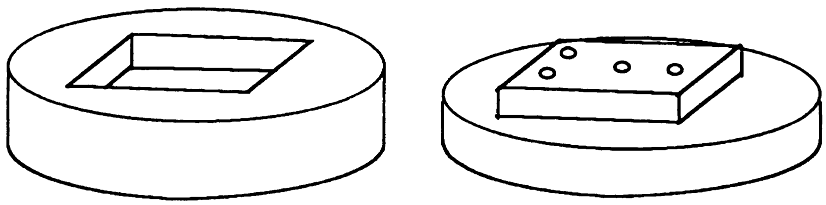

Figure 4.2 Schematic Sketch of the Teflon Mold

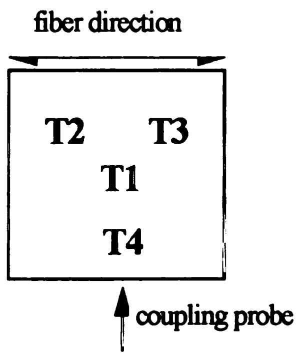

Figure 4.3 Temperature Measurement Locations

4.2 Mode Heating Characteristics

The frequencies of the empirical modes were obtained by locating the frequencies with locally minimal power reflectance. By tuning the frequency from 2 GHz to 4 GHz, eight empirical modes were found for the sample-loaded cavity at a fixed cavity length of 15 cm and a fixed coupling depth of 20mm. There is not much change of the locations of the modes with the reloading of the material. Therefore, when a new part is loaded for a new run these mode locations provide reliable start-points for mode tuning. Temperature also had minimals effect on the mode frequencies, as shown in Table 4.1, which could be a result of small sample size.

Typically, the reproducibility of microwave heating profile of conductive fiber reinforced composites was not very good, due to high sensitivity to sample loading position, sample size, fiber orientation, fiber content, and fluctuations of microwave frequency and power. In this study, samples were very carefully prepared to increase reproducibility. Although the exactly same heating profiles were hard to reproduce, the trends were quite reproducible and were used for characterizing the heating preference of each mode.

After characterizing the heating pattern for each mode, an optimum heating cycle can be designed to maximize the uniformity of heating. Computer control algorithm can be constructed to further include the consideration of the heating rates of each mode so as to optimize the material processing.

Table 4.1 Frequency Shift of Empirical Modes Due to Temperature Change

	Frequency Tuned for Each Mode (GHz)							
	Mode 0	Mode 1	Mode 2	Mode 3	Mode 4	Mode 5	Mode 6	Mode 7
30°C	2.1477	2.1653	2.1904	2.2446	2.3078	2.3730	2.5555	2.6310
110°C	2.1472	2.1640	2.1918	2.2460	2.3074	2.3722	2.5575	2.6338
f shift (GHz)	-0.0005	-0.0007	0.0014	0.0014	-0.0004	-0.0008	0.0020	0.0028

The heating characteristics were measured at these frequencies. Thermal images and temperature profiles of four of these modes (modes 1, 2, 3, and 5) are presented in Figure 4.4 and Figure 4.5, respectively. As revealed by the thermal images and the temperature profiles, single mode heating usually results in non-uniform temperature distribution.

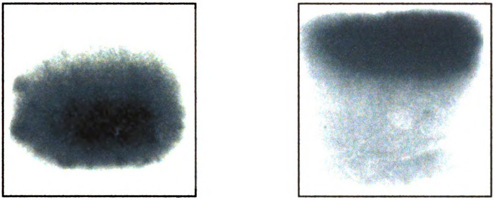

(a) mode 2 **(b)** mode 3

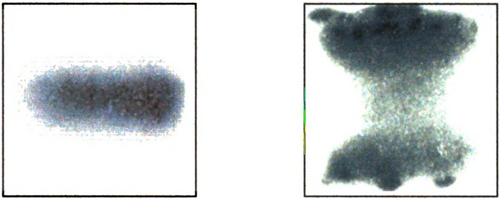

(c) mode 4 **(d)** mode 6

Figure 4.4 Thermal Paper Images of Four Selected Modes

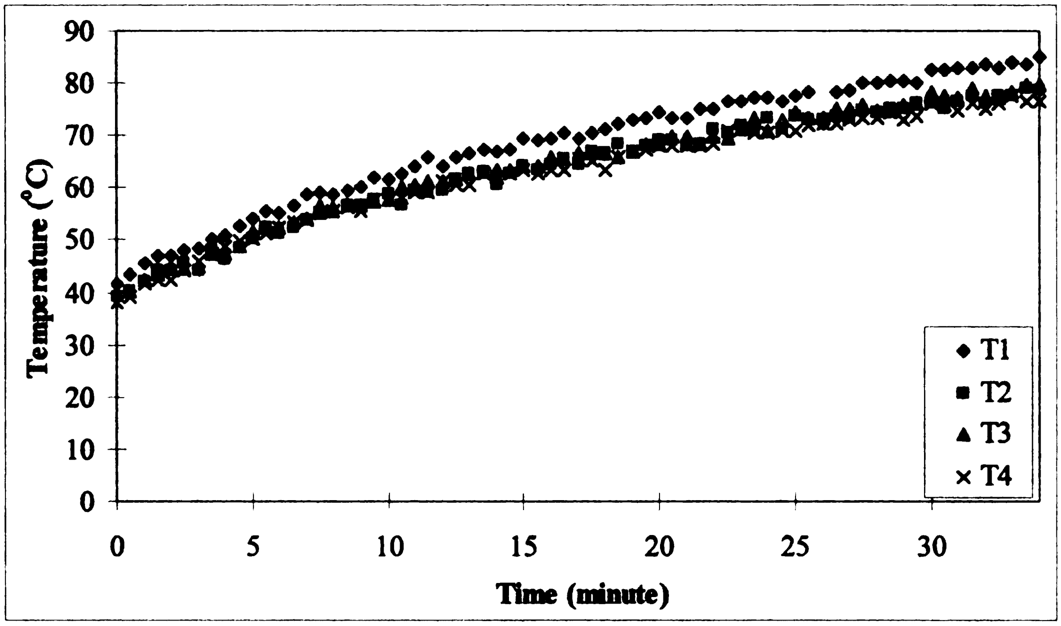

(a) Mode 1: f = 2.1653 GHz

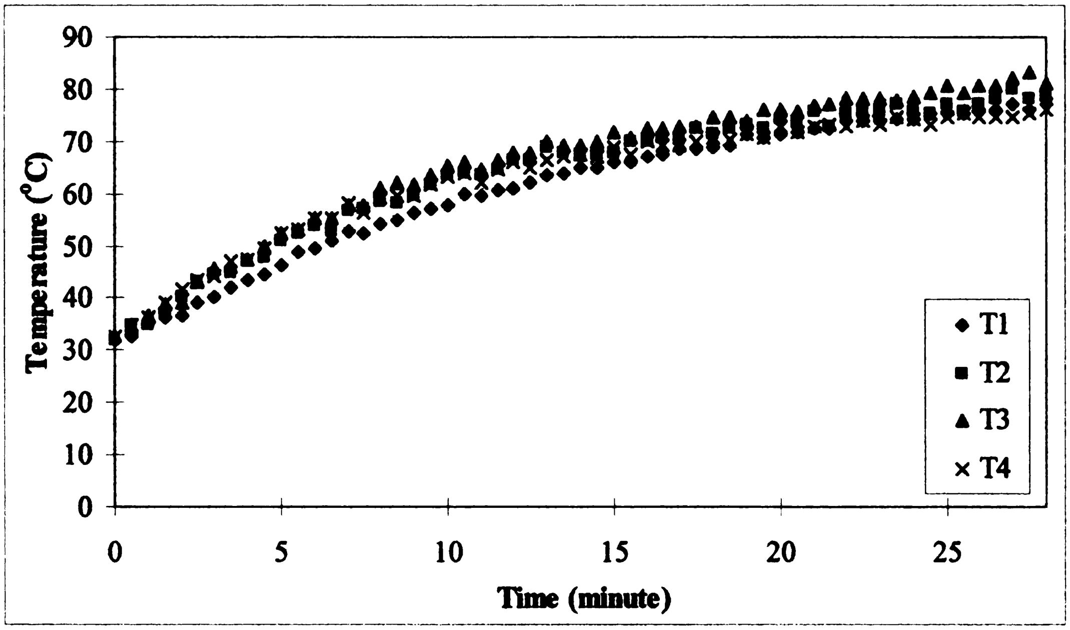

(b) Mode 2: f = 2.1904 GHz

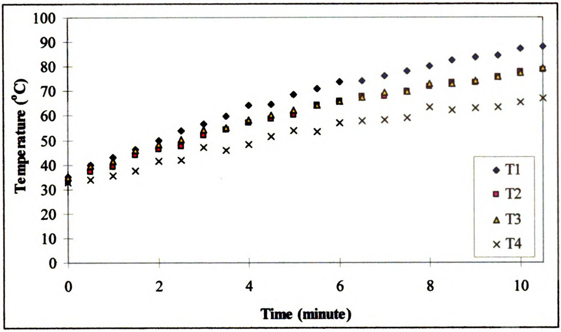

(c) Mode 3: f = 2.2446 GHz

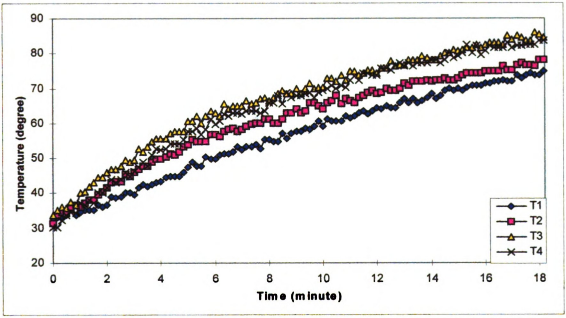

(d) Mode 5: f = 2.3730 GHz

Figure 4.5 Single Mode Heating Temperature Profiles of Selected 4 modes

4.3 Complementary Heating Concept and Mode Switching Technique

Due to the nature of electromagnetic fields, the field distribution of a single mode is generally uneven. Since microwave heating effects on non-magnetic material largely depend on electric field strength, this uneven field distribution often leads to uneven heating. From the thermal images and temperature profiles of the four selected modes, one can clearly see the hot spots and cold spots during heating.

Since different modes have different hot spots and cold spots, if the heating patterns of different modes are superimposed on one another, hot and cold spots tend to even out. If the hot spots of one mode are cold spots for another mode and vice versa, these two modes are said to have complementary heating patterns. It is obvious that the combined heating effects of complementary heating modes produce more even heating than any single mode heating. Figure 4.6 illustrates the concept of complementary heating by combining the heating effects of mode 3 and mode 5.

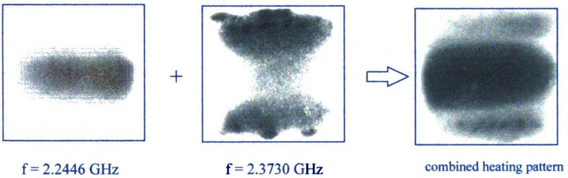

Figure 4.6 Complementary Heating Using Two Modes

The way to combine the heating effects of different modes is by exciting the modes in a particular sequence, which is called mode switching. Different design of this sequence

leads to different effectiveness. One example is to excite the modes in a pre-ordered sequence, which is termed Mode Sweeping technique. More advanced techniques determine when to select which mode by taking the mode characteristics and on-line temperature information into consideration. These techniques will be discussed in the following chapters.

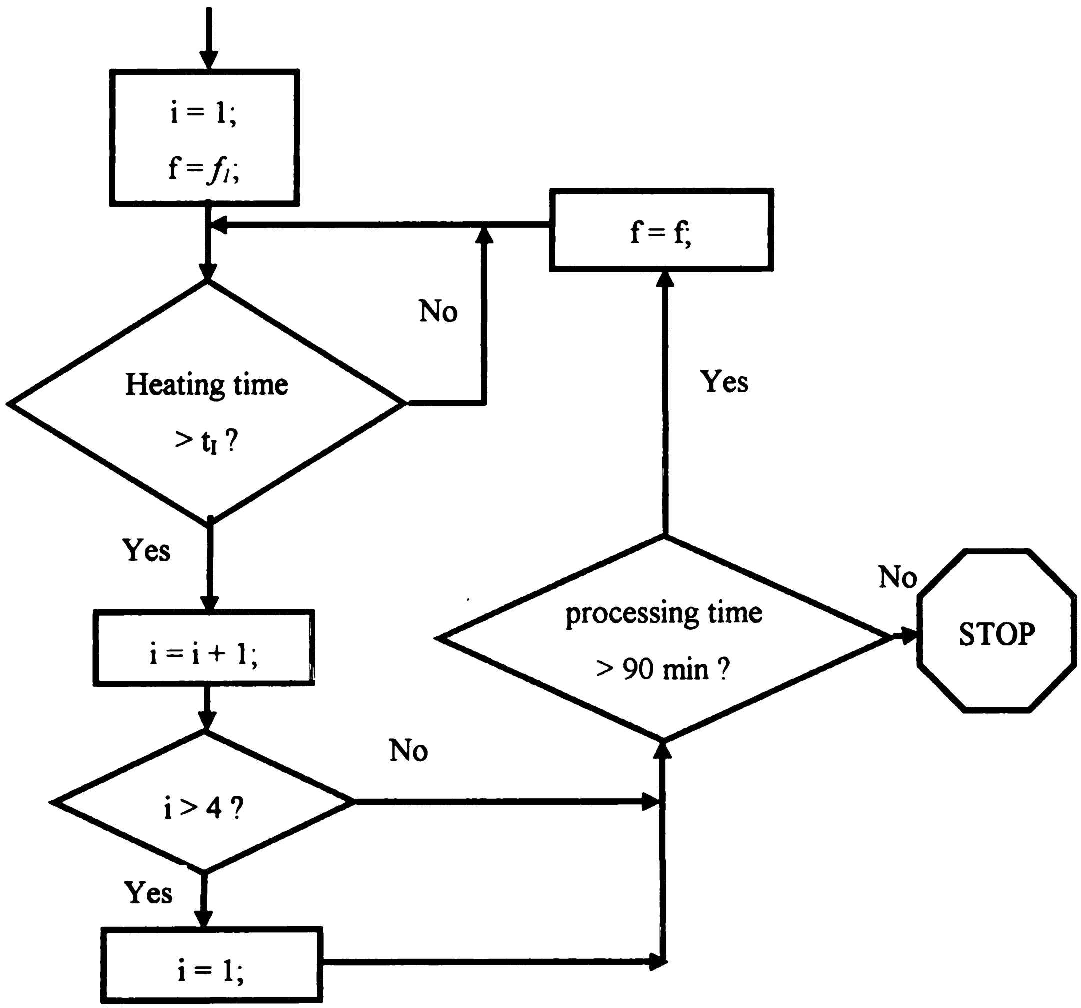

Figure 4.7 Mode Sweeping Algorithm

4.4 Control Algorithm and Program

The algorithm for mode sweeping heating is very straightforward, which is given in Figure 4.7. The computer wrote the frequency value to the HP Oscillator in a predetermined order. The frequency would remain the same for a certain period of time. Different frequencies could have different duration. The software program (modesweep.vi) was written in LabVIEW, and presented in Appendix D.

4.5 Selective Mode Sweeping Heating Results

These four modes with heating characteristics presented in Figures 4.4 and 4.5 have relatively high heating rates and complementary heating patterns. Therefore they were selected to heat the sample by discretely sweeping of the mode frequencies. During the heating, one frequency corresponding to a mode was selected at a time and remained for some time, then another frequency would be selected. The heating time for each mode and the order of the modes were programmed. Then the constructed heating cycle was used to heat the sample until the highest temperature reached 85 °C. Only the frequency was controlled by computer, by setting the value of the frequency output of the oscillator. The probe depth was fixed at 24.0 mm during the heating experiments. And the power was not controlled with a fixed dial knob position. Measurements for all four modes showed that the power output ranged from 23 Watts to 28 Watts.

The first mode sweeping heating experiment let each mode have the same heating time: 0.1 second. The order of the modes within a cycle was: mode 1, mode 2, mode 3 and mode 5. The thermal image and temperature profile, shown in Figure 4.8 and Figure 4.9 respectively, showed that the middle and lower part of the sample had higher temperature than the upper part. However, the temperature gradients shown by the temperature profiles were less than 6 °C. Since the thermal image of the first run looks similar to the heating pattern of mode 1, the residence time of mode 1 should be decreased. In the heating cycle of the second run, mode 1 had a heating time of 0.5 second in one cycle. The other ones all had 0.1 second heating time. The thermal image and temperature profile of the second run showed better uniformity of heating (Figure 4.8 and Figure 4.9). The temperature gradients were less than 3 °C when the temperature reached 85 °C, as shown in Figure 4.9.

Due to the heat loss, the edges of the sample tended to have lower temperature than that of the center. Both thermal images showed that the center temperature eventually tended to be higher than other ones when the heating is uniformly initially. This non-mechanistic temperature gradient increase affects the uniformity of the heating, and thus the properties of the product. To eliminate the heat loss, the cavity may be insulated or heated from outside using thermal method to provide a pseudo-insulating condition.

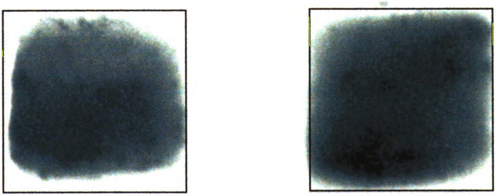

(a) Mode Sweeping Heating I **(b)** Mode Sweeping Heating II

Figure 4.8 Thermal Paper Images of Mode Sweeping Heating

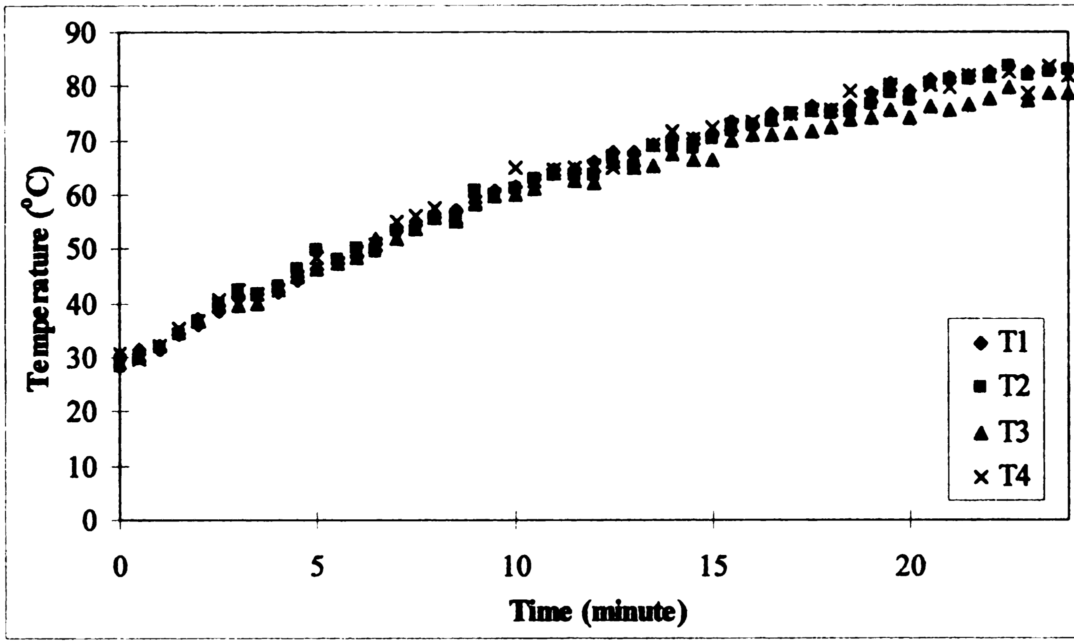

(a) Mode Sweeping Heating I

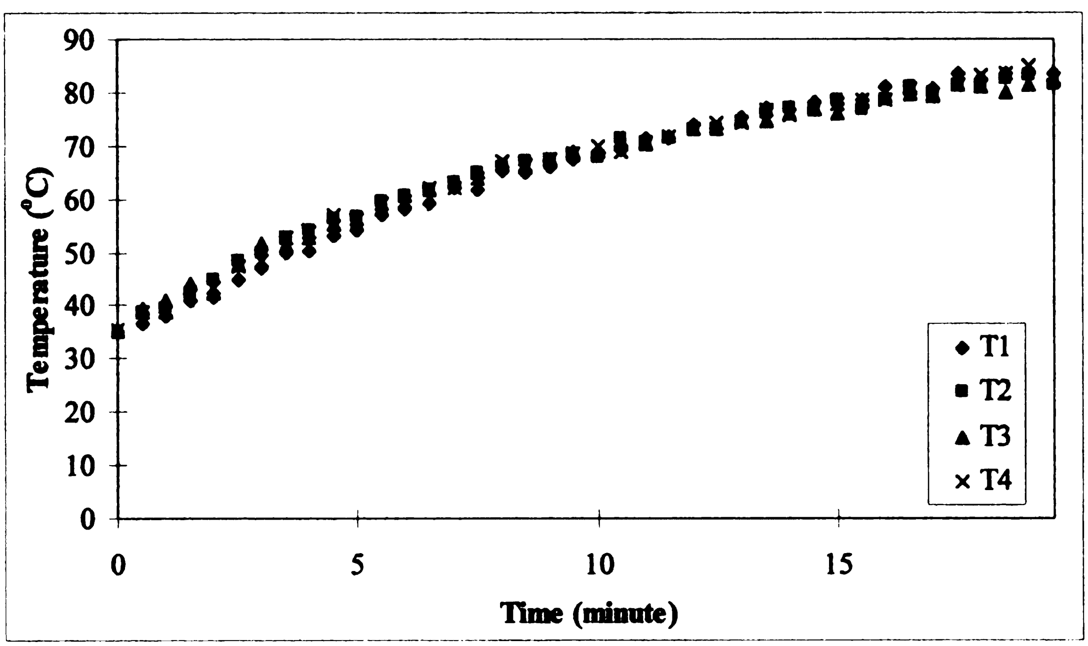

(b) Mode Sweeping Heating II

Figure 4.9 Mode Sweeping Heating Temperature Profiles

4.6 Summary and Conclusions

The experiments demonstrated that the power source consisting of an oscillator, a RF plug-in and a TWT worked well as a variable frequency power supply. This variable frequency microwave system, using a cylindrical cavity as the applicator, was able to obtained heating modes with a variety of heating patterns when graphite/epoxy material was loaded. A more uniform heating pattern resulted when two modes with complementary heating preferences were used alternatively for heating.

A mode sweeping heating technique was designed to take advantage of complementary heating concept and improve the temperature uniformity of microwave heating. Mode selection cycles were designed. In each mode selection cycle, a sequence of modes was used to heat the sample, each mode for a certain period of time. The mode selection cycle was repeated until the end of processing.

Mode sweeping method was shown to heat the 2" square graphite/epoxy composite parts not only uniformly, but also efficiently. The efficiency of mode sweeping heating lied between the highest one and the lowest one among those of the modes used. As observed in the experiments, mode sweeping with equal time intervals did not obtain optimum heating. To get even more uniform heating, the heating characteristics of each mode should be considered in the optimum heating process design. The heating uniformity of this method shows the potential to achieve uniform curing of the graphite/epoxy material of small size.

CHAPTER 5

INTELLIGENT VARIABLE FREQUENCY MODE SWITCHING PROCESSING

Intelligent mode switching processing using variable frequency microwaves is presented in this chapter. The rationale of intelligent mode switching heating is discussed. Based on the fundamental concepts of the intelligent mode switching method, a process control system was developed, which includes a mode selection controller, a mode tuning controller, and a microwave power controller. A simple parabolic power control algorithm was used to provide stable curing temperature control. Both stepper motor and variable attenuator were used to microwave power adjustment. The material processing performances using these devices are compared. Experimental results of square and V-shaped graphite/epoxy composite parts are presented. The results show the effectiveness of mode switching heating technique in reducing processing temperature gradients.

5.1 Rationale of Intelligent Mode Switching Heating

Microwave heating is instantaneous, volumetric and non-uniform in nature. Different modes have different electric field distributions, which are typically non-uniform. However, uniform heating can be obtained using combination of modes. In a multi-mode oven, the applicator is over-moded and time averaged uniform heating can be obtained by frequency sweeping. However the energy efficiency of this practice is very low, since a large portion of the time microwave energy is not critically coupled into the cavity or the material. Single-mode cavities can provide uniform heating using mode-switching method, in which several modes with complementary heating patterns are alternatively excited.

With a fixed frequency microwave power source, mode switching can only be achieved by mechanically adjusting the volume of the cavity, which is usually accomplished by moving the sliding top via a stepper motor. This mechanical process slows down the response of the system to temperature changes. Experiments showed that it took from 30 seconds to more than one minute for the cavity length to be adjusted with a satisfactory precision.

When a variable frequency power source is available, the heating modes can be changed by varying the frequency. Frequency control is available as an electronic process, in the form of digital communication between the computer and the variable frequency microwave power source. As a result of the instantaneous variable frequency mode switching, not only the speed of the process but also the controllability of the process is much improved. The use of variable frequency microwave power source also enable the control system to periodically tune the mode to make sure that microwave energy is critically coupled into the material.

With the implementation of computer control system for controlling the heating modes, the benefits of microwave heating can be fully utilized while achieving uniform processing. An automated microwave processing system with variable frequency power source and single mode cavity is presented in this chapter. The control parameters were microwave frequency and power. Heating modes with certain frequencies were characterized before processing. The computer chose the frequency that can improve the temperature uniformity the most by comparing the heating characteristics at that frequency with current temperature distribution. When the maximum temperature reaches curing temperature, microwave power was adjusted so as to keep the maximum temperature at constant.

5.2 Process Control System - VFMPCS I

The process control system for intelligent variable frequency microwave processing consists of a mode tuning controller, a mode selection controller, and a power controller. Figure 5.1 shows the configuration of the process control system. The LabVIEW program (VFMPCSI.vi) is documented in Appendix D.

The intelligent mode switching heating requires a mode selection algorithm that chooses the optimal mode to heat the sample. In addition, during the processing, it is desirable to periodically tune the frequency or mode so as to minimize the power reflectance. Moreover, when the temperature is at the curing level, the control system must be able to keep the curing temperature at the desired level. The maximum of the surface temperatures was used as the feedback for curing temperature control.

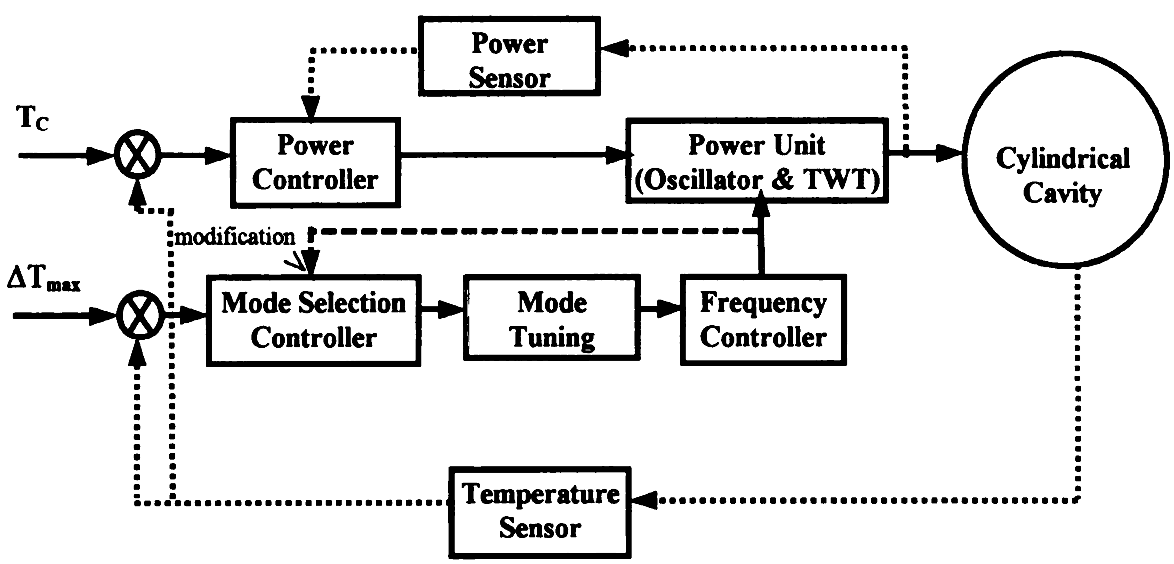

Figure 5.1 Process Control Diagram for Variable Frequency Mode Switching Heating

As seen in the diagram, the curing temperature is given as a set-point for the control system. The heating characteristics of each mode, including heating rate and heating pattern, are measured before the curing and stored in a database. When the heating is started, the temperatures are measured and the data are analyzed. If the temperature difference at different locations exceeds some value, the mode selection subprogram starts to search for another mode that has a heating pattern complementary to the current temperature distribution. The heating rate of the modes is also considered so as to obtain better energy efficiency as well. Once a mode is selected, the computer will adjust the microwave frequency and coupling probe depth to the corresponding values. Around these values, the mode tuning subprogram will tune the frequency and the probe depth, so as to minimize the reflected power. After the tuning, the frequency and probe depth values will be used to update the database. This will take into account the changes of mode locations due to the changes of the temperature and the degree of cure of the material. Also, during the heating, the heating pattern of the mode will be measured and the database will be updated. As the temperature reaches the curing temperature, the input power will be adjusted by a power controller to maintain a constant temperature.

5.2.1 Mode Tuning Controller

After the computer selects a heating mode, the frequency of this mode (f_o) will be given to the mode tuning controller. The task of the mode tuning program is to minimize the reflected power around the given frequency. The procedure is similar to that used in the mode characterization program. The difference is that the mode tuning controller searches for the mode in a small range ($f_o - \Delta f_o, f_o + \Delta f_o$). The mode tuning controller increases the frequency from (f_o - Δf_o) with an increment of Δf at each time. The input power is analyzed as a function of the frequency. If the reflected power curve reaches a minimum, the corresponding frequency will be recorded. If there are more than one minimum, the one with corresponding frequency closest to f_o will be selected. The sample will then be heated with the selected frequency.

5.2.2 Mode Selection Algorithm

Before microwave processing experiments, frequency scan was conducted from 2 GHz to 4 GHz for the cavity loaded with sample. Both input power and reflected power were measured. Power reflectance curve was obtained by plotting percentage of reflected power versus frequency. At frequencies with low power reflectance, the sample usually absorbs the microwave power significantly. Frequencies corresponding to locally minimal power reflectance are identified as frequencies of potential effective heating modes. Temperature rises were measured at six locations for each frequency. The heating rates were obtained by doing a linear fit to the temperature curves during heating-up stage. The heating rates for each mode were then normalized to between 0 and 5, using the following formula:

$$R_i' = (R_i - R_{min})/(R_{max} - R_{min}) \times 5, \ i = 1, .., m \tag{5.1}$$

Where m is the number of temperatures measured, R_i is the heat rate, R'_i is the normalized heating rate, R_{max} is the maximum heating rate, while R_{min} is the minimum.

During heating experiments, when the maximum difference between temperatures exceeds a preset limit (e.g., 10°C), the computer predicts of what the temperature profile would be like if other modes were used. Specifically, temperatures are predicted for each mode using the normalized heating rates:

$$T_i' = T_i + R_i' \times C, \ i = 1, .., m \tag{5.2}$$

where T_i' is the predicted temperature at location i. C is the time constant that can be adjusted to change the assumed heating time for the mode used for prediction. The standard deviation of the predicted temperatures will then be calculated. This will be used as the measure of temperature uniformity. The higher the standard deviation is, the less uniform the temperatures are. Therefore, the mode that produces the smallest standard deviation will be selected as the new heating mode. In essence, the controller picks a mode that will lead to most uniform temperature distribution after time *t*.

The larger C in Equation 5.2 is, the further in the future the prediction is made. For example, if the temperatures after time *t* are to be predicted, then C should be:

$$C = R_{max} \div 5 \times t \tag{5.3}$$

In our case, C had a value of 2, corresponding to a prediction about 30 seconds in advance. C can be different for heating-up stage and curing stage, because the temperature dynamics are different.

5.2.3 Power Control Algorithm

The purpose of the power control program is to maintain the maximum of the measured temperatures at the set point (the curing temperature of 160 °C). A parabolic algorithm was designed for this purpose. When the maximum of the temperatures is between the curing temperature control window, say 157 °C - 160 °C, the power output is parabolically related to the difference between the maximum temperature T and the curing temperature T:

$$P_i = (P_{\max} - P_{\min}) \times \left[\frac{T_{cure} - T}{T_{cure} - T_{low}} \right]^2 \tag{5.4}$$

where Pi is the input power, P_{max} is the set maximum power (100 Watts), P_{min} is the set minimum temperature, T is the maximum of the measured temperatures, T_{low} is the lower end of the curing temperature control window (157 °C), and T_{cure} is the curing temperature.

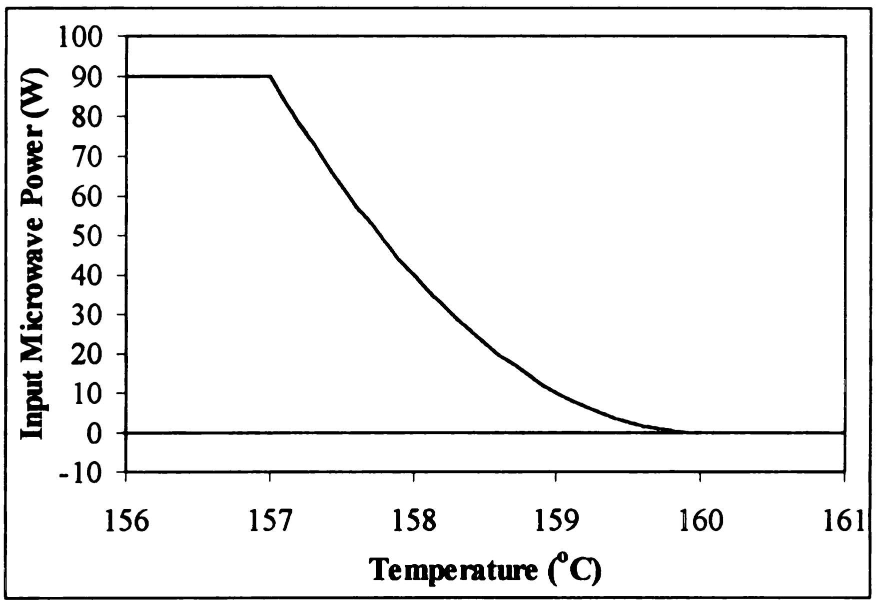

Figure 5.2 Power Temperature Relationship

If the maximum is higher than the curing temperature, then the microwave power will be turned off. If the maximum below the control window, then maximum power (100 watts) will be used. A curve representing the relationship is shown in Figure 5.2. The parabolic relationship was used because it is simple and requires no controller tuning. Also as shown in Figure 5.2, a slight change in temperature would cause more dramatic power change when the temperature is closer to 160 °C. This is desired because of two reasons. One is that when the temperature drops below 160 °C, microwave power needs to be increased quickly to prevent further drop of the temperature. The other reason is that when the temperature gets close to 160 °C, the microwave power needs to decrease quickly to prevent temperature overshoot.

5.3 Variable Frequency Microwave Processing of Square Graphite/Epoxy Composite Parts

5.3.1 Microwave Power Adjustment Using Stepper Motor

A parabolic power controller was used during the curing stage to keep the maximum surface temperature at the curing level. The microwave power control was achieved by adjusting the dial knob on the microwave power source via a stepper motor. The control algorithm and LabVIEW program are presented in Appendix B.

5.3.2 Experimental Results and Discussion

The material used was Hexel AS4-3501/6 graphite/epoxy prepreg. 24-ply unidirectional 3" by 3" parts were processed. The samples were placed in a Teflon mold and eight temperatures were measured on the sample surface. The mold was placed on the bottom of the single mode cavity with cavity length of 15 cm and coupling probe depth of 20 mm. The configurations are the same as in Figure 4.1 and Figure 4.2 in Chapter 4. Surface temperatures were measured at eight different sites on top of the sample, as shown in Figure 5.3. The sample was loaded into the cavity such that the fiber directions were perpendicular to the couple probe. During the experiments, the cavity length was fixed at 15 cm and the couple probe depth fixed at 20 mm.

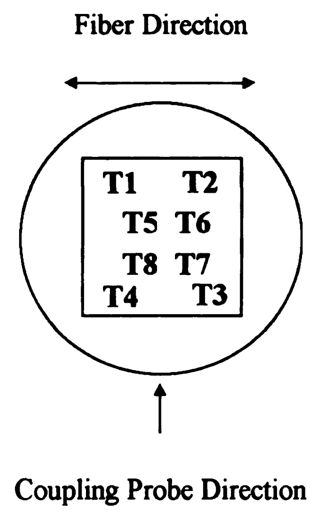

Figure 5.3 Temperature Measurement Locations

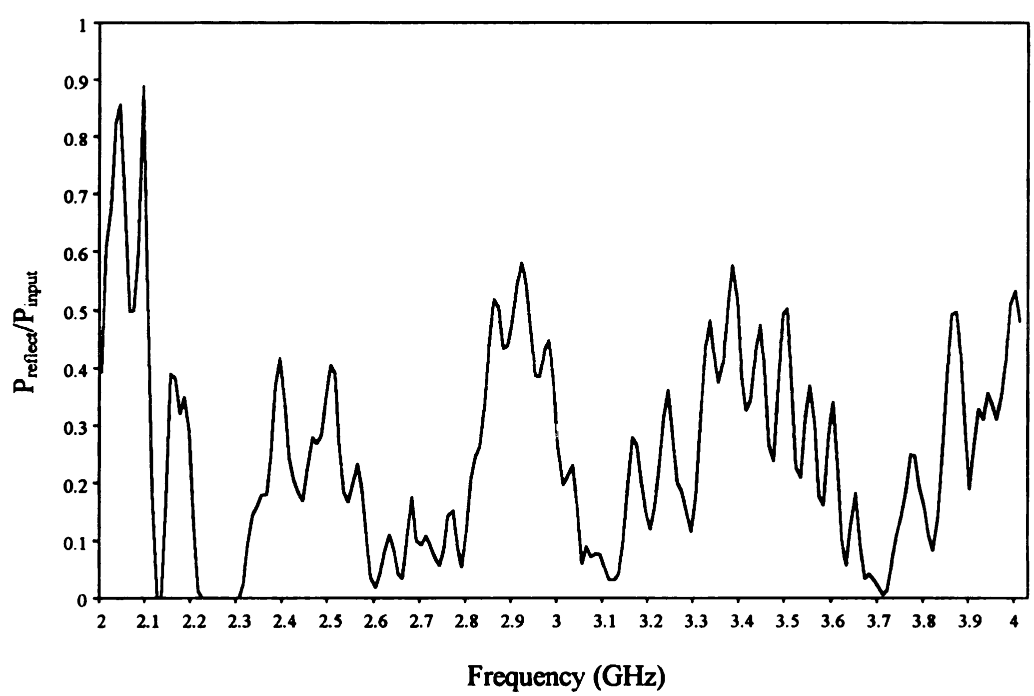

Figure 5.4 Percentage of Reflected Power versus Frequency

Before the curing studies, a scan of percentage of reflected power versus frequency was obtained by sweeping the frequency from 2 to 4 GHz with the sample inside the cavity (Figure 5.4). The frequencies at troughs with low percentages of reflected power usually correspond to heating modes, which can heat the sample rather significantly. Single mode heating experiments were performed at these frequencies.

The maximum of the measured temperatures was controlled as the curing temperature at curing stage. A description of the control program is given in Appendix D. Most of the modes demonstrated large thermal gradients, usually more than 40 degrees when the maximum temperature is at 100 °C. As the heating went on at the curing stage, the thermal gradients were slightly reduced due to thermal conduction. There was only one mode that showed relatively uniform heating. The difference of the temperatures was within 20 °C at the curing stage. However, thermal gradients exceeded 30 °C during the heating up stage. The heating profiles of a typical non-uniform heating mode and the rare uniform heating mode are presented in Figures 5.5 and 5.6, respectively. As seen in Figure 5.5, even after 90 minutes of heating, the thermal gradients were still large and the heating profile was still demonstrative of heating preference. Although the Teflon mold has low thermal conductivity, the heat loss from the sample to the ambient was significant due to large temperature difference (120 °C). To compensate for the heat loss, the sample needed to absorb necessary amount of microwave energy. Since microwave heating was uneven at that particular mode, the heating preference was preserved in the temperature profile throughout the heating experiment.

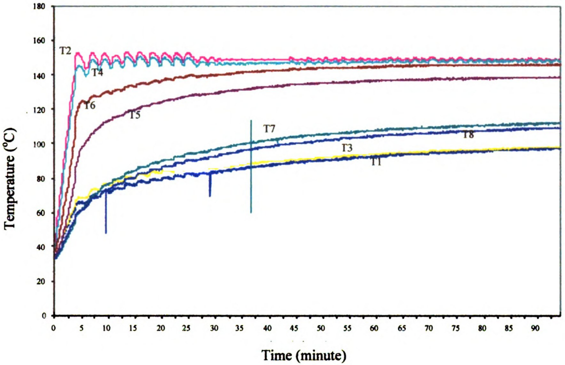

Figure 5.5 Single Mode Heating at f=2.5737 GHz

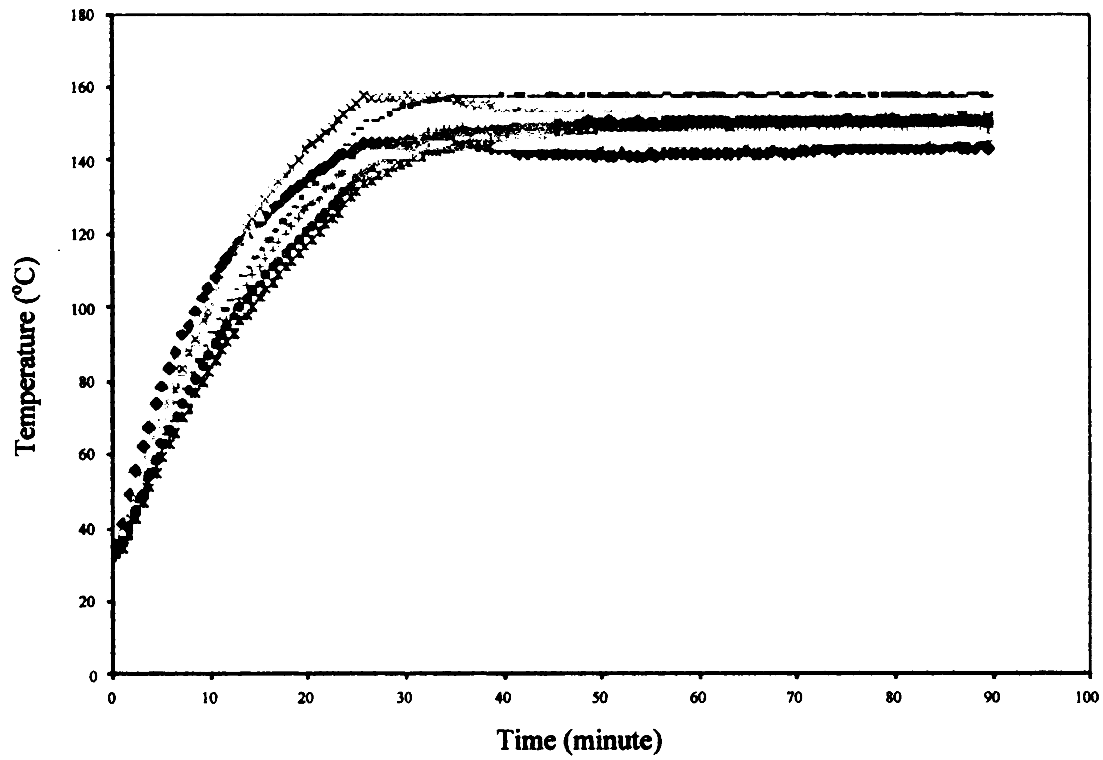

Figure 5.6 Single Mode Heating of 3" Square Sample - f = 3.0818 GHz

Six heating modes were selected for the mode switching heating experiment. The criteria of selection were the complimentariliness of the temperature profiles and the heating efficiency. The frequencies of the modes are given in Table 5.1. The temperature profiles of the variable frequency mode switching heating are presented in Figure 5.7. As can be seen, thermal gradients were significantly reduced compared with single mode heating. The temperatures were controlled to be within a window of 15 degrees throughout the processing. However, the temperature profiles were less stable due to the combination of mode switching and power control. The change of modes selected during the processing is illustrated in Figure 5.8. The six modes were quite evenly used during the

processing except for mode 5. The power adjustment is illustrated in Figure 5.9, which is rather sporadic. As shown in the single mode heating profile, the parabolic power controller performed reasonably well. However, during the mode switching heating, since the heating rates of the modes were different, which introduced fluctuations into the curing temperature control. Since the power control was actuated by mechanical movement of the stepper motor, the adjustment steps were slow and coarse. The less satisfactory performance of the power controller for mode switching heating was due to both the control algorithm and the control actuator.

Table 5.1 Frequencies of the Modes Used in the Mode Switching Heating

Modes	0	1	2	3	4	5
Frequency (GHz)	2.5772	2.7065	3.1009	3.1643	3.4415	3.6409

Since the heating characteristics of the modes were determined before the processing, the success of mode switching technique in alleviating thermal gradients proved that the heating characteristics are repetitive. The effectiveness of power control algorithm can be seen from single mode heating profiles.

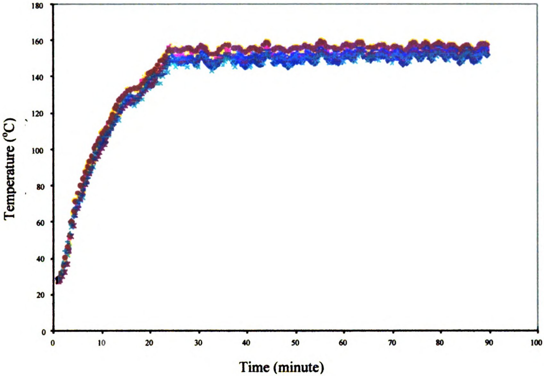

Figure 5.7 Mode Switching Heating of 3" Square Sample

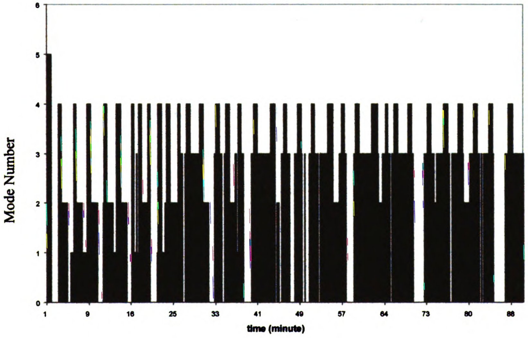

Figure 5.8 Mode Selection Histogram during Mode Switching Heating

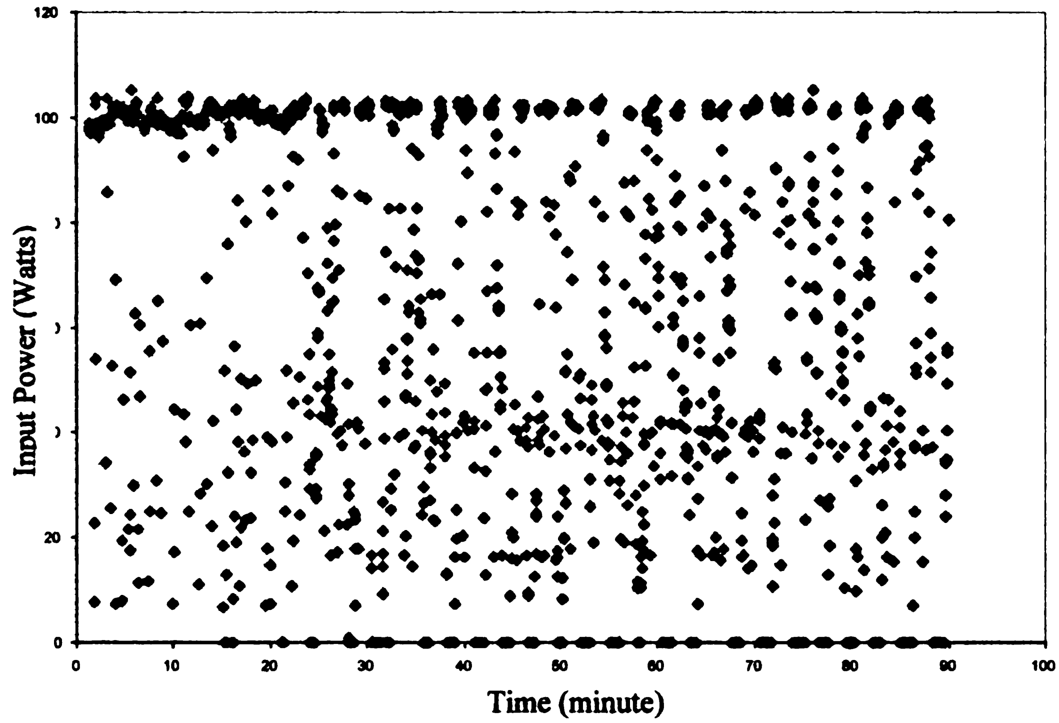

Figure 5.9 Input Power Change during Mode Switching Heating

5.4 Variable Frequency Microwave Processing of V-shaped Graphite/Epoxy Composite Parts

5.4.1 Microwave Power Adjustment Using Variable Attenuator

In order to improve the power controller performance, a new approach to microwave power control actuation was developed using a variable attenuator, the characteristics of which are presented in Chapter 3. The variable attenuator is connected between the HP Oscillator and the variable frequency microwave power amplifier. The attenuation can be changed via voltage control, by which the microwave power is controlled.

Compared with using a stepper motor to adjust the dial knob on the microwave power source so as to vary the amplification rate, the use of a variable attenuator provides much faster microwave power adjustment. An experimental comparison was conducted, in which the times used by the stepper motor and the variable attenuator to adjust to a new power level were measured and plotted in Figure 5.10. The initial microwave power was set at 50 watts, and the desired microwave power was from 10 watts to 90 watts. As shown in Figure 5.10, the larger the power change, the longer it took the stepper motor to adjust, while the adjustment time using a variable attenuator stayed pretty much the same. For example, when the power change was 20 watts, it took the stepper motor 4 seconds to adjust to the desired power level, and about 1 second using the variable attenuator.

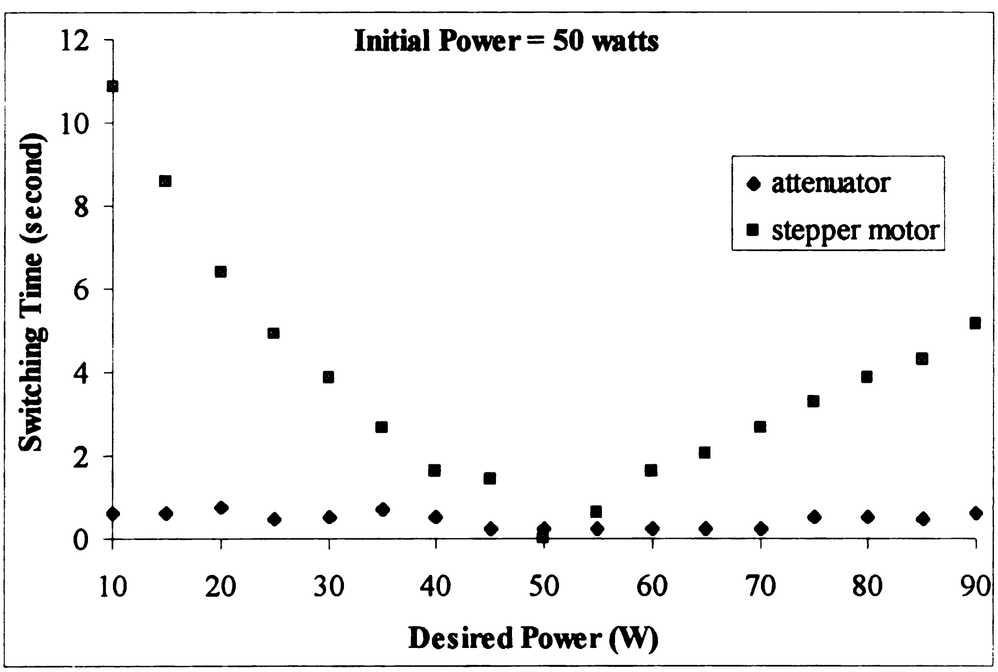

Figure 5.10 Comparison of Power Control Performance between Variable Attenuator and Stepper Motor

5.4.2 *Experimental Results and Discussion*

The variable frequency mode switching process control system was used to process V-shaped graphite/epoxy composite parts. The same material (Hexel AS4-3501/6 continuous graphite/epoxy prepreg) as used for square sample was used. Prepregs were cut into 3 inch by 3 inch pieces. Twenty-four of them were laid up uni-directionally to give a sample thickness about 0.17 inches (4.3 mm). The panels were bent to form a V-shape and placed in a Teflon mold, as shown in Figure 5.11. Temperatures were measured using fluoroptic temperature probes at six locations, the numbering of which is shown in Figure 5.12. The fluoroptic temperature probes are transparent to microwave. Thus the probes do not interfere with the electromagnetic fields and do not heat up under the microwave radiation during the experiments.

The Teflon mold with the sample was loaded into the cavity such that the fiber direction was perpendicular to the microwave coupling probe. It was determined by experiments that this was the optimal orientation, with efficient heating and diverse heating profiles. A power reflectance curve was obtained for loaded cavity and presented in Figure 5.13. In the next step, the sample was heated using the frequencies at which low power reflectance was observed. Temperature profiles were measured to obtain the heating characteristics of each mode.

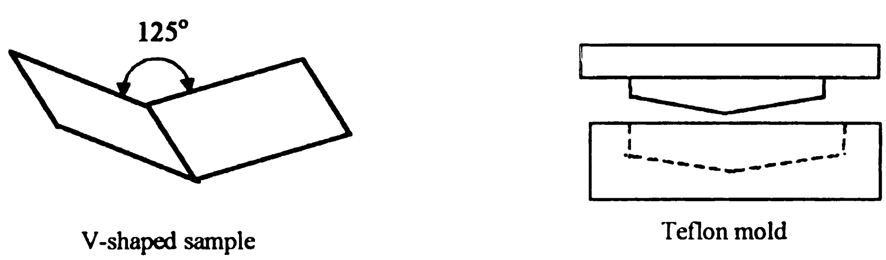

Figure 5.11 V-shaped Sample and Teflon Mold Configurations

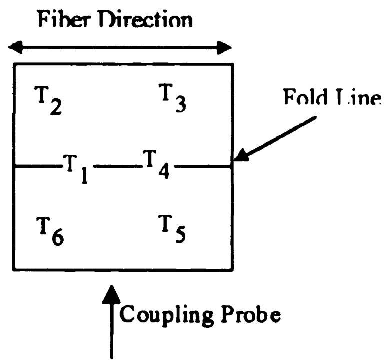

Figure 5.12 Temperature Measurement Configuration

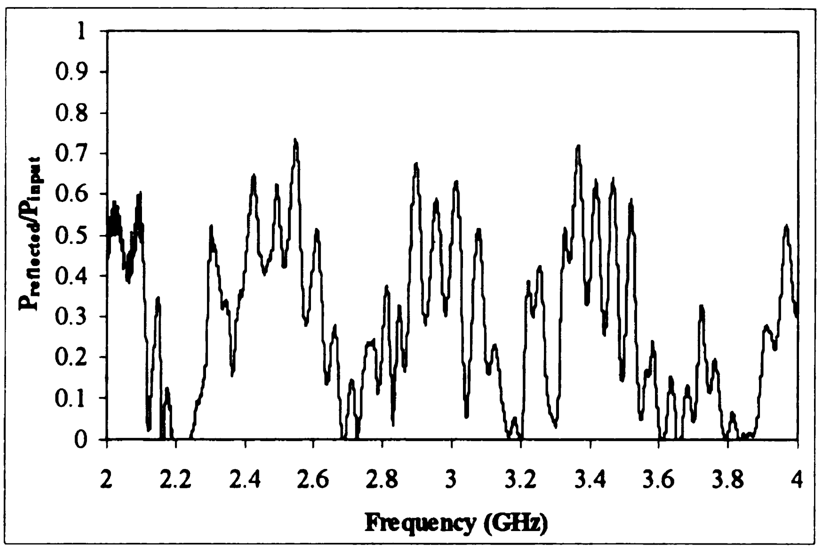

Figure 5.13 Power Reflectance versus Frequency

During the frequency scan, the temperatures were also monitored (Figure 5.14). With this measurement, one can see whether there are modes that heat different regions of the sample. As shown in Figure 5.14, the overall heating effect was quite uniform. Most temperatures had ups and downs during the frequency scan, which indicated that there were modes with different heating preference. Using this approach, one can monitor temperature changes over the frequency range for different sample loading positions and determine the optimal position that will give diverse heating patterns. The more diverse heating patterns are, the more uniform heating can be achieved by mode switching heating.

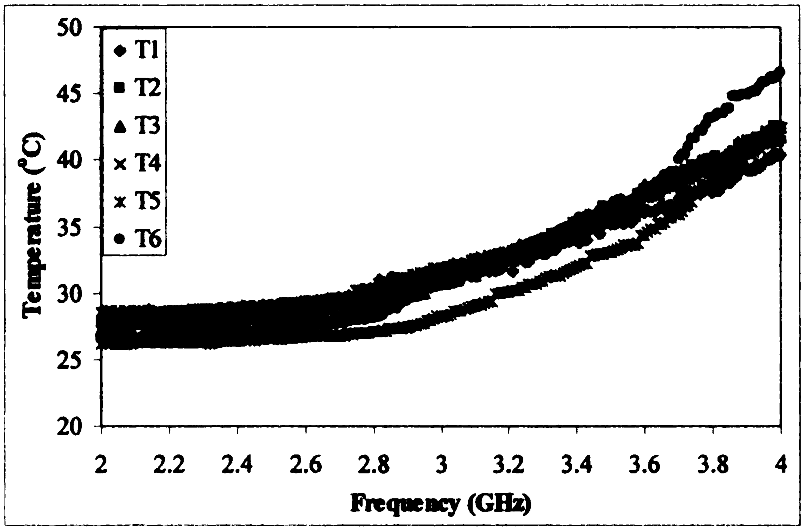

Figure 5.14 Temperature Change during Frequency Scan

The heating characteristics of the heating modes were analyzed and six modes that had complementary heating patterns were selected for mode switching heating. The heating profiles of the modes are given in Figure 5.15. As shown in Figure 5.15, single mode heating was quite uneven. Since the cold spots for some modes were hot spots for others, uniform heating was obtainable by combining the heating effects of these modes. Single mode processing was conducted with frequency at 3.6506 GHz (Figure 5.16). This was the most uniform modes among the available ones. The largest temperature gradient during processing was about 45°C. The temperature gradient decreased slightly as the

as the curing proceeds. This was because of heat conduction from center to cold spots along the edges.

Mode switching heating was conducted using a curing temperature control window of 155°C - 160°C, as described in power control algorithm. The temperature profiles were much more uniform compared with single mode heating, especially during the heating stage (Figure 5.17). At the curing stage, the edge temperatures were always lower than the center temperatures due to two reasons. One was the heat loss at the edges. The other was that the modes that heated the edges preferentially also heated the center somewhat. Because the maximum temperature must not exceed the curing temperature, the input power at curing stage was low, this further reduced the effectiveness of edge heating modes. A second mode switching heating experiment was conducted with a curing temperature control window of 157°C - 160°C. By narrowing the control window, the average input power increased and the difference between center and edge temperatures was reduced by about 15% (Figure 5.18).

The heating uniformity during the heating-up stage demonstrated the effectiveness of mode selection controller. The stability of the maximum temperature during the curing stage showed that the power controller was successful in maintaining a constant curing temperature. The curing temperature control was much more stable than using a stepper motor. The power variation during the processing also showed much smaller fluctuations than in the case of using a stepper motor. By narrowing the control window, the accuracy of temperature control can be improved as well as uniformity if heating of the edges was difficult. On the other hand, over-narrowing of the control window decreases the control system stability. Since control actions are stronger when control window is smaller, temperature fluctuations would be more pronounced which could result in severe temperature overshoot.

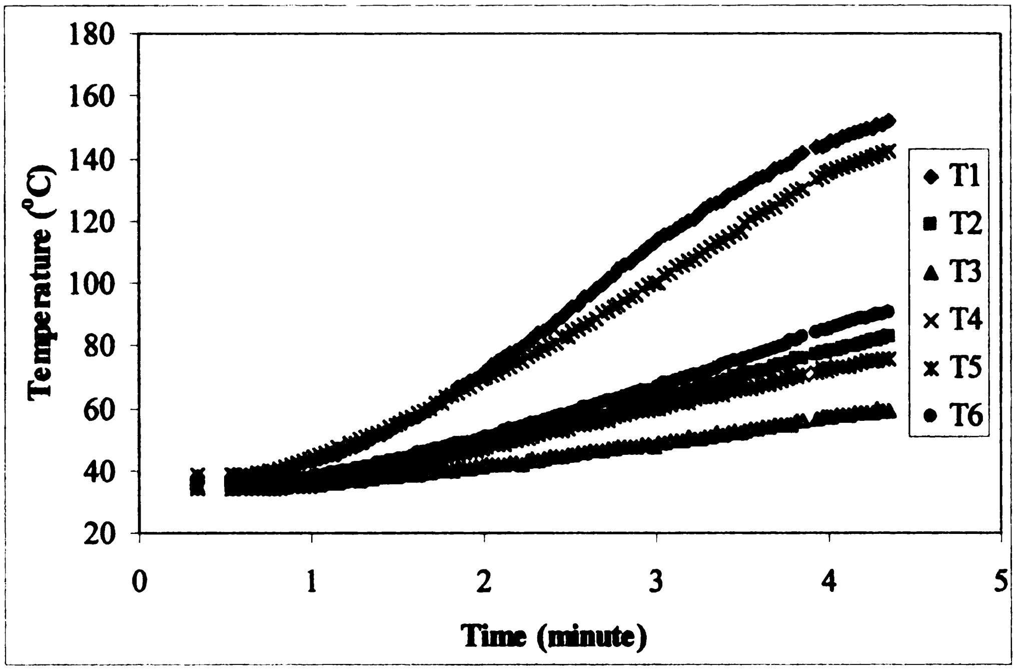

(a) Mode 0: f = 2.1605 GHz

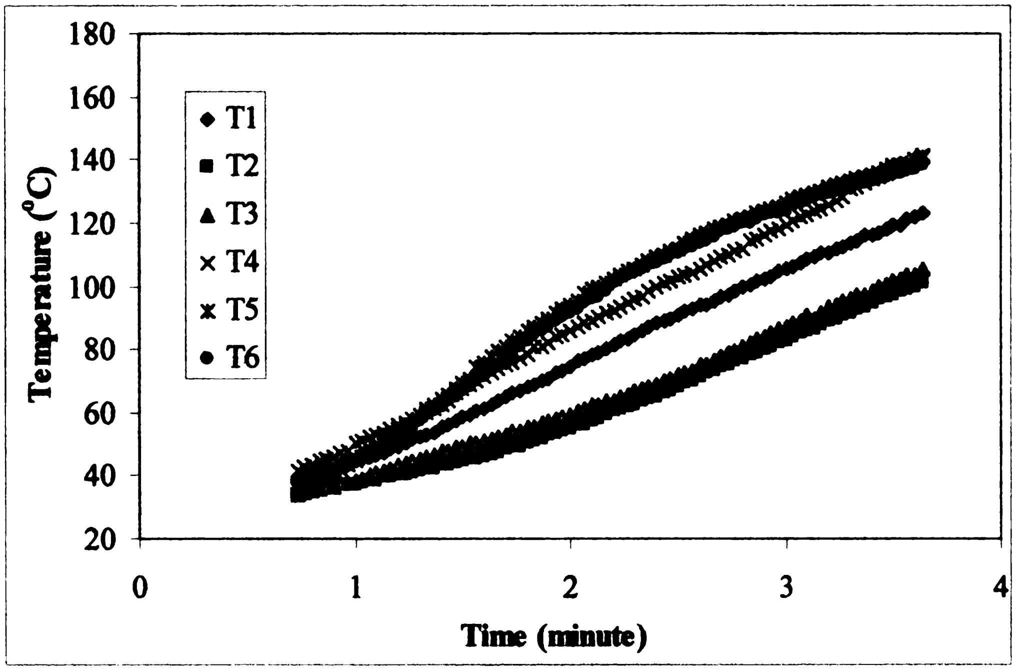

(b) Mode 1: f = 2.7243 GHz

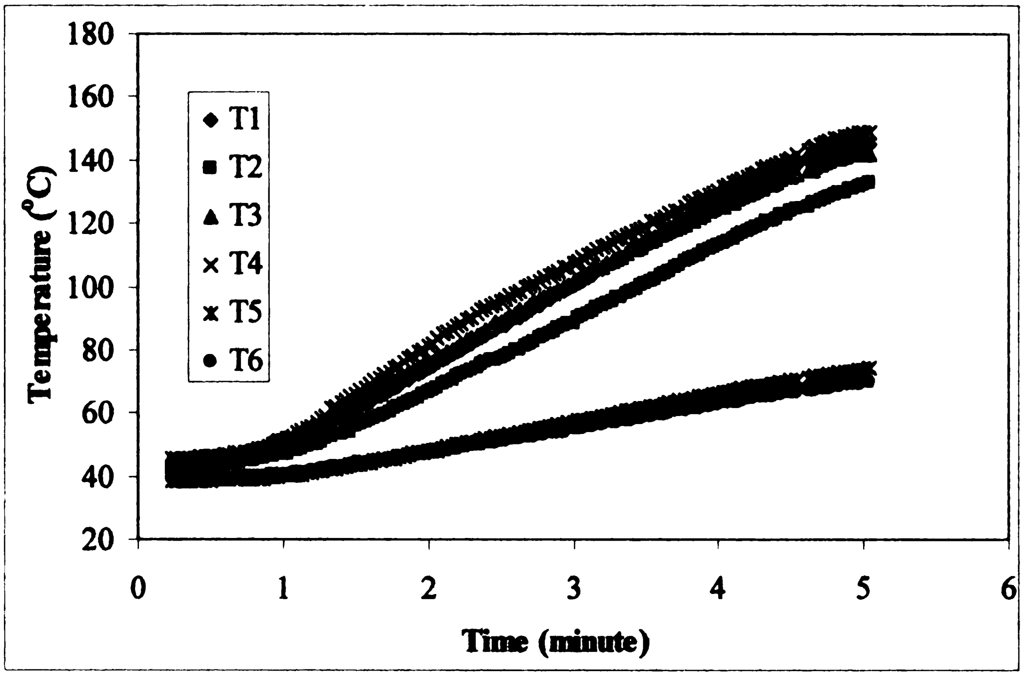

(c) Mode 2: f = 3.1610 GHz

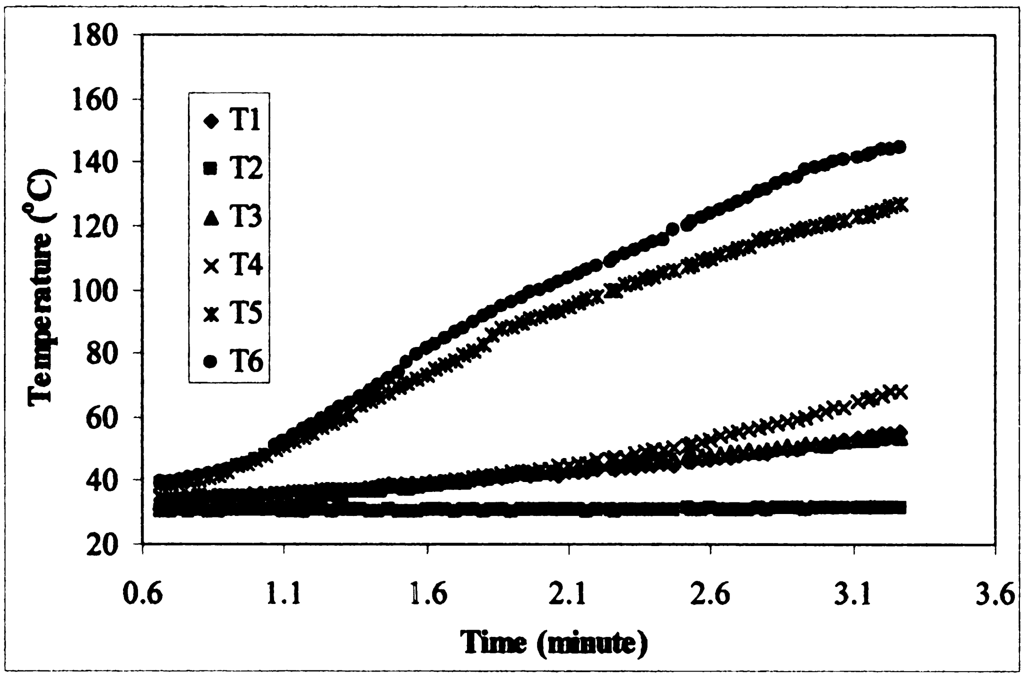

(d) Mode 3: f = 3.5420 GHz

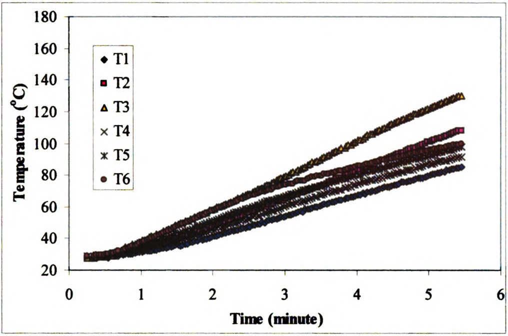

(e) Mode 4: f = 3.6506 GHz

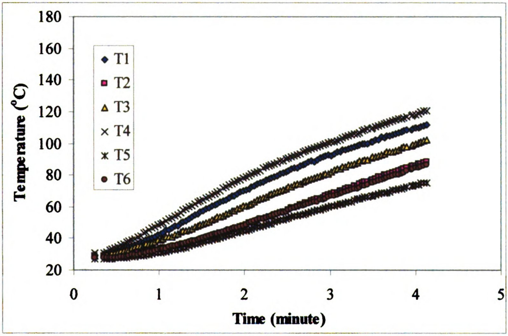

(f) Mode 5: f = 3.7911 GHz

Figure 5.15 Temperature Profiles of Single Mode Heating

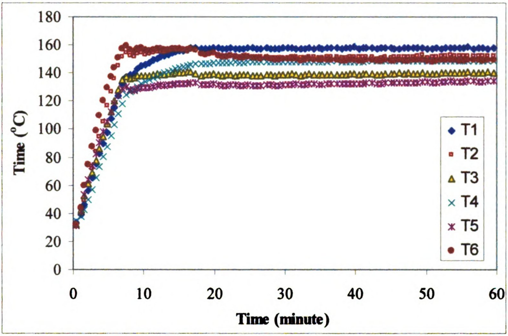

Figure 5.16 Single Mode Heating at f = 3.6506 GHz

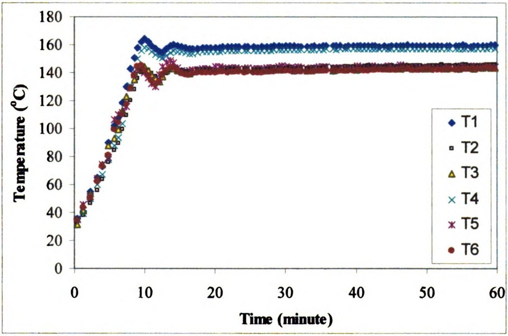

(a) Temperature Profiles

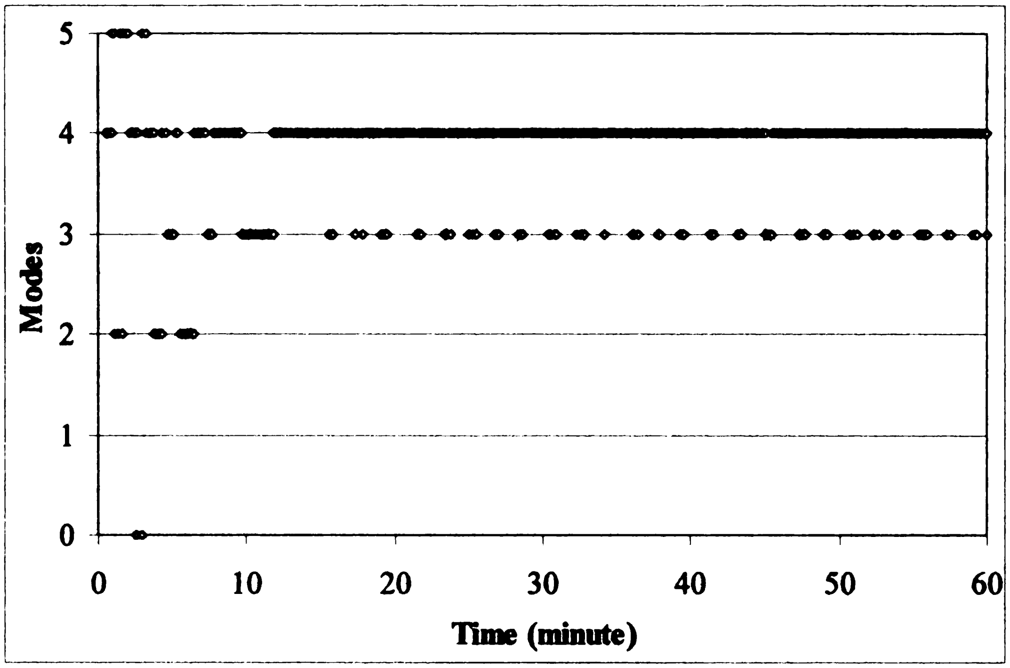

(b) Mode Selection Histogram

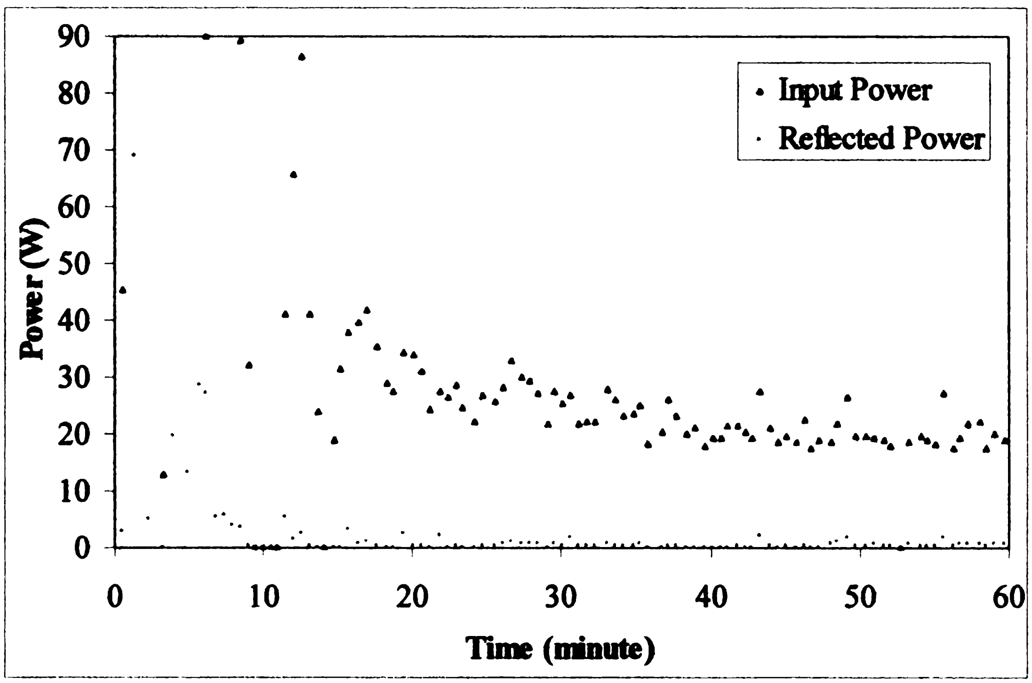

(c) Power Variation During the Processing

Figure 5.17 Mode Switching Heating 1 with Curing Temperature Control Window:

155°C - 160°C

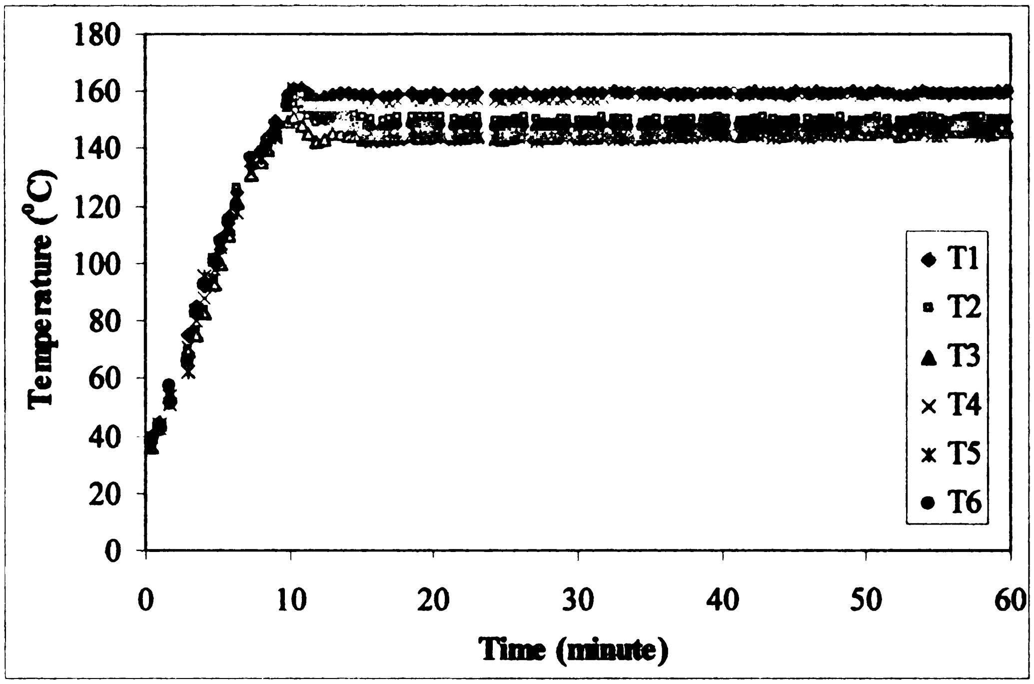

(a) Temperature Profiles

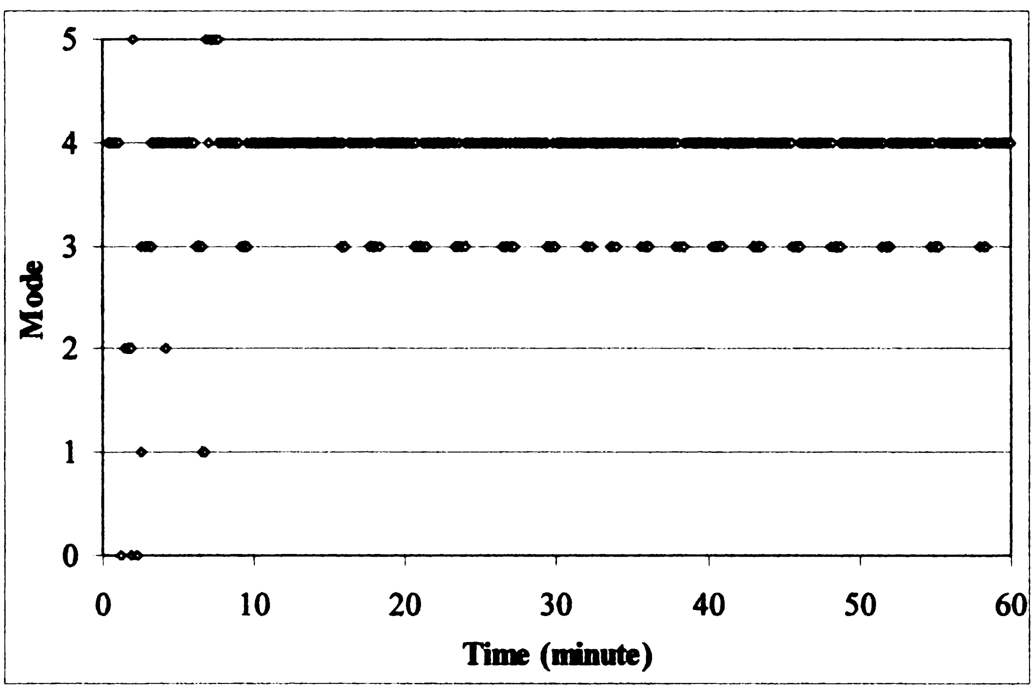

(b) Mode Selection Histogram

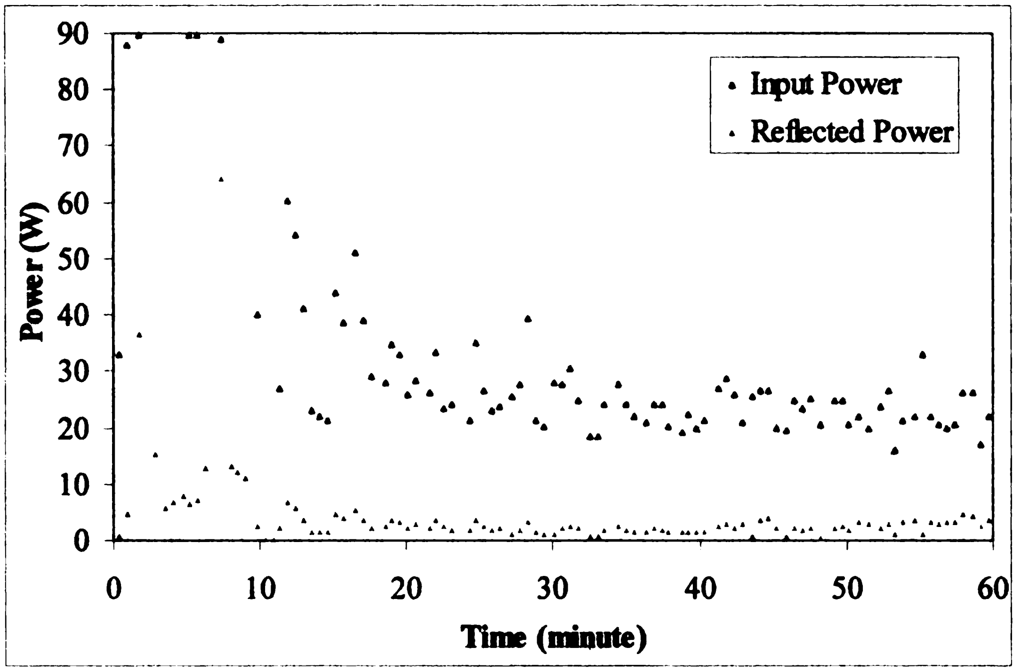

(c) Power Variation During Processing

Figure 5.18 Mode Switching Heating 2 with Curing Temperature Control Window:

157°C - 160°C

5.5 Summary and Conclusions

In variable frequency mode switching heating, processing cycles were designed based on the mode heating patterns only. However, during the processing of composites, the temperature distribution varies. Different temperature distributions call for mode with different heating preferences. An intelligent variable frequency mode switching technique was designed and developed in LabVIEW (VFMPCSI) to match mode characteristics with sample temperature distribution when selecting the heating mode.

The control system predicts the temperatures using the mode heating rates and the measured temperature distribution. The mode that will result in the smallest standard deviation of the predicted temperatures is selected for heating. A stepper motor was used to adjust the manual knob on the microwave power source. A parabolic power control algorithm was designed for simple microwave power control that did not require controller tuning. The power control algorithm was proved to be effective and stable. However fluctuations occurred during mode switching heating due to the different mode characteristics and the coarse and slow adjustment of the stepper motor for microwave power control. 24-ply unidirectional 3" by 3" graphite/epoxy composite parts were successfully processed using the intelligent variable frequency mode switching technique. Heating experiments proved that the heating characteristics of each mode was repetitive as long as the sample was loaded in the same way.

Variable frequency mode switching technique was also employed to significantly improve the heating uniformity of microwave processing of V-shaped graphite/epoxy panels. A different microwave power control hardware - variable attenuator, was used. The power adjustment time for the variable attenuator was much smaller than that of the stepper motor. The adjustment time using variable attenuator was less than 1 second, while the adjusment time for stepper motor ranged from 1 second to more than 10 seconds depending on the power change size.

CHAPTER 6

VARIABLE FREQUENCY MICROWAVE PROCESSING OF COMPLEX SHAPE COMPOSITE PARTS WITH ON-LINE MODE UPDATING

In this chapter, an on-line mode heating characteristics updating algorithm is presented. On-line mode updating ensures that the mode selection controller uses the accurate information about the mode heating characteristics when selecting the optimal mode to achieve uniform heating. The mode selection controller is upgraded to make more accurate comparison of the abilities of the heating modes to alleviate temperature gradients. A multi-staged PID controller was designed to provide more stable and precise curing temperature control. Complex shaped graphite/epoxy composite parts were processed using the process control system with on-line mode updating (VFMPCS II).

6.1 On-line Updating of Mode Heating Characteristics

For mode switching heating technique, the computer always tries to find a mode, when necessary, that will heat the sample most uniformly. To do so, the computer needs the information about the heating characteristics, i.e. heating preferences, so that it can predict how the temperature distribution will change if the mode is used to heat the sample. In order for the mode selection controller to be effective, the information about the mode heating characteristics must be accurate.

Mode heating preferences are characterized before processing experiments, as discussed in previous chapters. The heating rates at the temperature measurement sites during the heating-up stage are computed and stored in the computer. This information can be used for subsequent processing experiments as long as the sample material, configuration and loading position, and the cavity settings are the same. Obviously, these measured heating rates are only approximate representation of the mode heating preference, which varies with different batches of samples. In addition, mode heating characteristics or preferences change during the processing, not only because of the change of temperature distribution, but also because of material property changes during the processing, such as extent of cure, dielectric properties, and thermal properties. It is impossible to characterize exactly how each mode heats at certain stage of the processing. However, by on-line measuring the mode heating characteristics, the accuracy of mode heating preference information can be improved. This updating of mode heating characteristics can be carried out by computing the heating rates at each temperature measurement site for the mode that is being used.

6.2 Process Control System - VFMPCS II

The VFMPCS II process control system is consisted of a mode tuning controller, a mode selection controller, a multi-staged PID microwave power controller, and an on-line mode characteristics updating controller. The algorithms of these controllers are discussed in the following sections. The LabVIEW program (VFMPCS.vi) for the control system is documented in Appendix D.

6.2.1 Mode Tuning Controller

The mode tuning controller has the same algorithm as the one described in Chapter 5. The purpose of mode tuning is to minimize the power reflectance around the given mode frequency. Mode frequencies were determined by locating the valleys of the power reflectance versus frequency curve. The shape of the power reflectance versus frequency curve depends on the material dielectric properties. Since material dielectric properties change during processing, so do the valleys of the power reflectance versus frequency curve. Therefore, mode tuning can track the shift of the mode frequencies and make sure that the coupling between the microwave power and the sample is maximum. Mode tuning is carried out every time the heating mode is changed or the frequency is changed. After mode tuning, the tuned frequency will be used as the new frequency for the selected mode.

6.2.2 Mode Selection Controller

As similar in the mode selection controller in VFMPCS I described in Chapter 5, the standard deviation of the temperatures is used as the measure of temperature uniformity. The smaller the standard deviation, the more uniform the temperature distribution. The heating modes are characterized by the heating rates at the temperature measurement sites: dT_1/dt, ..., dT_6/dt; with $[dT/dt]$ = °C/second. For mode m (m = 0 to maximum number of modes), the heating characteristics are: $(dT_1/dt)_m$, …, $(dT_6/dt)_m$. The temperatures are measured during the processing: T_1, ... , T_6. The process controller assumes that mode m is used for heating and predicts what the temperature distribution will be after a series of time intervals: $T_1 + (dT_1/dt)_m \times n \times \Delta t$, ... , $T_6 + (dT_6/dt)_m \times n \times \Delta t$; where Δt is the time interval (e.g. 6 seconds), and n = 1,2,…, are the prediction steps (e.g. n = 1,2,…, 30). In other words, the process controller predicts how the mode will heat the sample every Δt (seconds), up to $\Delta t \times \max\{n\}$ (seconds) after the mode is used.

The process controller then computes the standard deviation of the temperatures at each prediction step:

$$\sigma_n = \sqrt{\frac{\sum_{i=1}^{6}\left[\left(T_i + \left(\frac{dT_i}{dt}\right)\times n\times\Delta t\right) - \overline{\left(T + \left(\frac{dT}{dt}\right)\times n\times\Delta t\right)}\right]^2}{6}} \tag{6.1}$$

where $\overline{\left(T + \left(\frac{dT}{dt}\right)\times n\times\Delta t\right)}$ is the average of the predicted temperatures. The minimum of all the standard deviations is then determined - σ^m, which is indicative of the ability of the mode to alleviate or aggravate the temperature gradients. After the same computation is carried out for each mode m, σ^m of all the modes are compared (m = 0, 1, ...). The mode with the smallest σ^m is considered as the best mode that will achieve most uniform heating after certain amount of time. Suppose $\sigma^k = \min_m \{\sigma^m\}$, then mode k is selected for heating the sample.

6.2.3 Multi-staged PID Microwave Power Controller

A multi-staged PID controller was developed for variable frequency microwave processing in order to achieve optimal processing. The processing of materials can be viewed as composed of different stages. The first stage is the beginning of the processing, when the microwave input power needs to be at maximum so as to heat the sample as fast as possible. When the sample temperature approaches the curing temperature, the control system should be able to slow down the heating appropriately to prevent temperature overshoot. At the curing stage, the microwave power should be just enough to maintain the curing temperature. Accordingly, the power controller needs to have different parameters at different stages. Microwave Processing of composite parts was divided into four stages as shown in Figure 6.1.

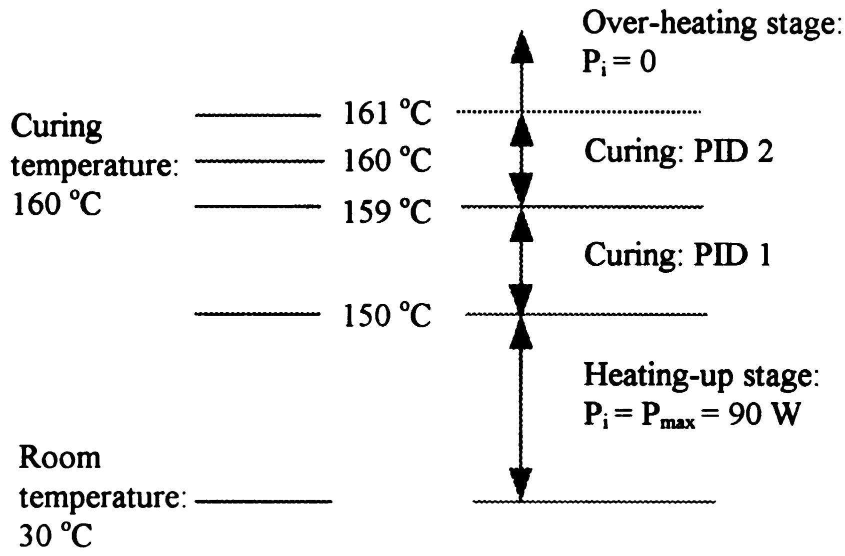

Figure 6.1 Multi-Staged PID Control

The maximum measured temperature is used to identify which stage the processing is in. The first stage is the heating-up stage, when the maximum surface temperature is well below the curing temperature and the maximum microwave is used to heat the sample as fast as possible. The maximum microwave power used in the experiments was 90 watts. The curing stage is defined as the temperature range from 10 °C below the curing temperature to 1 °C above the curing temperature. The curing stage is further divided into two stages. The curing stage I is between 150 °C and 159 °C, while the curing stage II is between 159 °C and 161 °C. In the curing stages, PID algorithm is used for microwave power control. Two sets of PID control parameters correspond to the two curing stages, (K_p1, T_i1, T_d1) and (K_p2, T_i2, T_d2). When the maximum surface temperature goes above 161 °C, the microwave power will be shut down.

Two different sets of PID parameters are used because in the two curing stages the temperature increasing rates are different, so are the process dynamics. In curing stage I, the heating rates and input microwave are still high, thus quick response of the controller is needed. In curing stage II, the temperatures are stabilizing, especially the controlled temperature - maximum measured temperature. The input microwave power also approaches to a steady level. Therefore, the control response need not be as quick. However, control accuracy becomes a more important issue. Generally speaking, $K_p1 > K_p2$, $T_i1 > T_i2$, and $T_d1 < T_d2$. Experiments were conducted to determine optimal values of the control parameters. The following are used for the PID control in the experiments:

$$K_p1 = 50,\ T_i1 = 1000,\ T_d1 = 10 \tag{6.2}$$

$$K_p2 = 20,\ T_i2 = 50,\ T_d2 = 30 \tag{6.3}$$

6.2.4 On-line Mode Characteristics Updating Controller

On-line mode characteristics updating is the measurement of heating rates for the modes during processing. It is necessary for mode selection controller to be successful. In order to filter out the temperature measurement errors, the controller computes the heating rates after the selected mode heats the sample for a certain period of time. Twenty seconds was used in the experiments. The controller throws away the first few temperature data, since there is time delay for the heating effects of the selected mode to show in the measured temperatures. In the processing experiments, the controller uses the temperature data during the last 15 seconds to compute the heating rates using linear fit. The heating rates are then stored as the heating characteristics of the particular mode.

6.3 Variable Frequency Microwave Processing of V-shaped Graphite/Epoxy Composite Parts with On-line Mode Updating

The same material, sample configuration, and loading position as the V-shaped part processing in Chapter 5 were used. The temperature measurement configuration is different from that described in Chapter 5, as shown in Figure 6.2.

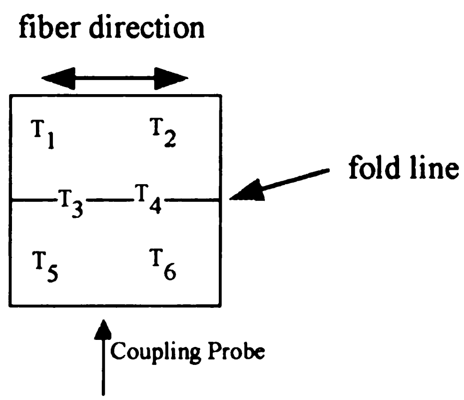

Figure 6.2 Temperature Measurement Configuration

6.3.1 Heating Modes and Their Characteristics

The same heating modes were used for the experiments, as in the experiments described in Chapter 5. The heating characteristics are described in Chapter 5. Complementary heating patterns can be found in the heating characteristics of these modes.

6.3.2 Mode Switching Heating Results and Discussion

The experimental results of variable microwave mode switching processing of V-shaped graphite/epoxy composite parts using VFMPCS II are presented in Figure 6.3. As shown by the temperature profiles, the temperature gradients are significantly reduced throughout the processing experiment. The final maximum temperature difference was only 15 °C. During the curing stage, T_3 and T_4 remained high because they were close to the center of the sample. Usually, the center of the sample would have higher temperature during the curing stage because of the temperature gradient created by the heat loss from the sample to its surroundings.

The microwave power control stabilized the maximum temperature at the curing temperature rather fast without much temperature overshoot. The temperature was less than 1 °C. At the beginning of the curing stage, there were some fluctuations of the temperatures. Those were due to the change of heating modes and the fact that microwave power level was not stabilized yet. The performance of the power controller was stable and accurate at the curing stage. The average microwave power kept decreasing, as seen in Figure 6.3 (c), and approached to a steady value at about 20 watts at the end of processing. The decrease of average input microwave power could be a result of the increase of ambient temperature, which reduced the heat loss from the sample.

From Figure 6.3 (a), it is shown that all modes were utilized at the heating-up stage. However, only three modes - 3, 4, and 5, were used at the curing stage. Modes 4 and 5 saw the most action, which indicates that modes 4 and 5 heated the edges of the sample more.

Mode sweeping heating was also conducted for V-shaped graphite/epoxy composite samples, following the procedure described in Chapter 4. The heating times in a cycle for mode 0 and 1 were 10 seconds, and 20 seconds for the rest of the modes. Modes 0 and 1 had less heating times because they had slower heating rates or lower energy efficiency. The results are presented in Figure 6.4. The temperature profiles in Figure 6.4

(a) shows that T_3 and T_4 are again high at the curing stage. The temperature gradients actually increased at the beginning of the curing stage. The reason was the heat loss from the sample to its surroundings. As the heating progressed, the ambient temperature increased and temperature gradients decreased. The power variation during the processing is presented in Figure 6.4 (b). The microwave power level was more sporadic as in mode switching heating because of the frequent change of modes. Each time the mode (i.e. the frequency) is changed, the microwave power had to be tuned down first in order to prevent a microwave power source fault. Therefore, power adjustment was very frequent. As in the mode switching heating experiments, the same trend was evident that the average microwave power was steadily decreasing as the heating progressed.

For comparison, the temperature profiles of a single mode heating experiment were also presented in Figure 6.5. The maximum temperature difference and standard deviation of temperatures are plotted versus time in Figure 6.6, for these three processing techniques. The significant improvement in temperature uniformity using intelligent mode switching heating is obvious. Both the maximum temperature difference and standard deviation of temperatures were small and stable in the case of variable frequency mode switching heating. The averages of maximum temperature difference and standard deviation of the temperatures are listed in Table 6.1. The maximum temperature difference seems to follow the same trend very closely as the standard deviation. Therefore, similar results could result if the maximum temperature difference were used as the measure of temperature uniformity.

Table 6.1 Average Maximum Temperature and Standard Deviation at Curing Stage

Average	Intelligent Switching	Mode Sweeping	Single Mode Heating
$(\Delta T)_{max}$	13.69 °C	30.07 °C	52.15 °C
$\sigma(T)$	5.51 °C	12.65 °C	21.64 °C

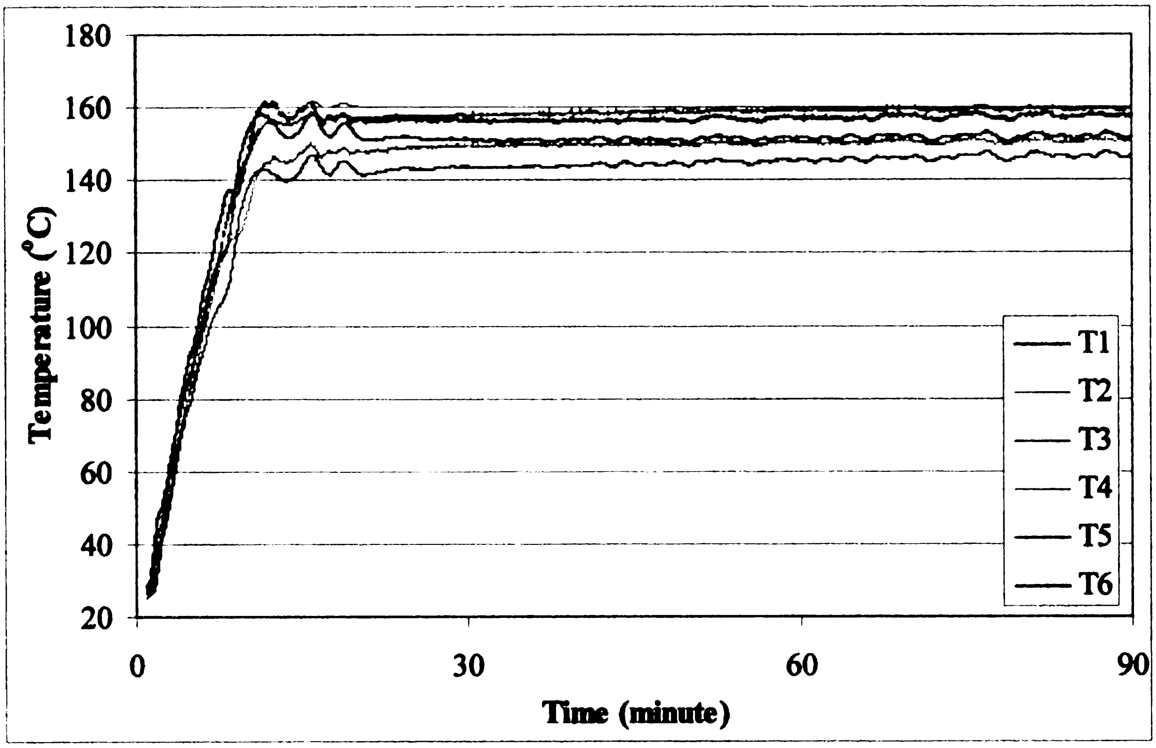

(a) Temperature Profiles

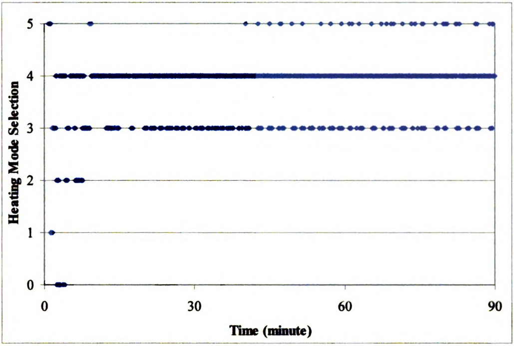

(b) Mode Selection Histogram

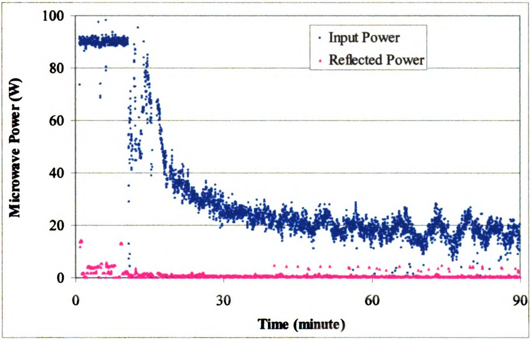

(c) Power Variation during Processing

Figure 6.3 Intelligent Variable Frequency Mode Switching Heating of V-shape Graphite/Epoxy Composite with On-line Mode Updating

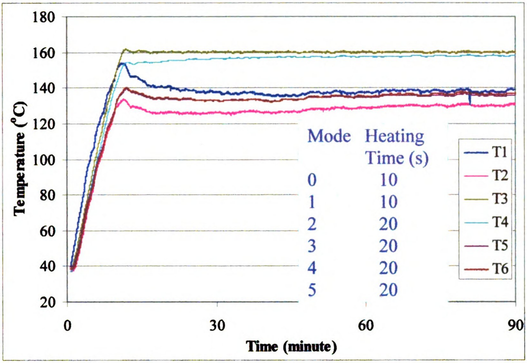

(a) Temperature Profiles

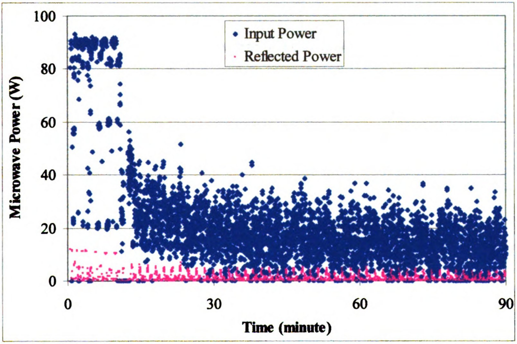

(b) Power Variation During Processing

Figure 6.4 Mode Sweeping Heating of V-shaped Graphite/Epoxy Composite

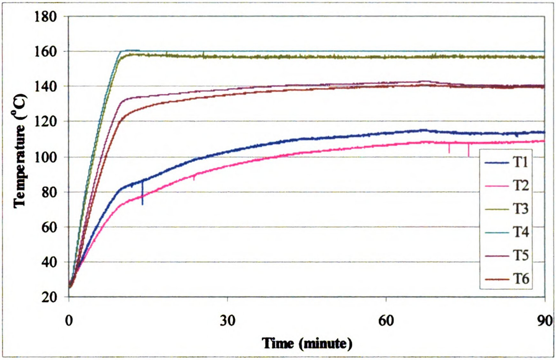

Figure 6.5 Single Mode Heating at f = 2.1605 GHz for V-shaped Graphite/Epoxy Composite

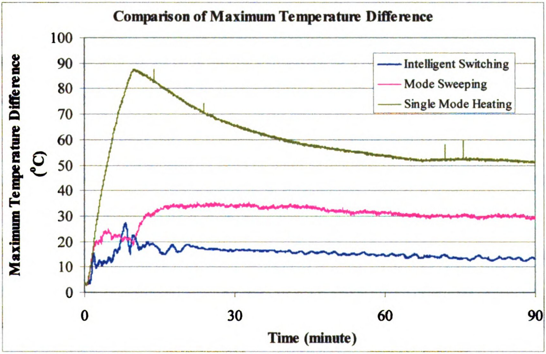

(a) Maximum Temperature difference Comparison

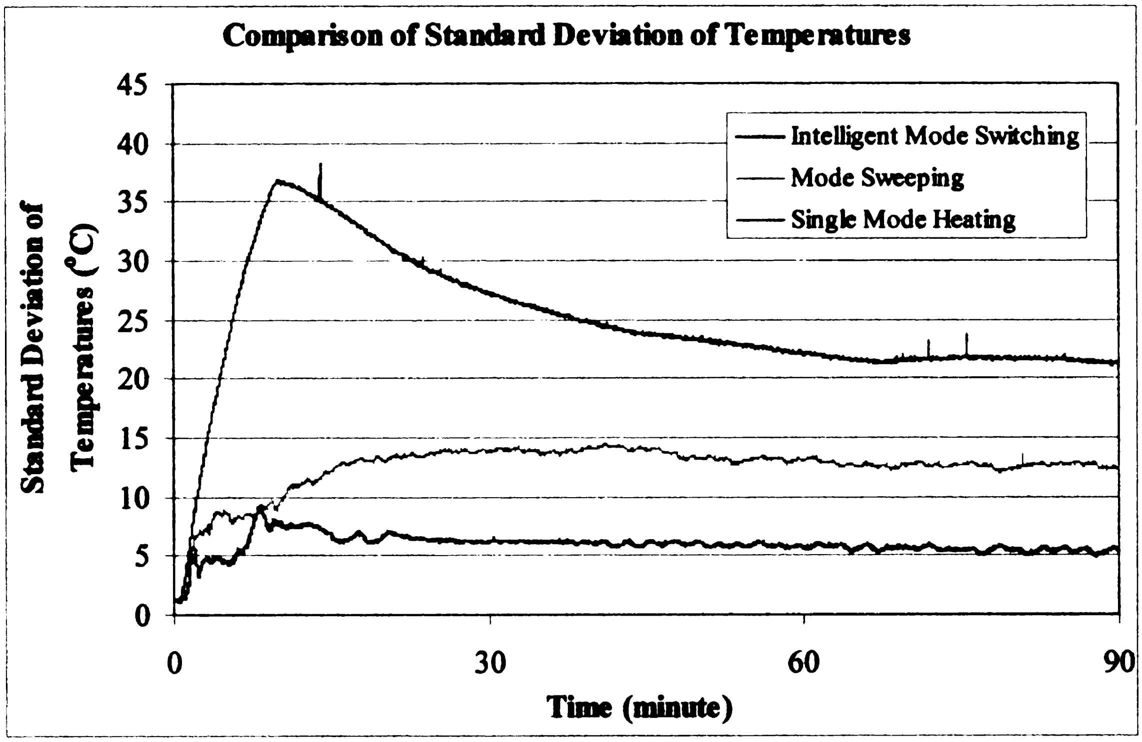

(b) Standard Deviation Comparison

Figure 6.6 Comparison of Temperture Uniformity for Single Mode Heating, Mode Sweeping, and Intelligent Mode Switching Heating of V-shaped Graphite/Epoxy

6.4 Variable Frequency Microwave Processing of Tri-planar Graphite/Epoxy Composites with On-line Mode Updating

In order to further test the performance of the variable frequency mode switching processing technique and the process control system, a more complexly shaped geometry was considered. Twenty-four-ply of uni-directionally laid-up graphite/epoxy prepregs (Hexel AS4-3501/6) were bent into tri-planar shape as shown in Figure 6.7. The sample was loaded into a Teflon mold and then into the microwave cavity. The fiber direction of the sample was perpendicular to the coupling probe. Temperatures were measured at six different sites on the sample surface, as shown in Figure 6.8. The lower edge of the

tri-planar sample was placed near the coupling probe. During the experiments, the cavity length was fixed at 15 cm, and the coupling probe depth at 20 mm.

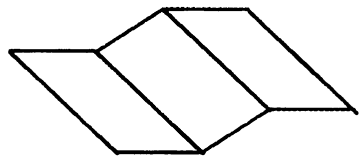

Tri-planar sample

Figure 6.7 Configuration of Tri-planar Graphite/Epoxy Samples

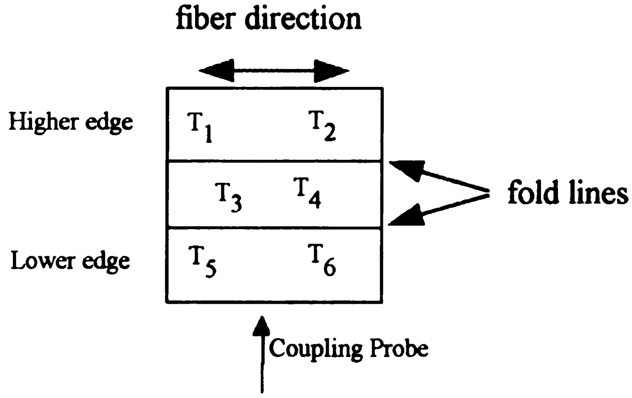

Figure 6.8 Temperature Measurement Configuration of Tri-planar Samples

6.4.1 Heating Modes and Heating Characteristics

In order to determine the frequencies of empirical heating modes, power reflectance was measured while the frequency was swept from 2 GHz to 4 GHz. The power reflectance versus frequency curve is shown in Figure 6 9. The frequencies with power reflectance less than 0.1 were used individually to heat the sample and only the ones with considerable heating effects were regarded as heating mode frequencies. Figure 6.10 shows the temperature change during the frequency scan. The temperature profile indicate the difficulty to obtain uniform heating because the heating preference remained almost the same throughout the frequency spectrum.

Six modes were selected for the experiements based on the heating characteristics and heating effectiveness. The heating characteristics of these modes are given in Figure 6.11, corresponding to the frequencies. Only the heating characteristics at the heating-up stage were measured, since on-line mode updating was going to be used in the experiments to provide accurate heating charateristics information. As shown in Figure 6.11, all the modes heated the higher edge (T_1 and T_2) of the sample preferentially except mode 0, which heated the lower edge (T_5 and T_6) preferentially.

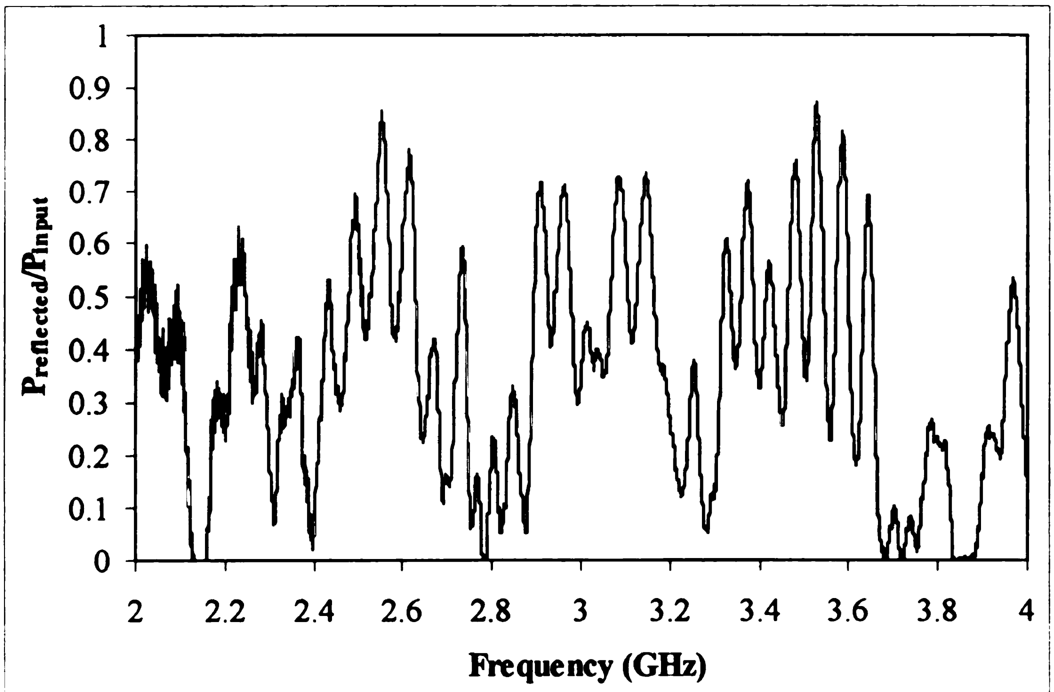

Figure 6.9 Power Reflectance versus Frequency Curve for a Tri-planar Sample

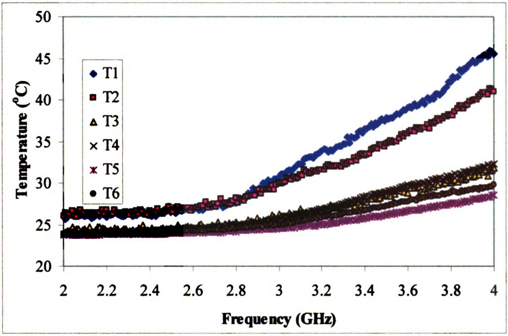

Figure 6.10 Temperature Change during Frequency Scan

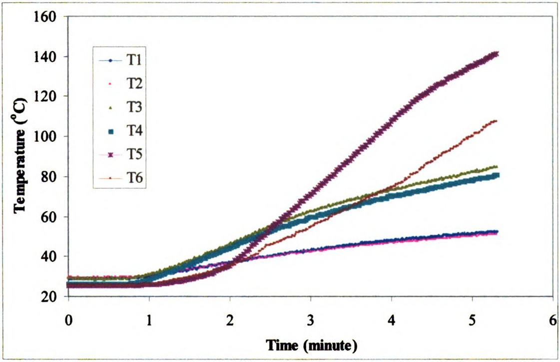

(a) Mode 0: f = 2.1501 GHz

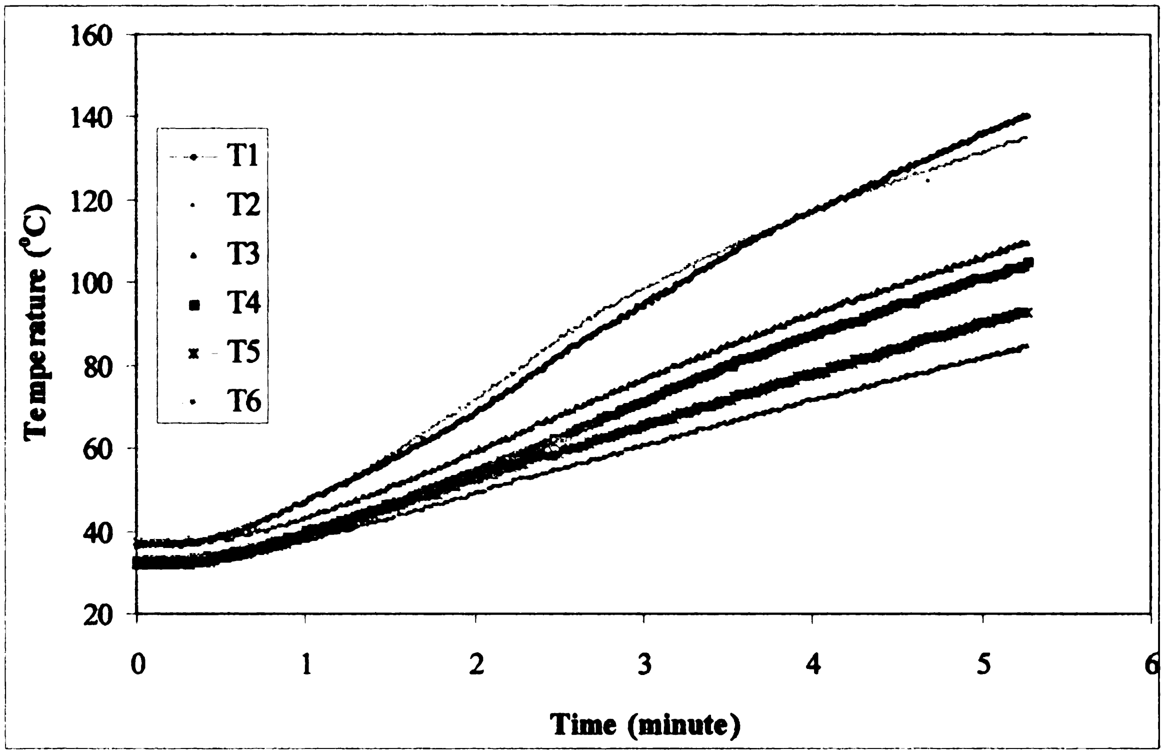

(b) Mode 1: f = 2.3019 GHz

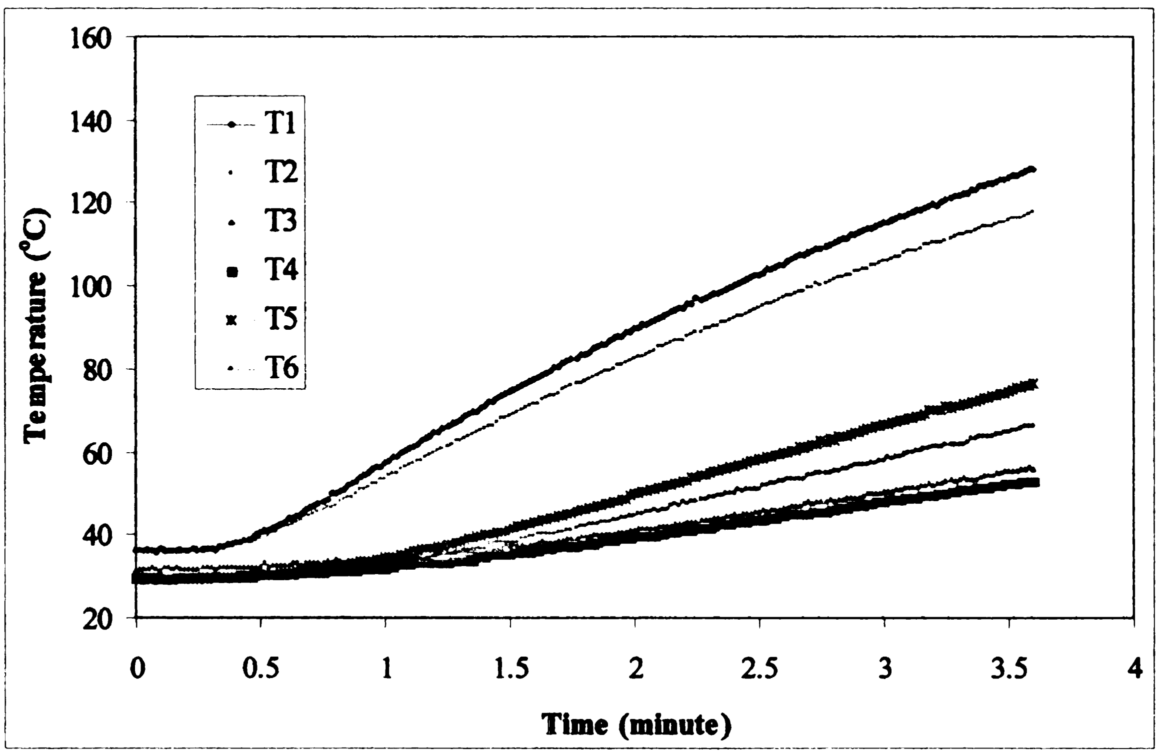

(c) Mode 2: f = 3.6692 GHz

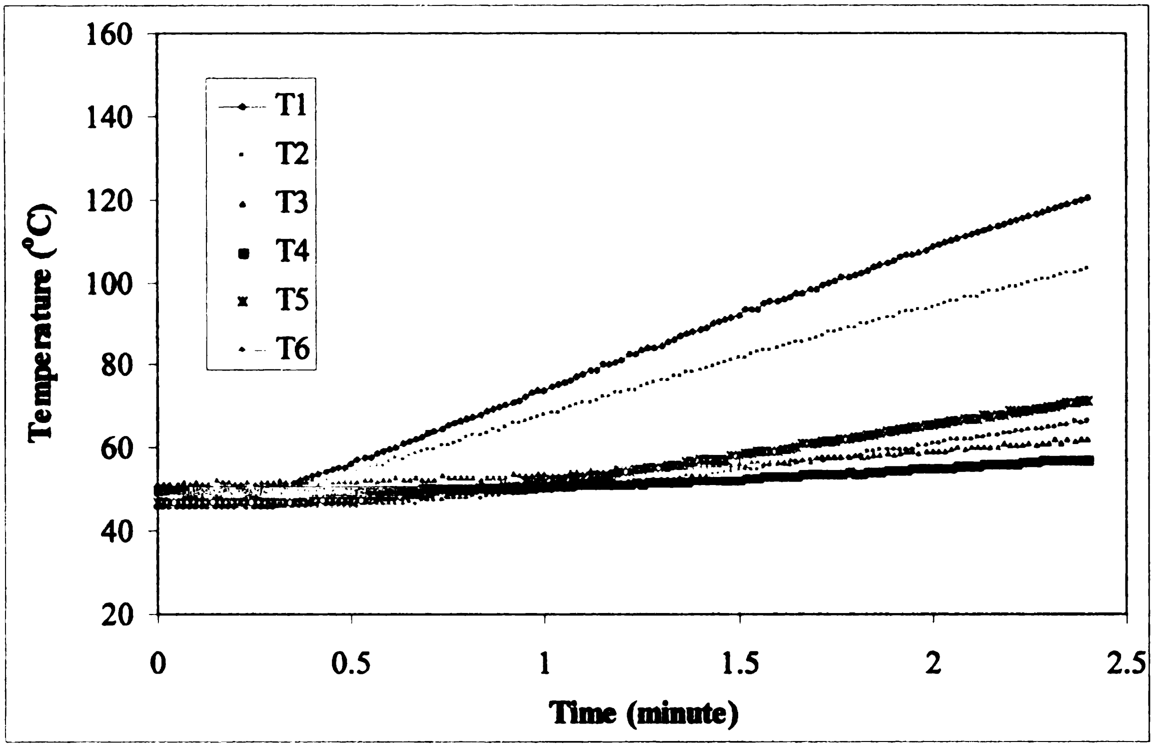

(d) Mode 3: f = 3.7104 GHz

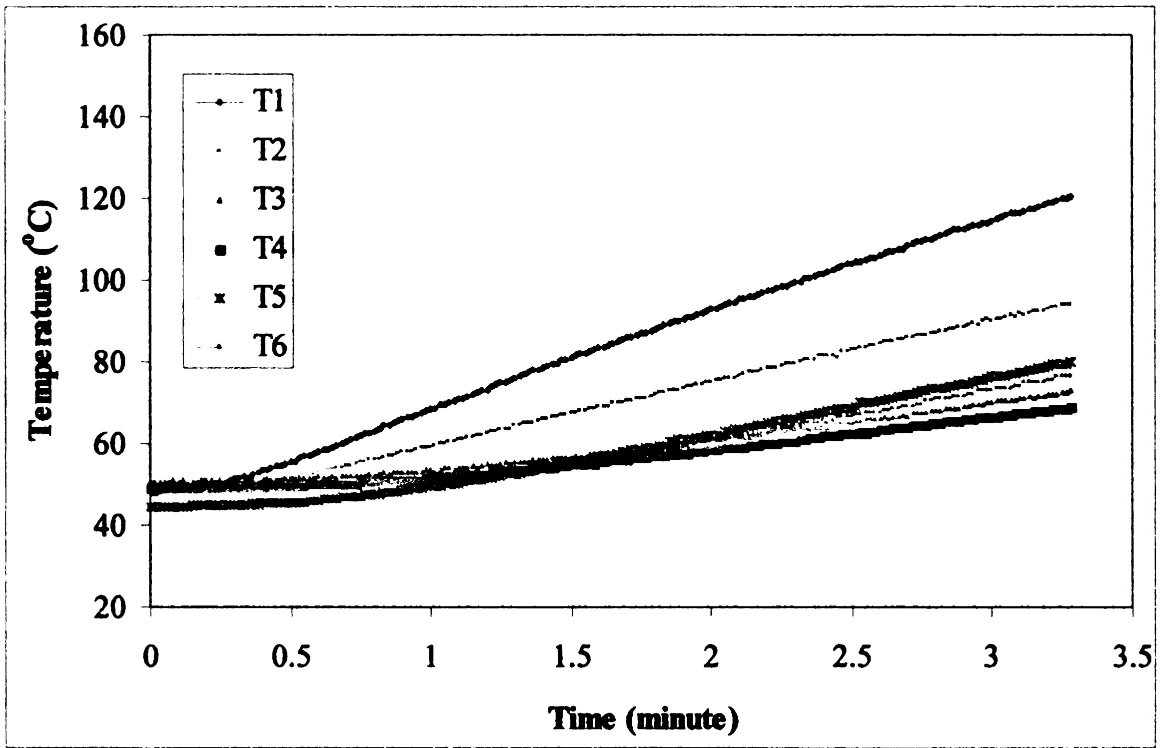

(e) Mode 4: f = 3.7472 GHz

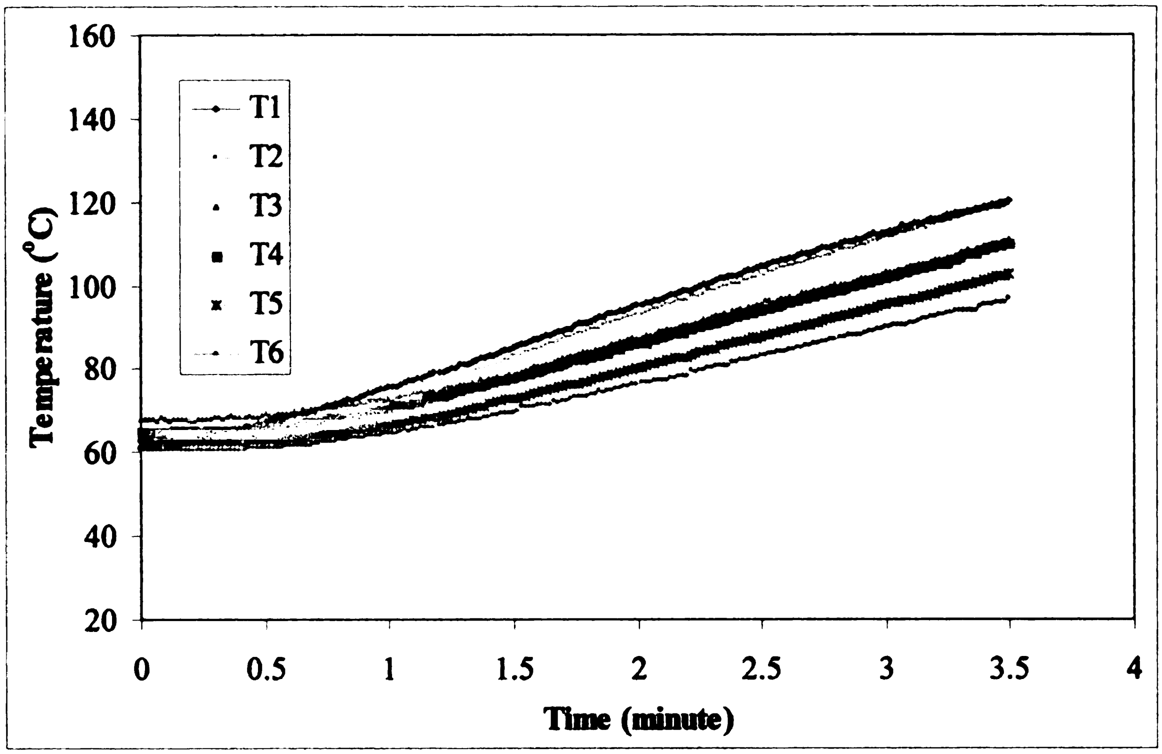

(f) Mode 5: f = 3.8356 GHz

Figure 6.11 Mode Heating Characteristics

Figure 6.12 shows the temperature profiles for the processing of a tri-planar graphite/epoxy composite sample at f = 3.8326 GHz. The heating was relative uniform at the heating-up stage, compared with general single mode heating. However, the temperature gradient increased at the curing stage and the maximum temperature difference stayed at about 30 °C.

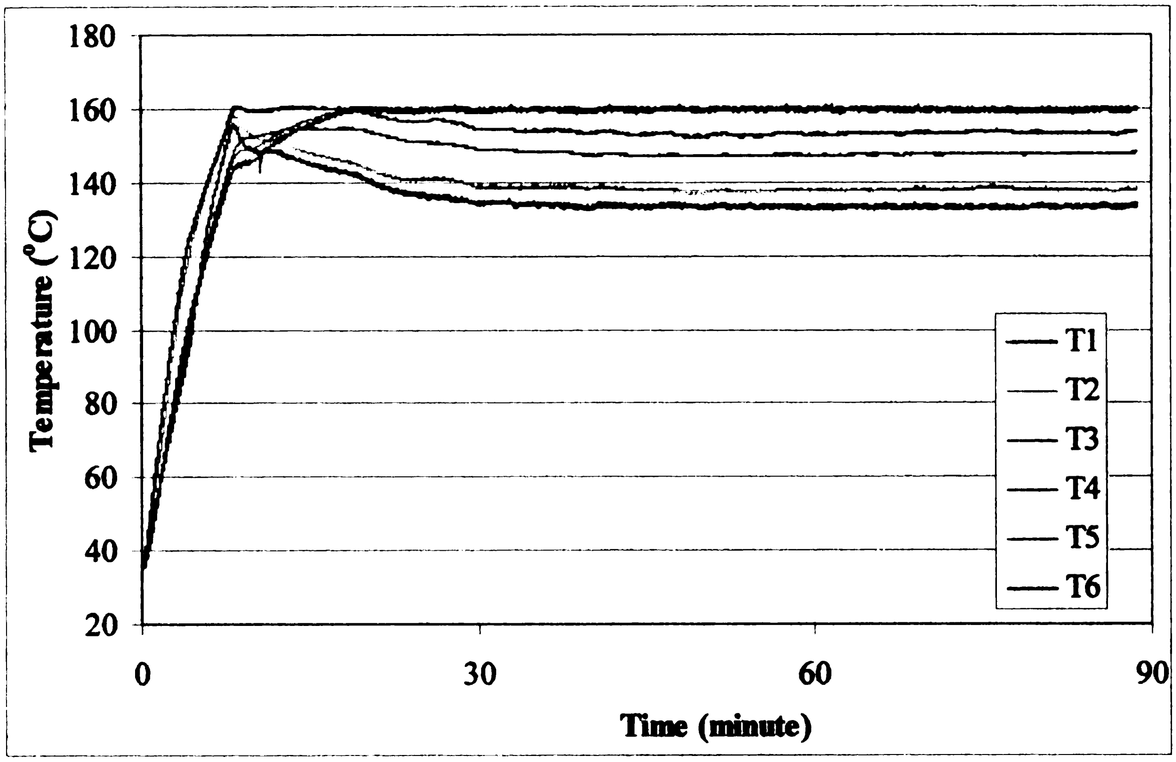

Figure 6.12 Single Mode Heating Profile at f = 3.8326 GHz

6.4.2 Intelligent Mode Switching Heating Results and Discussion

The heating results using variable frequency microwave mode switching technique and VFMPCS II are presented in Figure 6.13. The temperature profiles show that the heating was quite uniform with the final maximum temperature difference of about 15 °C. The power controller performed well and the maximum temperature (T_4) was stabilized within 160 °C ± 0.5 °C quickly after it reached curing stage. The temperature overshoot was less than 1 °C. Other than the fluctuations at the beginning of the curing stage, the temperatures remained stable with edge temperatures lower than the center temperatures. The microwave power decreased as the processing time increased and approached to a steady level around 25 watts.

Figure 6.13 (b) shows the mode selected for heating versus processing time. For this particular experiment, only three modes were actively used for heating. Modes 0, 1, and 5 were used at the heating-up stage. Both modes 1 and 5 were used at the beginning of the curing stage, after which only mode 1 was used for heating. Apparently, during the processing, the controller decided that mode 1 had the heating characteristics that would alleviate the temperature gradients the most. Although mode heating characteristics change during the processing, the initial heating characterization in Figure 6.11 (b) is indicative of the heating preference of mode 1. Therefore, the mode selection by the controller was reasonable, since at the curing stage T_1 and T_2 were the lowest temperatures and mode 1 heated T_1 and T_2 preferentially.

Mode sweeping heating was also conducted using the same six modes. The method was described in Chapter 4. Each mode was assigned a heating time of 10 seconds and the modes were used sequentially. The heating results are given in Figure 6.14. As shown in Figure 6.14, initially the center temperatures (T_3 and T_4) were the lowest, which is predictable since Figure 6.11 showed that all of these six modes heated the edges preferentially except mode 0. The overall heating effect would obviously show preference at the edges since all the modes have equal heating times. As the processing progressed, the center temperatures increased more rapidly and became the highest temperatures. This is due to the heat loss from the sample to its surroundings around the edges. Just as in the intelligent modes switching experiment, T_1 and T_2 became the lowest temperatures.

The comparison of temperature uniformity of single mode heating, mode sweeping heating, and intelligent modes switching heating is presented in Figure 6.15. The intelligent mode switching heating with mode updating proves to be far more superior than single mode heating and mode sweeping heating in terms of achieve temperature uniformity. The average maximum temperature difference and average standard deviation of temperatures at curing stage are listed in Table 6.2.

Table 6.2 Average Maximum Temperature and Standard Deviation at Curing Stage

Average	Intelligent Switching	Mode Sweeping	Single Mode Heating
$(\Delta T)_{max}$	13.52 °C	15.83 °C	26.83 °C
$\sigma(T)$	5.39 °C	7.29 °C	11.17 °C

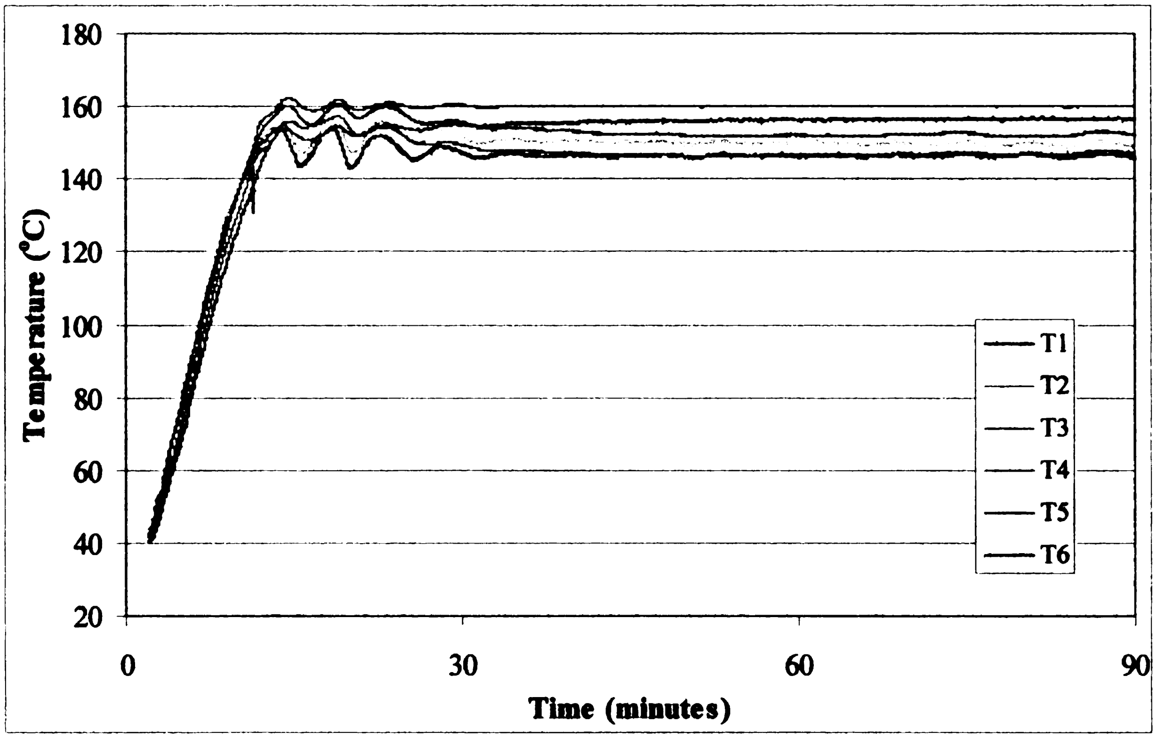

(a) Temperature Profiles

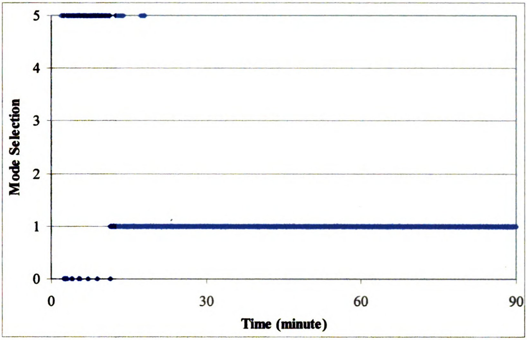

(b) Mode Selection Diagram

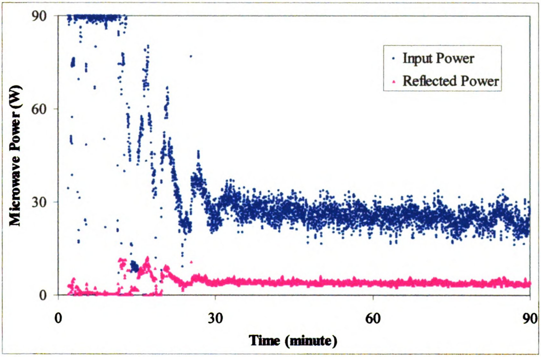

(c) Power Variation during Processing

Figure 6.13 Intelligent Mode Switching Heating of Tri-planar Graphite/Epoxy

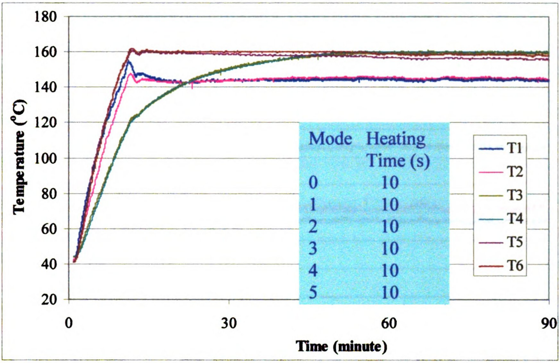

(a) Temperature Profiles

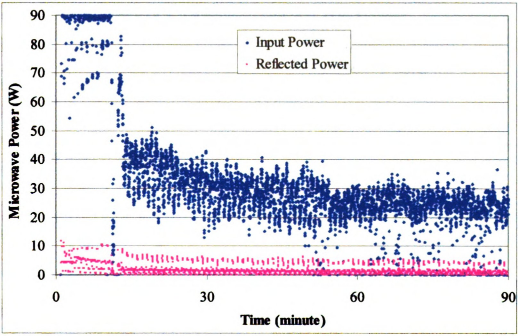

(b) Power Variation during Processing

Figure 6.14 Mode Sweeping Heating of Tri-planar Graphite/Epoxy

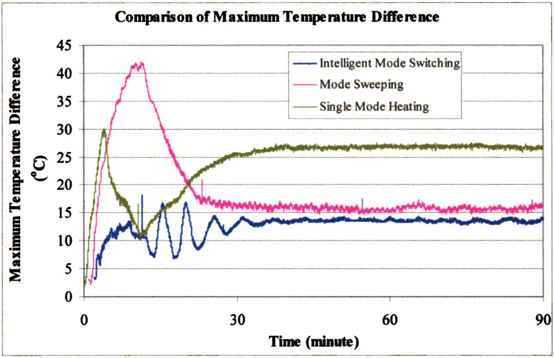

(a) Comparison of Maximum Temperature Difference

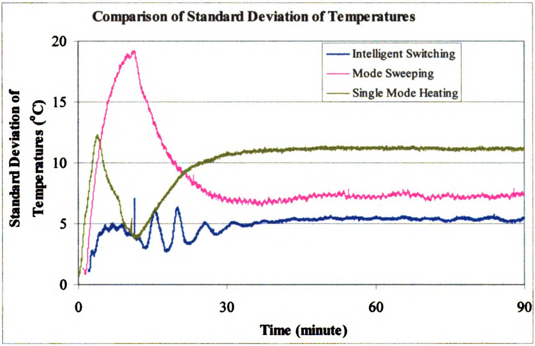

(b) Comparison of Standard Deviation

Figure 6.15 Temperature Uniformity Comparison of Single Mode heating, Mode Sweeping Heating, and Intelligent Mode Switching Heating of Tri-planar Graphite/Epoxy

6.5 Summary and Conclusions

The process control system VFMPCS II has been added the capability of on-line updating the mode heating characteristics. Mode heating characteristics change during the processing due to material property changes and temperature change. This feature enables the control system to obtain accurate heating characteristics and ensure the effectiveness of the mode selection controller. On-line mode characteristics updating is especially important for complexly shaped composite parts since the processing conditions vary in a larger degree.

A mode selection controller with a series of prediction steps was designed. Instead of comparing the heating uniformity at some point in the future, the controller predicts the temperatures at a number of points in the time after. Only by computing the predicted temperatures at different points of time, can the potential of each mode to alleviate the temperature gradient be accurately predicted. A multi-staged PID controller was designed to take advantage of the quick response of variable attenuator. The processing of composite materials was divided into four stages, and power control strategies were designed accordingly.

Experiments were conducted for both V-shaped and tri-planar graphite/epoxy composite parts. Results showed significant improvement of heating uniformity over single mode heating and mode sweeping heating. The mode selection controller and the on-line mode characteristics updating controller proved to be effective and accurate, and improved the robustness of the process control system. The power controller performed well and provided quick, stable, and accurate curing temperature control.

CHAPTER 7

SUMMARY AND CONCLUSIONS

This work was intended to accomplish two main objectives. One is the development of an automated microwave processing system that employs variable frequency technology. The other is the development of a process control system for uniform processing of polymer composites using variable frequency microwave energy.

Microwave processing of materials, especially polymers and polymer composites, has proved in the past to be advantageous over thermal processing approach. Previous research has demonstrated benefits including faster heating, increased reaction rates, enhanced glass transition temperatures, improved conductive fiber matrix adhesion, and better mechanical properties of the products. However, these advantages have not been exploited at industrial scale because of the difficulty of developing a microwave processing system easy to operate while providing desired and consistent performance. In particular, lack of process automation and inability to provide uniform processing are the major obstacles. Good process control systems can simply the operation of the microwave processing system and ensure the consistency of good performance. The use of variable frequency technology in microwave processing eases the task of process automation because same effects can be achieved by electronically adjusting frequency rather than mechanically changing the microwave applicator dimension(s).

In this research, a variable frequency microwave processing system has been developed and automated. Both frequency and power of the microwave energy source were controllable by the computer. Processing parameters were measurable by computer through a data acquisition system. A process control system was developed to achieve uniform processing of polymer composites while maintaining a stable and constant curing temperature. The results and conclusions are summarized as follows.

7.1 Development of an Automated Variable Frequency Microwave Processing System

A variable frequency microwave processing system was developed based on the configuration of the fixed frequency microwave processing system. The major difference was the microwave power source. The variable frequency microwave power source consisted of an HP oscillator as the signal generator and a TWT amplifier. The oscillator frequency output range was from 1.7 GHz to 4.3 GHz. However, only the frequency range of 2 GHz to 4 GHz was used in the processing experiments for a power level high enough for effective heating. Other microwave circuit components and the circuit configuration were the same as the fixed frequency microwave system. However the microwave components were required to be operational from 2 GHz to 4 GHz. The variable frequency microwave processing system was automated and characterized.

7.1.1 Automation of the Microwave Processing System

The automation of the microwave processing system mostly involved achieving computer control of the microwave frequency and power. The frequency of the microwave power source was controlled through the GPIB interface between the computer and the HP Oscillator. The computer could write the desired frequency directly to the Oscillator through GPIB. A variable attenuator was used for the computer control of microwave power. The attenuation was controllable via the control voltage. The variable attenuator was connected between the HP Oscillator and the TWT amplifier because of the maximum input power to the attenuator was 30 dBm.

Measured processing parameters included input microwave power, reflected microwave power, and the surface temperatures of the material being processed. Microwave power was measured by power meters with analog outputs. Temperatures were measured using Luxtron fluoroptic thermometer with analog outputs. The analog signals were obtained by the computer through a National Instruments™ data acquisition board. The process control system analyzes the measured processing parameters and adjusts the microwave frequency and power accordingly to achieve the processing goals.

7.1.2 Characterization of the Variable Frequency Microwave Processing System

The characteristics of the microwave circuit components have been studied. The microwave power source showed a varying power output level at different frequencies. The microwave power output tended to be higher at higher frequencies. The time for the computer to write the frequency to the oscillator was measured at about 0.1 seconds. The cut-off frequency curves measured for the empty cylindrical cavity agreed well with theoretical predictions, which ensured that the quality of the single mode resonant cavity.

Characterization program for loaded microwave cavity was also designed. Microwave power reflectance was measured versus frequency. Mode frequencies were obtained by locating the frequencies with minimal power reflectance. The temperature profiles measured during the frequency scan were used to determine the variety of heating preferences of the modes, which was used as the criterion for the optimal sample loading position.

The variable attenuator was characterized to determine the relationship between the control voltage and attenuation. The relationship turned out to be linear over a wide range and nonlinear when the control voltage is close to 0. The characterization of the power meters showed that a certain amount of time was necessary for the meter to give accurate readings after power step changes. It was determined that the power reading would be within 5% of the true value after 170 ms of a power step change.

Dielectric properties of DGEBA/DDS showed little change over the frequency range from 2 GHz to 4 GHz. The scattered data did not indicate any trends. Therefore, the frequency effects on epoxy dielectric properties were considered as minimal.

7.2 Variable Frequency Mode Sweeping Heating

The experiments demonstrated that the power source consisting of an oscillator, a RF plug-in and a TWT worked well as a variable frequency power supply. This variable frequency microwave system, using a cylindrical cavity as the applicator, was able to obtained heating modes with a variety of heating patterns when graphite/epoxy material was loaded. A more uniform heating pattern resulted when two modes with complementary heating preferences were used alternatively for heating.

A mode sweeping heating technique was designed to take advantage of complementary heating concept and improve the temperature uniformity of microwave heating. Mode selection cycles were designed. In each mode selection cycle, a sequence of modes was used to heat the sample, each mode for a certain period of time. The mode selection cycle was repeated until the end of processing.

Mode sweeping method was shown to heat the 2" square graphite/epoxy composite parts not only uniformly, but also efficiently. The efficiency of mode sweeping heating lied between the highest one and the lowest one among those of the modes used. As observed in the experiments, mode sweeping with equal time intervals did not obtain optimum heating. To get even more uniform heating, the heating characteristics of each mode should be considered in the optimum heating process design. The heating uniformity of this method shows the potential to achieve uniform curing of the graphite/epoxy material of small size.

7.3 Variable Frequency Mode Switching Processing

In variable frequency mode switching heating, processing cycles were designed based on the mode heating patterns only. However, during the processing of composites, the temperature distribution varies. Different temperature distributions call for mode with different heating preferences. An intelligent variable frequency mode switching technique was designed and developed in LabVIEW (VFMPCSI) to match mode characteristics with sample temperature distribution when selecting the heating mode.

The control system predicts the temperatures using the mode heating rates and the measured temperature distribution. The mode that will result in the smallest standard deviation of the predicted temperatures is selected for heating. A stepper motor was used to adjust the manual knob on the microwave power source. A parabolic power control algorithm was designed for simple microwave power control that did not require controller tuning. The power control algorithm was proved to be effective and stable. However fluctuations occurred during mode switching heating due to the different mode characteristics and the coarse and slow adjustment of the stepper motor for microwave power control. 24-ply unidirectional 3" by 3" graphite/epoxy composite parts were successfully processed using the intelligent variable frequency mode switching technique. Heating experiments proved that the heating characteristics of each mode was repetitive as long as the sample was loaded in the same way. Mode switching heating resulted in much improved temperature uniformity.

Variable frequency mode switching technique was also employed to significantly improve the heating uniformity of microwave processing of V-shaped graphite/epoxy panels. A different microwave power control hardware - variable attenuator, was used. The power adjustment time for the variable attenuator was much smaller than that of the stepper motor. The adjustment time using variable attenuator was less than 1 second, while the adjusment time for stepper motor ranged from 1 second to more than 10 seconds depending on the power change size. The procedure used in this study can be readily applied to processing of other complex-shaped composite parts.

7.4 Variable Frequency Microwave Processing of Complex Shape Composite Parts with On-line Mode Updating

An on-line mode characterization capability was added to the variable frequency microwave processing system and resulted in a much improved process control system - VFMPCS II. On-line mode characterization was necessary because mode heating characteristics change during the processing due to material property changes and temperature change. This feature enables the control system to obtain accurate mode heating characteristics and ensure the effectiveness of the mode selection controller. On-line mode characterization is especially important for complexly shaped composite parts since the processing conditions vary in a larger degree than simply shaped composite parts.

A mode selection controller with a series of prediction steps was designed. Instead of comparing the heating uniformity at some point in the future, the controller predicts the temperatures at a number of points in the time after. Only by computing the predicted temperatures at different points of time, can the potential of each mode to alleviate the temperature gradient be accurately predicted. A multi-staged power controller was designed to take advantage of the quick response of the variable attenuator. The processing of composite materials was divided into four stages, and power control strategies were designed accordingly. At the heating-up stage, maximum microwave power was used. When the maximum measured temperature was within 10 °C of the curing temperature - 160 °C, a PID controller was used for microwave power control. When the maximum measured temperature was within 160 °C ± 1 °C, the second PID controller was used for microwave power control. The parameters of the two PID controllers were tuned in such a way that the first PID controller had faster response, while the second controller was more stable and accurate.

Experiments were conducted for both V-shaped and tri-planar graphite/epoxy composite parts. Results showed significant improvement of heating uniformity over single mode heating and mode sweeping heating. The final maximum temperature differences for both samples were less than 15 °C. Quantitative comparisons were made for these three processing techniques. For the V-shaped samples, the intelligent mode switching heating reduced the standard deviation of temperatures by 56% and 75% as compared with mode sweeping heating and single mode heating respectively. For the tri-planar samples, the intelligent mode switching heating reduced the standard deviation of temperatures by 26% and 52% as compared with mode sweeping heating and single mode heating respectively. The mode selection controller and the on-line mode characteristics updating controller proved to be effective and accurate, and improved the robustness of the process control system. The power controller performed well and provided quick, stable, and accurate curing temperature control. The temperature overshoot was less than 1 °C and the maximum measured temperature was controlled within 160 °C ± 0.5 °C.

7.5 Summary

Compared with previous research results in single microwave cavity processing, the results accomplished in this work showed significant improvement. Adegbite et al. [20] used fixed frequency mode switching technique to process 3" 24-ply square graphite/epoxy composite parts. The final maximum temperature difference was less than 15 °C. However, large temperature fluctuations were present not only in the heating-up stage, but also in the curing stage. The temperature fluctuation reached 25 °C at times. Fellows et al. [17] used fixed frequency mode switching technique to process V-shaped polyester/glass composite parts. The desired curing temperature was 120 °C. The maximum temperature difference was about 25 °C throughout the processing experiment. Large temperature fluctuations were also observed and exceeded 15 °C at many occasions. The curing temperature varied from 120 °C to 130 °C. The reasons for instability of temperature control, large temperature fluctuations, and non-uniform temperature distribution were not only the slow mechanical adjustment of cavity length for mode switching, but also lack of a stable and accurate process control system. As comparison, the results in this work showed uniform temperature distribution throughout the processing, with maximum measured temperature difference less than 15 °C most of the time. The temperature control was stable and accurate. No large temperature fluctuations were observed. Curing temperature overshoot was kept within 1 °C and curing temperature was controlled within 1 °C of the desired value.

The significance of this work is in the development of a variable frequency microwave processing technology that provide uniform and stable processing with consistent performance and great flexibility and applicability. Advantages of using variable frequency microwave technology have been explored and demonstrated. A systematic processing procedure was established, including selection of sample loading positions, location of the mode frequencies, characterization of the heating modes, and finally computer controlled variable frequency microwave processing of the materials. A complete set of variable frequency techniques has been created to optimize microwave processing. The process control system that included optimal mode selection and robust temperature control has be designed and developed. Specifically, this work made the following contributions to the microwave material processing technology advancement:

1. The design and implementation of hardware and software for the automation of a variable frequency microwave processing system to achieve fast and precise control.

2. The development and implementation of a process control system using innovative control methodologies, to achieve uniform and controlled heating by mode sweeping or switching, mode tuning, and power control.
3. A microwave cavity characterization program that would determine the frequencies of the heating modes and the optimal loading position of the samples.
4. A predictive mode selection algorithm that would select an optimal heating mode to alleviate the temperature gradients by matching the sample temperature distribution with the heating characteristics of the modes.
5. Power control execution programs that provided fast and precise tuning of the power control devices, stepper motor and variable attenuator.
6. An on-line mode heating preference characterization program that would update the mode heating characteristics database so as to improve the robustness of temperature uniformity control.
7. A variable frequency mode tuning program that provides fast and timely tuning of the mode frequency so as to minimize reflected microwave power.
8. Analysis and characterization of the performance of microwave circuit components, such as power meters, in variable frequency processing.
9. Automatic data acquisition for fast, reliable and convenient data collection, tracking, and maintenance.
10. Demonstration of the ability of the variable frequency microwave processing system to provide uniform and controlled processing of complex-shaped graphite/epoxy composite parts.

11. A tested procedure for variable frequency microwave processing of polymer composites, including: optimization of sample loading position, location and characterization of the modes, mode sweeping heating or intelligent mode switching heating with the option of on-line mode characterization.
12. An intuitive graphical user interface for the operation and control of the variable frequency microwave processing system.

CHAPTER 8

RECOMMENDATIONS AND FUTURE WORK

In this work, variable frequency technology has been successfully applied in microwave processing of polymer composites in a single mode cavity. The energy efficiency of the single mode resonant cavity was exploited while a uniform processing temperature was achieved, which had been the obstacle of the application of microwave processing systems in the industry. The advantages of variable frequency technology included more available heating modes, fast mode switching, and easy characterization of the loaded microwave cavity.

The benefits of variable frequency technology can be further realized in on-line cure monitoring of microwave processing of polymers and composites, because of the capability of power reflectance scan. Combining thermal heating with variable frequency microwave heating can further increase the uniformity of the material processing temperature. As indicated by the experimental results, the temperature gradients at the curing stage of variable frequency microwave processing were mainly due to the heat loss from the sample to the ambient. With the utilization of variable frequency technology and the development of the robust process control system, the microwave processing system has become a viable system for industrial use. Scale-up studies need to be carried out to further reduce the gap between the lab-scale system and the industrial processing system.

Three recommendations for future work are proposed in this chapter. They are: 1) on-line cure monitoring, 2) hybrid heating for ultimately uniform processing, and 3) scale-up studies and application of variable frequency microwave processing in industrial processes. These recommendations are presented in the following sections respectively.

8.1 On-line Cure Monitoring for Microwave Processing of Polymers and Composites

When the composite material is loaded inside a single mode cavity, a power absorption curve can be obtained by sweeping the frequency and measuring the percentage of reflected power. There will be numerous troughs, some of which indicate low percentage of reflected power, which are characteristics of resonant modes. The absorption of electromagnetic energy depends on both the frequency and the material properties, if other parameters are unchanged. Therefore, if we fix frequency by selecting a clearly defined trough, the frequency at the dip and the bandwidth will only depend on the material properties, namely dielectric properties. For the material being processed, its dielectric properties change with temperature and extent of cure, or chemical composition. During curing stage, it is desired that the temperature will remain constant, which can be achieved by the control system. Therefore, by monitoring the change of frequency and bandwidth of the selected trough, it is possible to detect the change of extent of cure.

In order to accomplish this task, experiments should be carried out to establish the relationship between extent of cure and dielectric properties of the polymer or composite material to be processed. An example is given in Figure 8.1. In addition, a theoretical or empirical model for electromagnetic absorption peak shift due to dielectric property changes should be developed. Small perturbation method can be used by considering the change of dielectric properties as small perturbations.

8.2 Hybrid Heating for Ultimately Uniform Processing

As indicated by the processing results in Chapters 4 to 6, at the curing stage of variable frequency microwave processing, temperature gradients always existed. The center temperatures were higher than the rest, especially compared to the temperatures around the edges of the sample. The cause of the temperature gradients from the center of the sample to the edges was the heat loss from the sample to the surroundings, because the ambient temperature was always lower than the sample temperature. The temperature gradients reduced as the processing progressed and the ambient temperature increased.

For applications that require ultimately uniform temperature distribution during processing, a hybrid heating approach can be taken by combining variable frequency microwave heating with thermal heating. Hardware modifications are required for the microwave processing system. A thermal heater, such as an electrical resistive heating tape, can be installed around the cavity wall. Computer control of the thermal heater is crucial to have optimally coordinated heating between microwave heating device and thermal heating device. A control algorithm will be necessary to control the thermal heater such that the ambient temperature around the sample will follow the sample temperature.

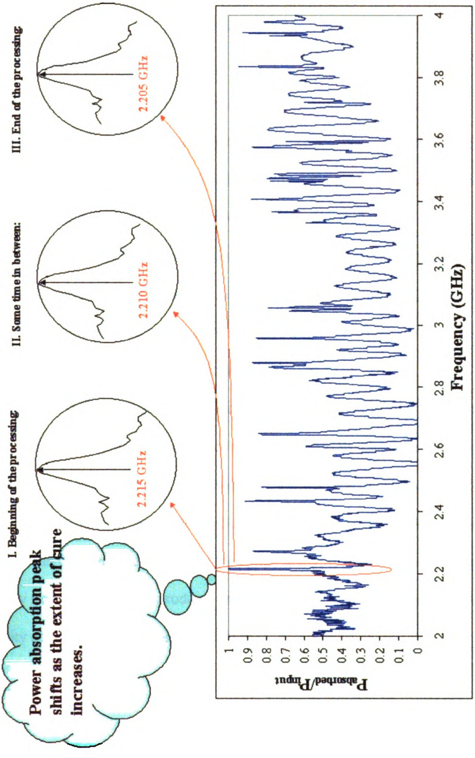

Figure 8.1 An Example of Relating Power Absorption Curve Change to Extent of Cure Change

8.3 Scale-up Studies and Industrial Application of Variable Frequency Microwave Processing System

The variable frequency microwave processing techniques developed on batch process can be applied to microwave pultrusion process and microwave resin transfer molding process. Process modeling should be carried out for both pultrusion and Resin Transfer processes. Heating modes should be identified and characterized. The control parameters should be determined both empirically and with the aid of mathematical modeling. Experiments should be conducted to process composite parts using these systems. The research findings will be the basis of further efforts to develop prototype industrial pultrusion and Resin Transfer Molding systems.

For the scale-up studies, an 18-inch cavity can be used to carry out experiments at the large scale. A new variable frequency power source with frequency range from 0.5 GHz to 2 GHz will be necessary to provide microwaves than can establish single resonant modes inside the 18-inch cavity. Proportionally enlarged samples should be processed and results should be compared with those for 7-inch cavity. Composite parts with complex geometry similar to industrial products can also be processed so as to investigate the feasibility of commercializing this technology.

APPENDICES

APPENDIX A

Control Hardware Instrumentation

1. Stepper Motor Power Control Module

Connecting the data acquisition board with the stepper motor is a 15 pin DSUB connector for the directional motor control with automatic directional shutoff at end stalls. The assignments for the pin connections are listed in Table A.1

Table A.1 Connector and cable wire assignments

Pin #	Wire Color	Signal	Comments
1	Red	5 V DC	External Source
2	-	-	-
3	-	-	-
4	-	-	-
5	Yellow	High end TTL Signal	-
6	-	-	-
7	-	-	-
8	Blue	Decrease	TTL 3 mA
9	Brown	Ground	+ 5 V DC Return
10	-	-	-
11	-	-	-
12	Orange	Low End TTL Signal	-
13	-	-	-
14	-	-	-
15	Green	Increase	TTL 3 mA

2. ARRA 4752-60D Voltage Controlled Variable Attenuator

The configuration of the ARRA 4752-60D Voltage Controlled Variable is given in Figure A.1.

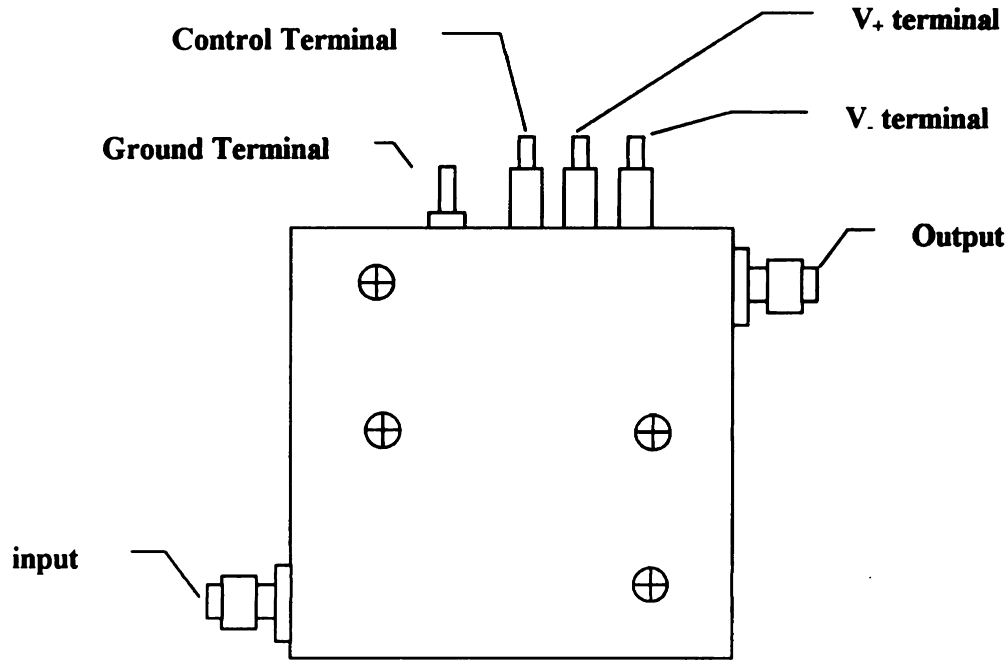

Figure A.1 Device Configuration of the Variable Attenuator

The general specifications of the variable attenuator are as follows:

Frequency Range	1.0 - 18.0 GHz
Attenuation Range	0 - 60dB
RF Power Max	+20 dBm
	+30 dBm survival
Rise & Fall Time	1.5 μ sec/ 50 ns
Power Supply	± 12 Volts, 100 mA
Control Voltage	0 - 6 Volts

3. Data Acquisition Board - National Instruments™ PCI-MIO-16XE-50

The National Instruments™ PCI-MIO-16XE-50 (20 kS/s, 16-Bit, 16 Analog Inputs) is one of the PCI E series boards supplied by National Instruments Inc. This model of data acquisition boards has bus master capability that makes possible robust, multitasked DAQ applications. Bus Mastering improves overall system performance through direct transfer of data between the plug-in board and computer memory, without burdening the CPU. The PCI standard enables the same application to run on a variety of operating systems and computers.

The PCI-MIO-16XE-50 board is a multifunction analog, digital, and timing I/O board for PCI bus computers. It features 16-bit ADCs with 16 analog inputs, 16-bit DACs with voltage outputs, eight lines of TTL-compatible digital I/O, and two 24-bit counter/timers for timing I/O. Because the PCI board has no DIP switches, jumpers, or potentiometers, it is easily software-configured and calibrated. This feature is made possible by the National Instruments MITE bus interface chip that connects the board to the PCI I/O bus. The MITE implements the PCI Local Bus Specification so that the interrupts and base memory addresses are all software configured. Data-acquisition-related configuration includes such settings as analog input polarity and range, analog input mode, and others.

Calibration for the PCI-MIO-16XE-50 board:

Calibration refers to the process of minimizing measurement and output voltage errors by making small circuit adjustments. On the PCI E series boards, these adjustments take the form of writing values to onboard calibration DACs (CalDACs). Some form of board calibration is required for all but the most forgiving applications. If the board was not calibrated the signals and measurements could have very large offsets, gain, and linearity errors. Since both power measurement and power control requires high precision in this study, calibration was carefully carried out.

There are three levels of calibration available for the PCI E series boards.

1. Loading calibration constants. Loading calibration constants refers to the process of loading the CalDACs with the values stored in the EFPROM, the onboard nonvolatile memory. NI-DAQ software dtermines when this is necessary and does it automatically.

2. Self-Calibration. The PCI board can measure and correct for almost all of its calibration-related errors without any external connections. The national Instruments software provides a self-calibration method, which can be initiated by the user. This self-calibration process, which generally takes less than a minute, is the preferred method of assuring accuracy. Self-calibration should be sufficient if the user is interested primarily in relative measurements. Otherwise, the external calibration should be used to address the gain error due to time or temperature drift of the onboard voltage reference, which could not be eliminated by the self-calibration process.

3. External Calibration. The PCI E series board has an onboard calibration reference to ensure the accuracy of self-calibration. This voltage is stable enough for most applications, but if the board is used at an extreme temperature or if the onboard reference has not been measured for a year or more, the board needs to be externally calibrated. An external calibration refers to calibrating the board with a known external reference rather

than relying on the onboard reference. The external calibration can be conducted by calling the NI-DAQ calibration function.

I/O Connector Pin Assignments:

The pin assignments are illustrated in Figure A.2 [99]. A NationalInstruments™ R6850 Ribbon Cable was used to connect the 68-pin data acquisition board to a 50-pin I/O connector block. This greatly simplified the labeling associated with the pins. The I/O connector block terminals are listed in Table A.2 along with corresponding signals.

ACH8 -	34	68	- ACH0
ACH1 -	33	67	- AIGND
AIGND -	32	66	- ACH9
ACH10 -	31	65	- ACH2
ACH3 -	30	64	- AIGND
AIGND -	29	63	- ACH11
ACH4 -	28	62	- AISENSE
AIGND -	27	61	- ACH12
ACH13 -	26	60	- ACH5
ACH6 -	25	59	- AIGND
AIGND -	24	58	- ACH14
ACH15 -	23	57	- ACH7
DAC0OUT -	22	56	- AIGND
DAC1OUT -	21	55	- AOGND
UNASSIGNED -	20	54	- AOGND
DIO4 -	19	53	- DGND
DGND -	18	52	- DIO0
DIO1 -	17	51	- DIO5
DIO6 -	16	50	- DGND
DGND -	15	49	- DIO2
+ 5 V -	14	48	- DIO7
DGND -	13	47	- DIO3
DGND -	12	46	- SCANCLK
PF10/TRIG1 -	11	45	- EXTSTROBE
PF11/TRIG2 -	10	44	- DGND
DGND -	9	43	- PF12/CONVERT
+ 5 V -	8	42	- PF13/GPCTR1_SOURCE
DGND -	7	41	- PF14/GPCTR1_GATE
PF15/UPDATE -	6	40	- GPCTR1_OUT
PF16/WFTRIG -	5	39	- DGND
DGND -	4	38	- PF17/STARTSCAN
PF19/GPCTR0_GATE -	3	37	- PF18/GPCTR0_SOURCE
GPCTR0_OUT -	2	36	- DGND
FREQ_OUT-	1	35	- DGND

Figure A.2 Pin Assignments for PCI-MIO-16XE-50 Board

Table A.2 I/O Connector Block Terminals and Corresponding Signals

PHYSICAL SIGNAL	PIN ASSIGNMENTS	PIN #		PIN ASSIGNMENTS	PHYSICAL SIGNAL
	AIGND	1	2	AIGND	
Cavity Length	ACH0	3	4	ACH8	Temperature 1
Probe Depth	ACH1	5	6	ACH9	Temperature 2
Input Power	ACH2	7	8	ACH10	Temperature 3
Reflected Power	ACH3	9	10	ACH11	Temperature 4
	ACH4	11	12	ACH12	Temperature 5
	ACH5	13	14	ACH13	Temperature 6
	ACH6	15	16	ACH14	Temperature 7
	ACH7	17	18	ACH15	Temperature 8
	AISENSE	19	20	DAC0OUT	VA_V/SM_Inc[1]
SM_Dec[2]	DAC1OUT	21	22	*UNASSIGNED*	
	AOGND	23	24	DGND	
Probe Direction	DIO0	25	26	DIO4	
Probe Pulse	DIO1	27	28	DIO5	
Cavity Direction	DIO2	29	30	DIO6	
Cavity Pulse	DIO3	31	32	DIO7	
	DGND	33	34	+ 5 V	Probe/SM Power
Cavity Power	+ 5 V	35	36	SCANCLK	
	EXTSTROBE	37	38	PFI0/TRIG1	
	PFI1/TRIG2	39	40	PFI2/CONVERT	
	PFI3/GPCTR1_SOURCE	41	42	PFI4/GPCTR1_GATE	
	GPCTR1_OUT	43	44	PFI5/UPDATE	
	PFI6/WFTRIG	45	46	PFI7/STARTSCAN	
	PFI8/GPCTR0_SOURCE	47	48	PFI9/GPCTR0_GATE	
	GPCTR0_OUT	49	50	FREQ_OUT	

Notes:

1. Pin #20 was connected to either VA_V or SM_Inc, where VA_V is the control voltage for the variable attenuator and SM_Inc is the "increase" voltage for the stepper motor.
2. SM_Dec is the "decrease" voltage for the stepper motor.

4. Schematic for Teflon Molds

All Teflon molds were composed of two parts, a top part (cover) and a bottom part (holder). Latches are used to put the two parts together. The Diameters for the latch holes are all 0.375 ". Eight probing holes are to be drilled with locations and dimensions sketched below. The diameters for the probing holes are all 0.125 ".

1. Teflon Mold for V-Shaped Samples

A Teflon mold was made for a V-shaped composite part. The mold is consisted of a holder and a cover. The mold looks like a cylindrical block when closed. The sample is loaded in the center of the mold. The schematics for the Tri-planar Teflon mold are presented in Figure A.6 through Figure A.8.

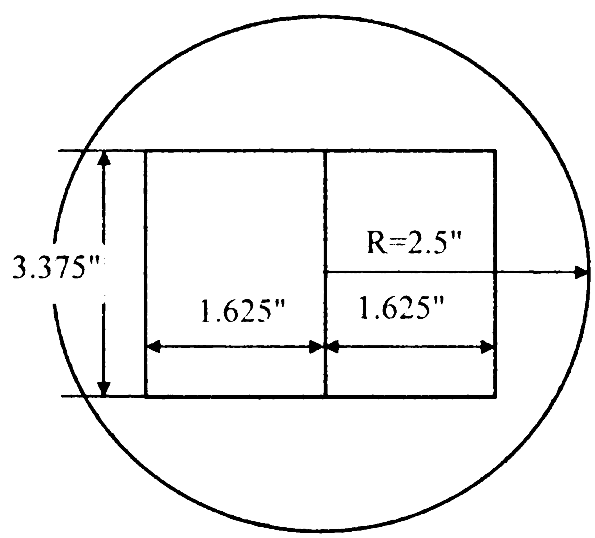

(a) Top View

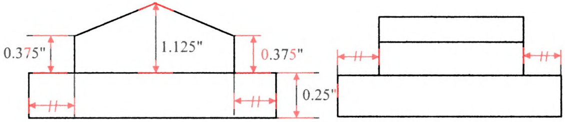

(b) Side Views

Figure A.3 Schematic for V-Shaped Teflon Mold Cover

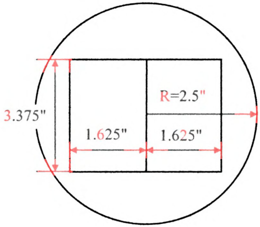

(a) Top View

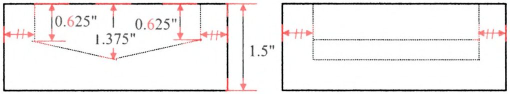

(b) Side Views

Figure A.4 Schematic for V-Shaped Teflon Mold Holder

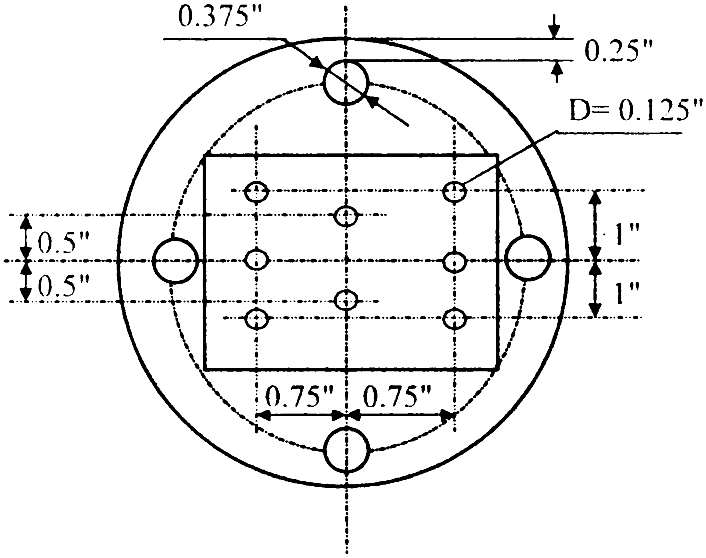

(a) Cover

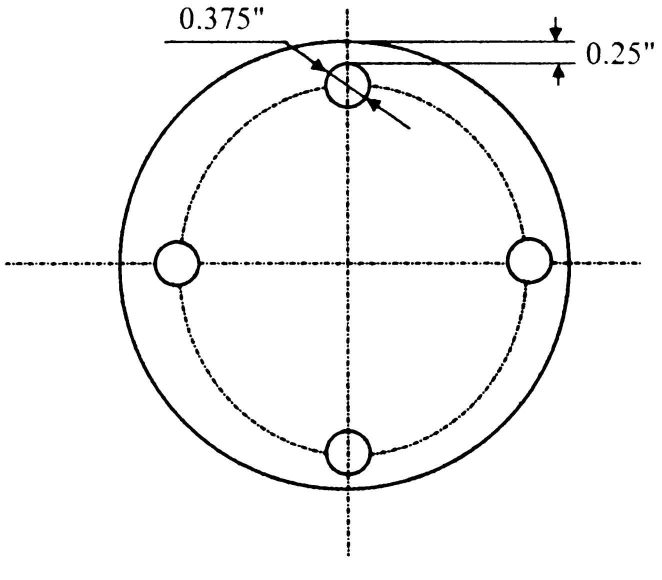

(b) Holder

Figure A.5 Schematic for V-Shaped Teflon Mold Latches and Probing Holes

2. Teflon Mold for Tri-Planar Samples

A Teflon mold was also made for processing tri-planar composite parts. The mold is consisted of a holder and a cover. The mold looks like a cylindrical block when closed. The sample is to be centered in the mold. The schematics for the Tri-planar Teflon mold are presented in Figure A.6 through Figure A.8.

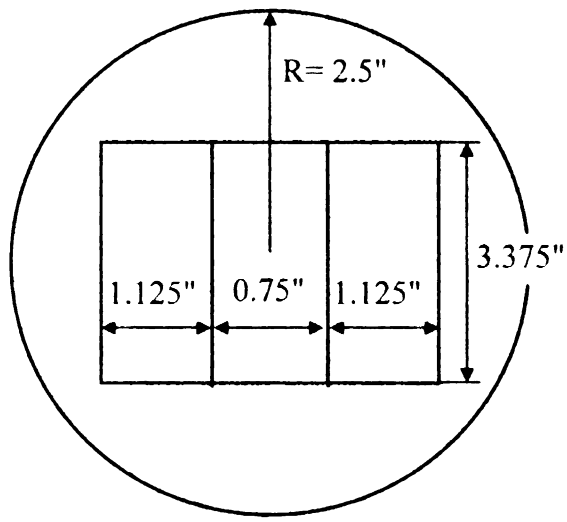

(a) Top View

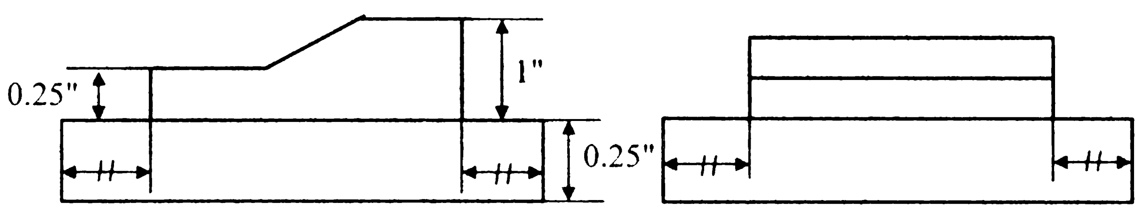

(b) Side Views

Figure A.6 Schematic for Tri-Planar Teflon Mold Cover

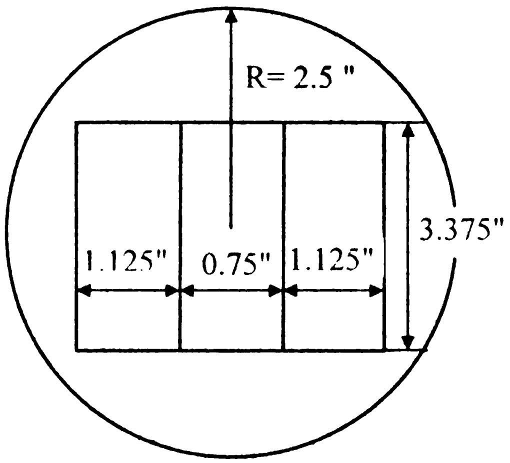

(a) Top View

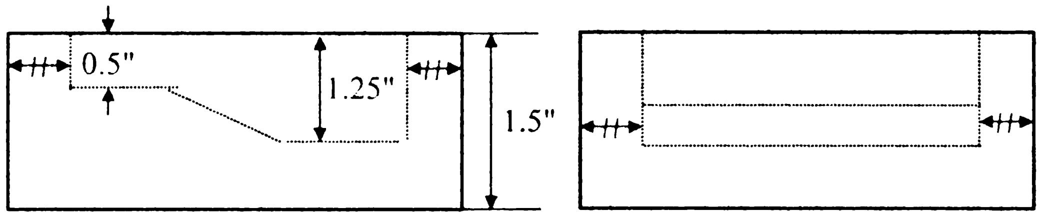

(b) Side Views

Figure A.7 Schematic for Tri-Planar Teflon Mold Holder

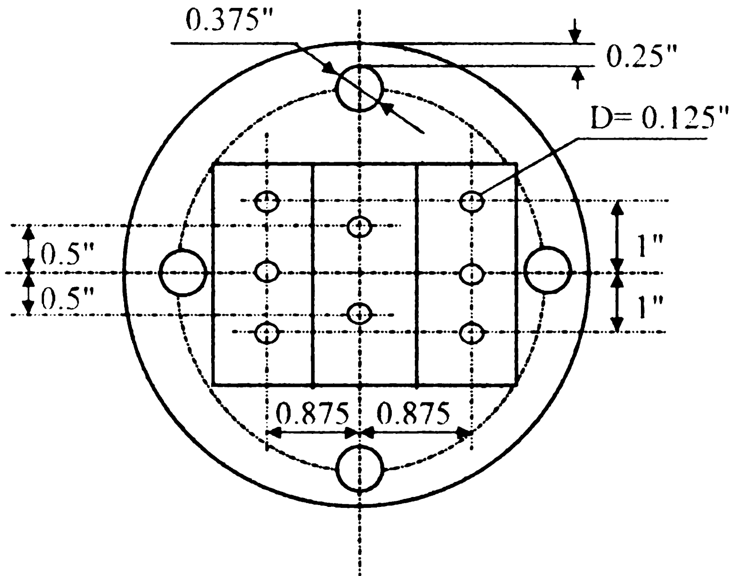

(a) Cover

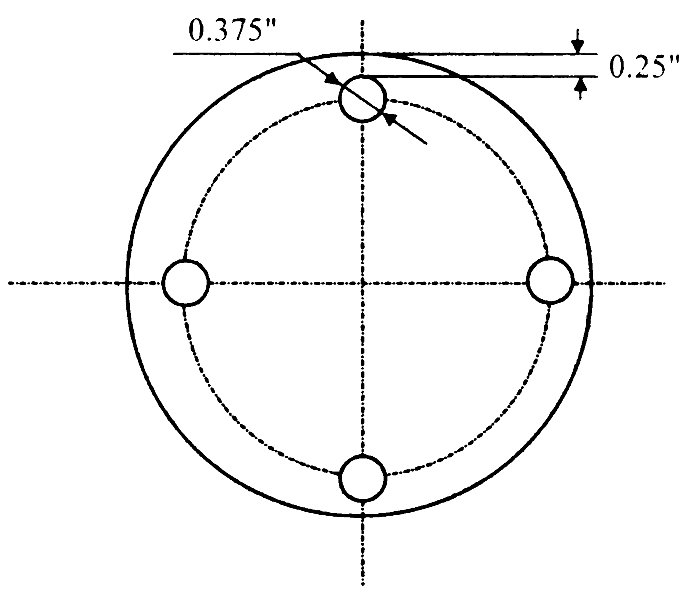

(b) Holder

Figure A.8 Schematic for Tri-Planar Teflon Mold Latches and Probing Holes

APPENDIX B

LabVIEW Subvi's

1. f-write#.vi

This program sets single microwave frequency. A formatted string for the frequency is written to the Oscillator through the GPIB interface. "CW" sets the mode of operation for the oscillator, which is followed by frequency value and unit. The GPIB address of the oscillator is 19.

The LabVIEW program front panel and diagram of f-write.vi are presented in Figure B.1.

*2. **va1step.vi***

This program changes the attenuation of the variable attenuator by changing the control voltage. The control voltage of the variable attenuator can be controlled on the front panel. The device number for the National Instrument Data Acquisition board is 1. The attenuator control voltage is connected to the analog output 0 of the DAQ board (Figure A.2). The control voltage range is 0 – 6 volts.

The LabVIEW program front panel and diagram of va-1-step.vi are presented in Figure B.2.

*3. **vapwrctrl.vi***

This program is used for variable attenuator (microwave) power control. Given a desired microwave power, this program adjusts the control voltage so that the microwave power output is close enough to the desired power. The logarithmic relation between the control voltage and the attenuation was used to provide a starting estimate of the control voltage. A linear search method based on the logarithmic relation was used for tuning of the control voltage. The measurement of microwave power is carried out after 175 ms of each control voltage change.

The LabVIEW program front panel and diagram of vactrl.vi are presented in Figures B.3 and B.4.

4. pwrctrl.vi

This program is used for the control of microwave power using stepper motor. The desired microwave power is compared with the measured microwave power. If the desired power is higher than the measured power, the polarity of the control voltages are such that the stepper motor turns in the increasing direction of the microwave power, and vice versa. At each stepper motor adjustment, the control voltages are applied for 50 ms and then zero voltages are applied to halt the stepper motor for 150 ms. In this way, more stable stepper motor adjustment is achieved.

The LabVIEW program front panel and diagram of pwrctrl.vi are presented in Figures B.5 and B.6 respectively.

5. m-tuning.vi

The purpose of this program is used for mode tuning. The frequency is tuned within the given range in order to minimize the reflected microwave power. The granularity of frequency tuning can be adjusted.

The LabVIEW program front panel and diagram of mtuning.vi are presented in Figures B.7 and B.8 respectively.

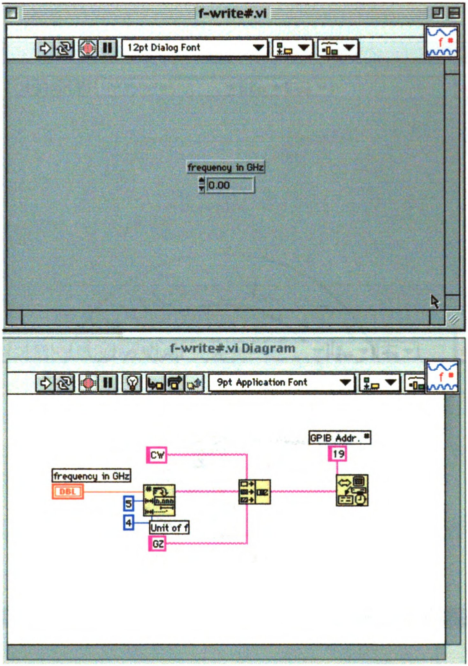

Figure B.1 LabVIEW Program of f-write#.vi - Front Panel and Diagram

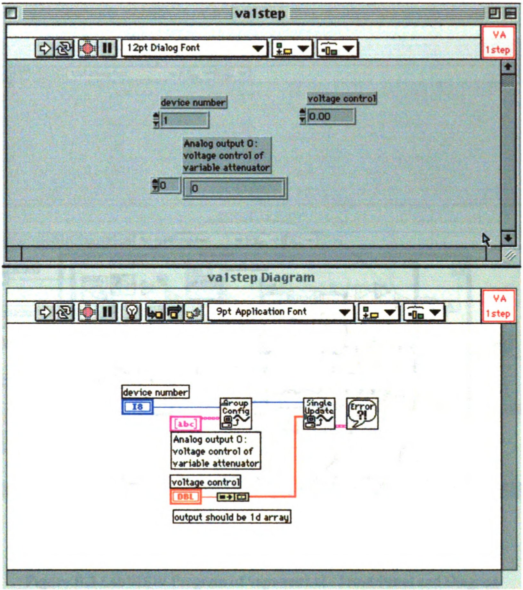

Figure B.2 LabVIEW Program of va1step.vi - Front Panel and Diagram

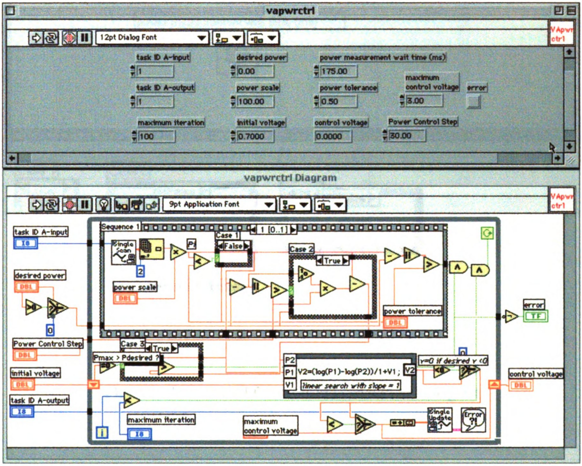

Figure B.3 LabVIEW Program of vapwrctrl.vi - Front Panel and Diagram

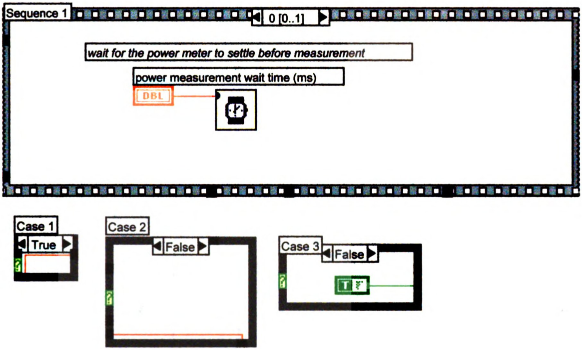

Figure B.4 Additional Elements of vapwrctrl.vi - Diagram

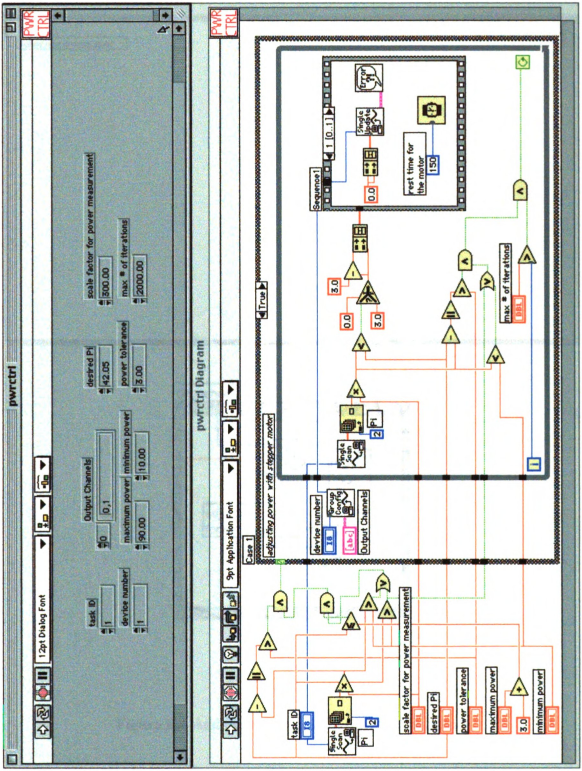

Figure B.5 LabVIEW Pogram of pwrctrl.vi - Front Panel and Diagram

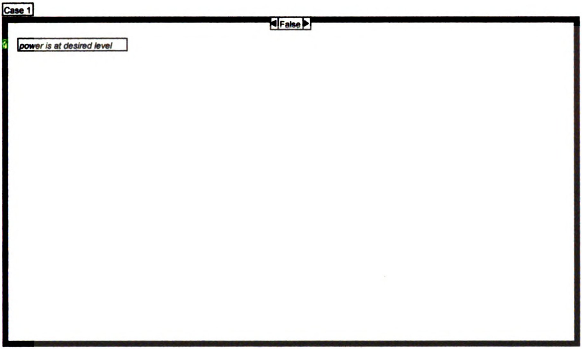

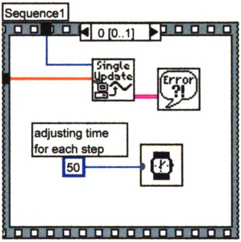

Figure B.6 Additional Elements of pwrctrl.vi Diagram

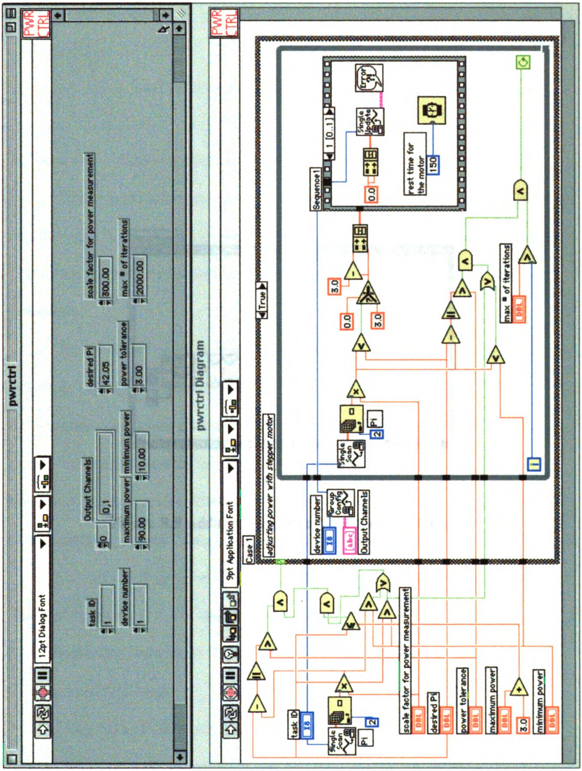

Figure B.7 LabVIEW Program for m-tuning.vi - Front Panel and Diagram

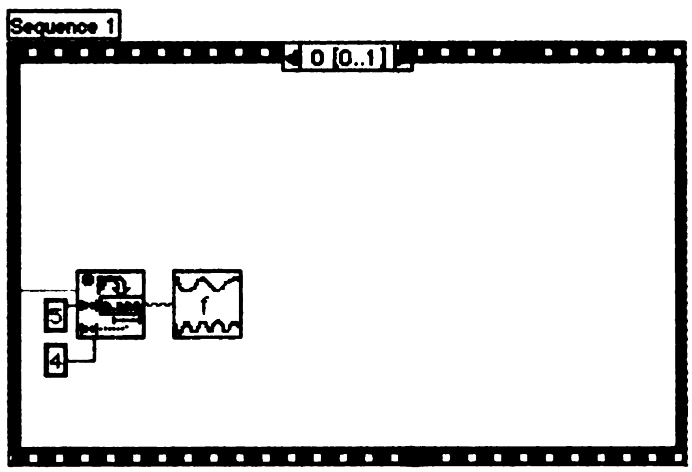

Figure B.8 Additional Elements of m-tuning.vi Diagram

APPENDIX C

LabVIEW Programs for System Characterization

1. vapwrtest.vi (Characterization of Variable Attenuator)

This program is used to characterize the variable attenuator in order to determine how the relationship between attenuation and control voltage changes with frequency. Microwave power was measured while changing the control voltage at different frequencies.

The LabVIEW program front panel and diagram of vapwrtest.vi are presented in Figures C.1 and C.2 respectively.

2. p-response-test.vi (Measurement of Power Meter Response Time)

The response time of the power meters was measured using this program. Microwave power is measured as function of time after a power step change due to variable attenuator control voltage change. The magnitude of power change can be varied.

The LabVIEW program front panel and diagram of p-response-test.vi are presented in Figures C.3, C.4, and C.5 respectively.

2. Characterization&temp.vi (Measurement of Power Reflectance Curve and Temperature Change)

Using this LabVIEW program, the power reflectance curve is measured, along with the temperature change while varying the frequency. Six temperatures are measured, which can be expanded to eight. During the run, frequency is changed from lower end to higher end with specified increment. The input and reflected microwave powers are measured and the reflectance is computed and plotted. Temperatures are measured during the frequency sweep.

The LabVIEW program front panel and diagram of characterization&tempe.vi are presented in Figures C.6, C.7, C.8, and C.9 respectively.

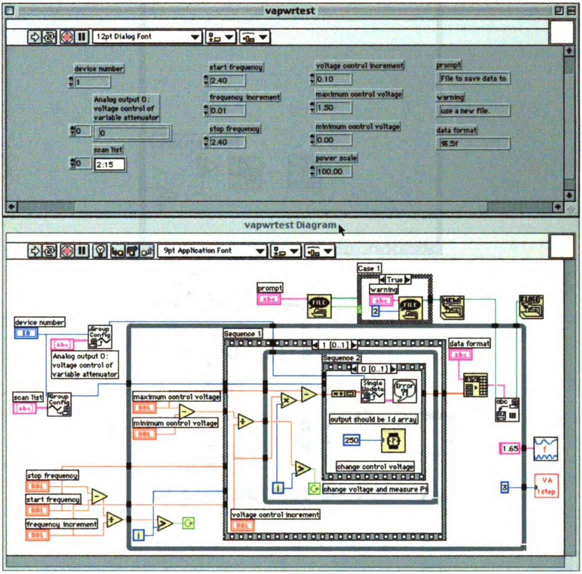

Figure C.1 LabVIEW Program of vapwrtest.vi - Front Panel and Diagram

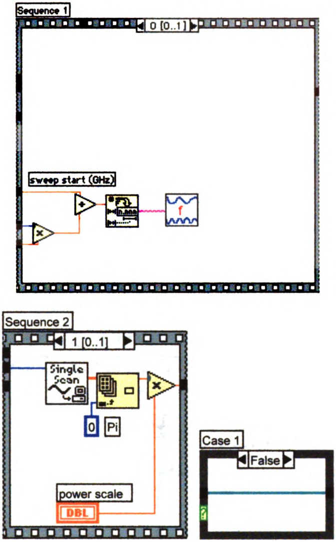

Figure C.2 Additional Elements of vapwrtest.vi Diagram

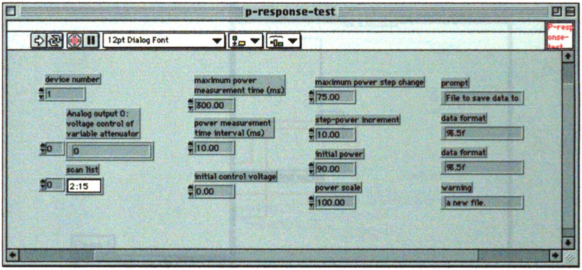

Figure C.3 LabVIEW Program of p-response-test.vi - Front Panel

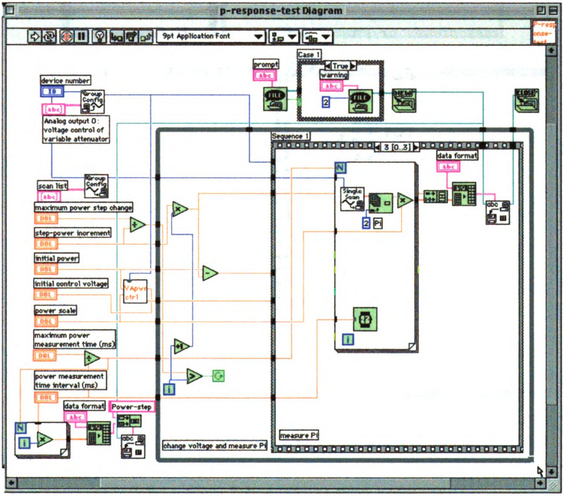

Figure C.4 LabVIEW Program of p-reponse-test.vi - Diagram

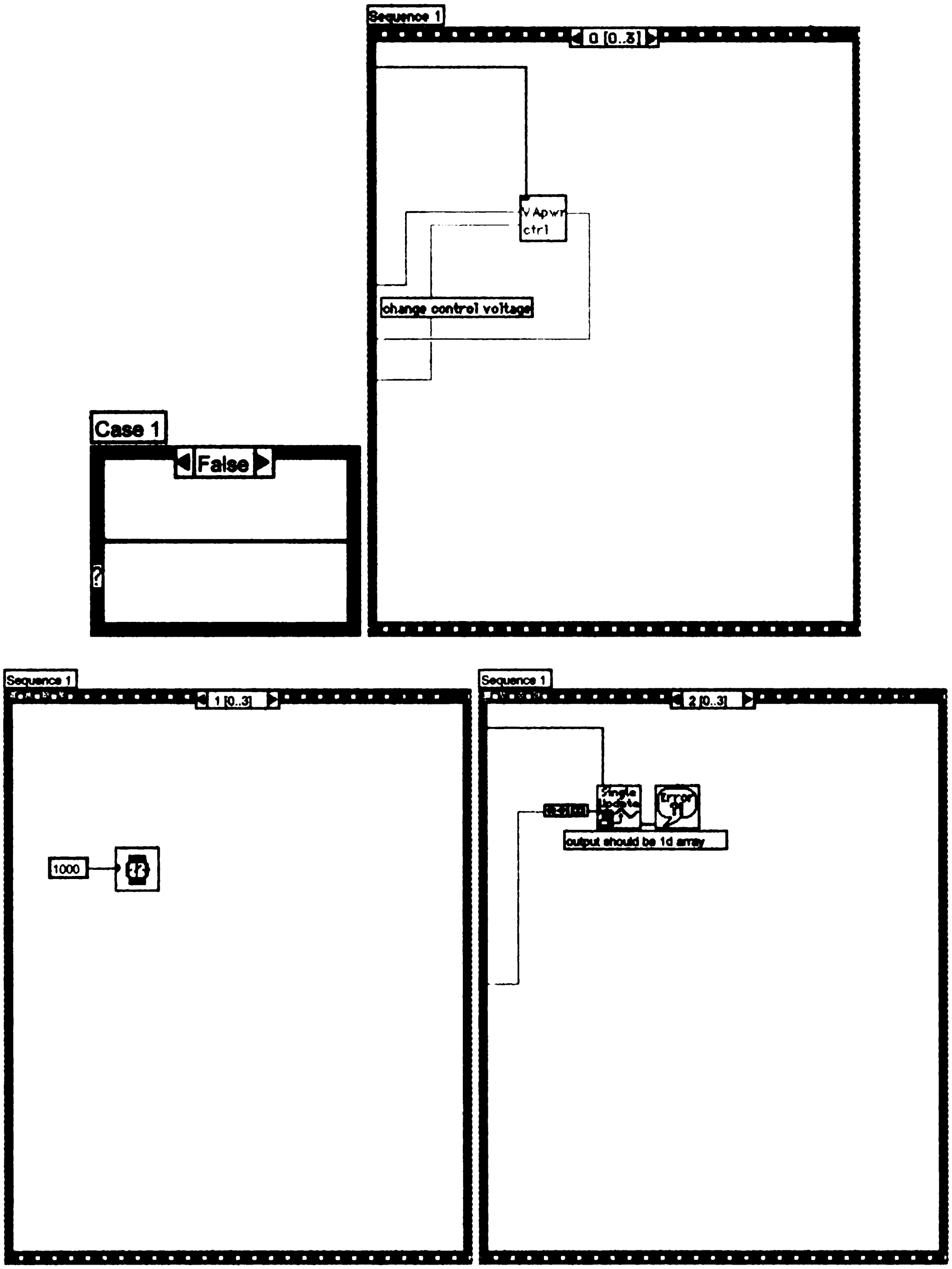

Figure C.5 Additional Elements of p-reponse-test.vi Diagram

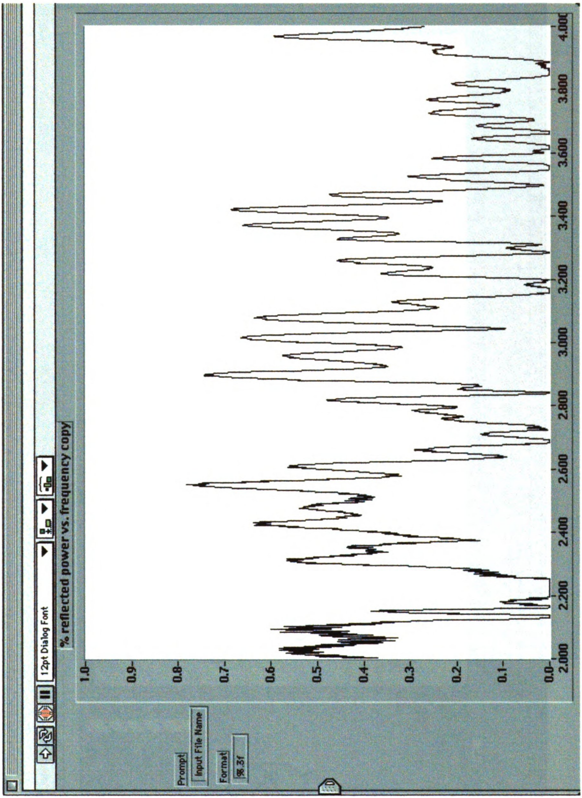

Figure C.6 LabVIEW Program of characterization&temp.vi - Front Panel (Left Half)

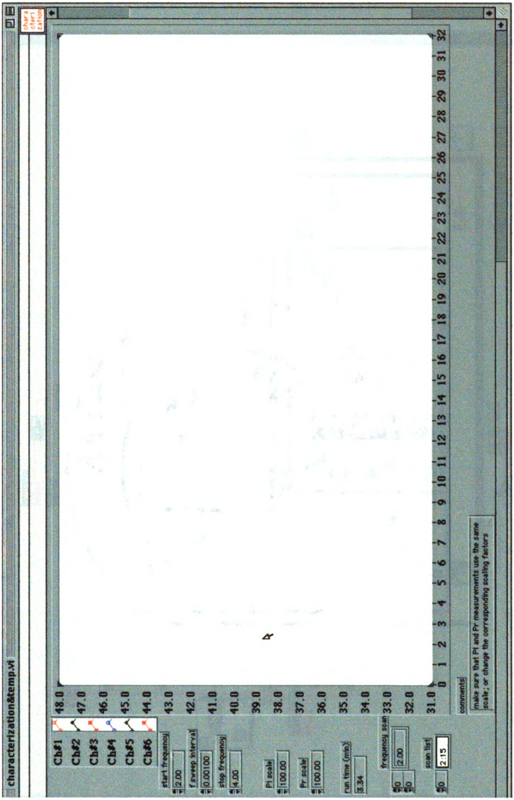

FIGURE C.7 LabVIEW Program of characterization&temp.vi - Front Panel (Right Half)

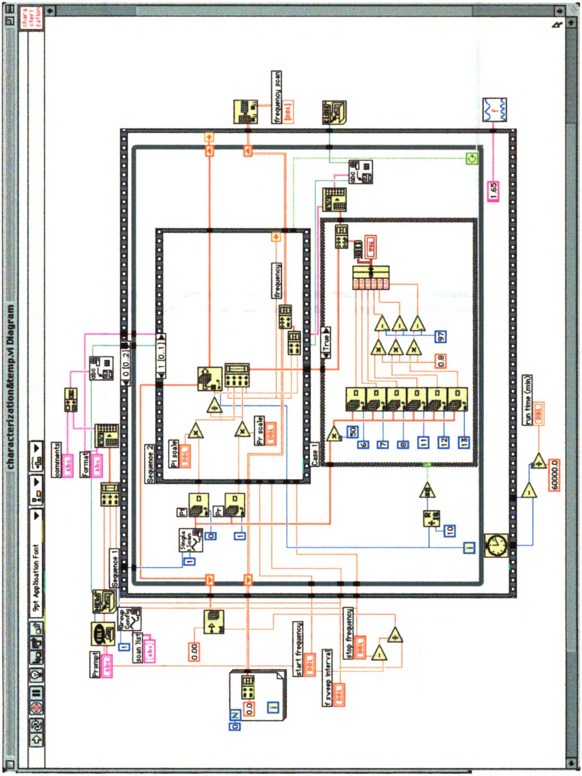

Figure C.8 LabVIEW Program of characterization&temp.vi - Diagram

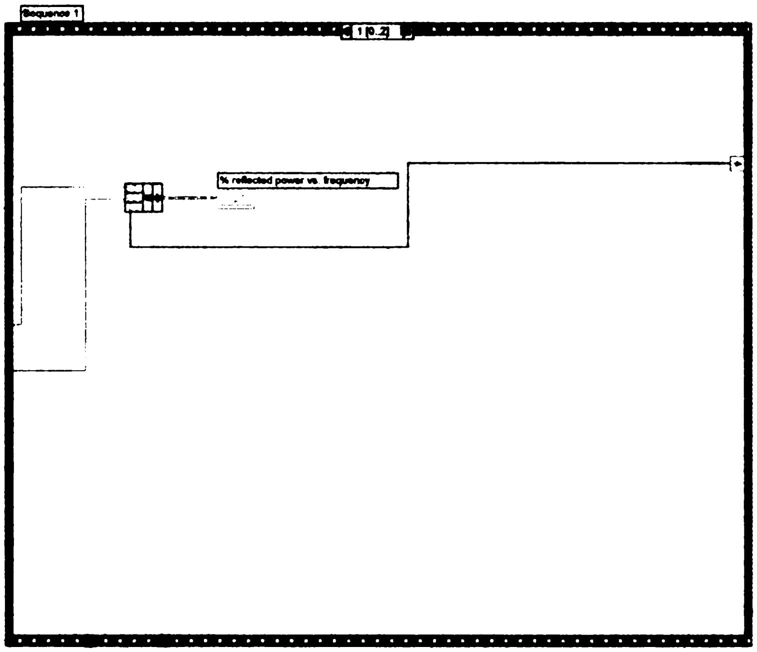

Figure C.9 Additional Elements of characterization&temp.vi Diagram

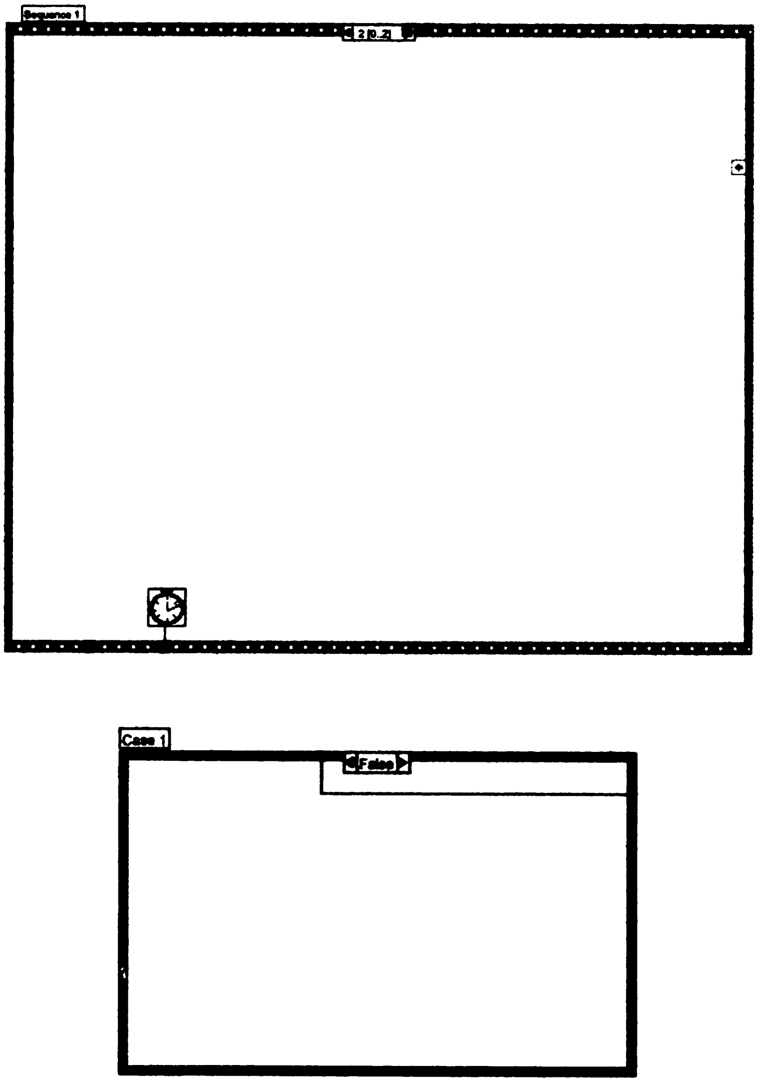

Figure C.9 (Continued)

APPENDIX D

LabVIEW Programs for Process Control System

1. *Singlemode.vi - single mode heating*

This is the LabVIEW program for microwave heating experiment using a single mode with PID microwave power control. The heating experiment starts at room temperature with the initial frequency. The program shown measures six temperatures at the sample surface. As the temperatures approach the curing temperature, a PID control algorithm is used to maintain the highest temperature at the curing temperature. The user can determine how long the experiment lasts.

As the sample is being heated, the program tunes the frequency in the vicinity of the initial frequency in order to minimize the reflected microwave power. The tuning ranges and tuning granularity can be different for heating stage and curing stage. A tuning period is used to determine how often the frequency is tuned. A minimal microwave power is required for the frequency tuning to ensure the accuracy.

Other parameters that can be adjusted include power measurement and control parameters and temperature measurement and control parameters. Two sets of PID control parameters are used for the two-staged PID control. The microwave power reflectance curve and the temperature profiles are displayed on the LabVIEW control panel.

The LabVIEW program front panel and diagram of singlemode.vi are presented in Figures D.1, D.2, and D.3 respectively.

2. modesweep.vi - variable frequency mode sweeping heating

Six modes are used in this program for the microwave heating experiment. These modes are used in a sequence with each mode assigned a heating time. Frequency tuning is used to minimize the reflected microwave power for each mode. A two-staged PID control algorithm is used for the microwave power control. The sample is heated from room temperature and the maximum temperature is maintained at the curing temperature by PID control. An on-line monitoring option is provided for measuring the minimum reflectance frequency for a selected mode. The user can adjust the parameters for PID control, on-line characterization, mode tuning, and power and temperature measurement. Temperatures are plotted on the control panel.

The LabVIEW program front panel and diagram of modesweep.vi are presented in Figures D.4, D.5, and D.6 respectively.

2. VFMPCSI.vi - variable frequency mode switching heating with process control

This program is used to process composite parts following the similar procedure as described in singlemode.vi . The number of measured and controlled temperatures can be changed in the program. The major difference from singlemode.vi is that in this program, mode switching technique is implemented to achieve more uniform heating. In addition, the power control algorithm uses a parabolic relation between the temperature and the microwave power. The mode switching algorithm is described in details in Section 5.2.

The LabVIEW program front panel and diagram of vfmpcsI.vi are presented in Figures D.7, D.8, and D.9 respectively.

3. VFMPCSII.vi - variable frequency mode switching heating with process control and on-line mode characteristics updating

This program is based on VFMPCSI.vi and uses a two-stage PID control algorithm. The mode switching algorithm follows a similar idea but uses a different implementation compared with that of VFMPCSI.vi. Furthermore, this program adopts an On-line Mode Characteristics Updating Controller to adapt the mode selection to the heating characteristics change of the modes. The details of the algorithms are presented in Section 6.2.

The LabVIEW program front panel and diagram of vfmpcsII.vi are presented in Figures D.10, D.11, and D.12 respectively.

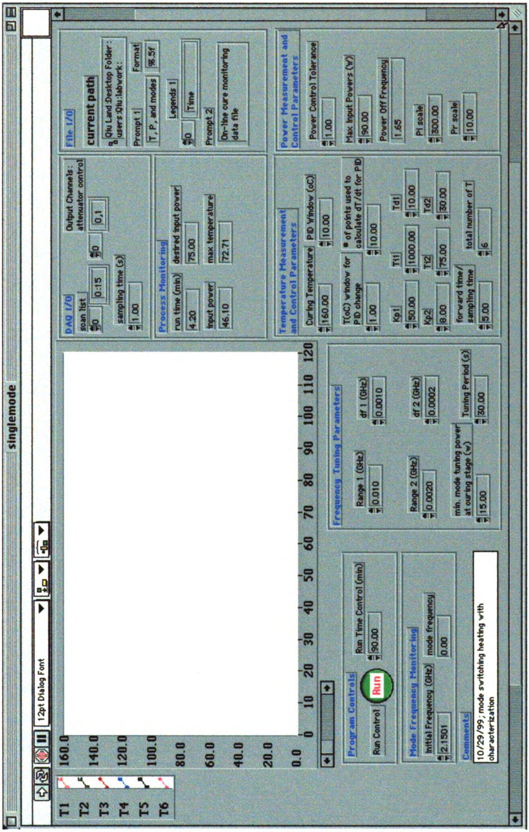

Figure D.1 LabVIEW Program of singlemode.vi - Front Panel

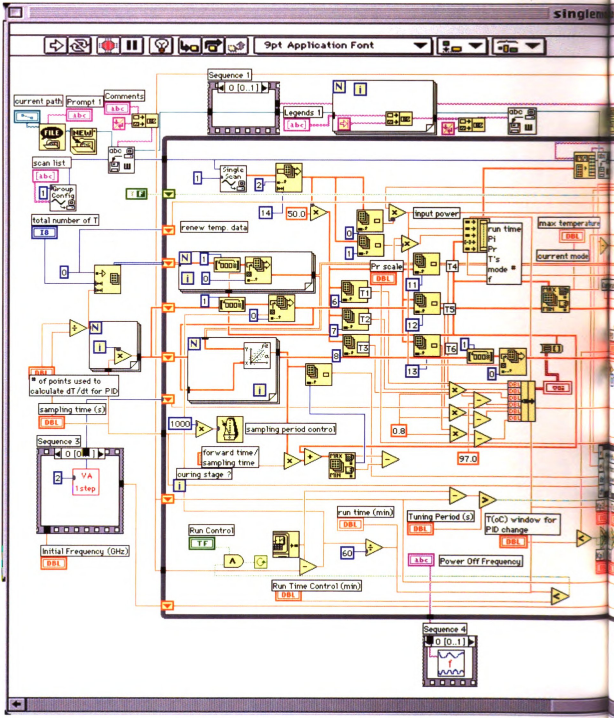

Figure D.2 LabVIEW Program of singlemode.vi - Diagram

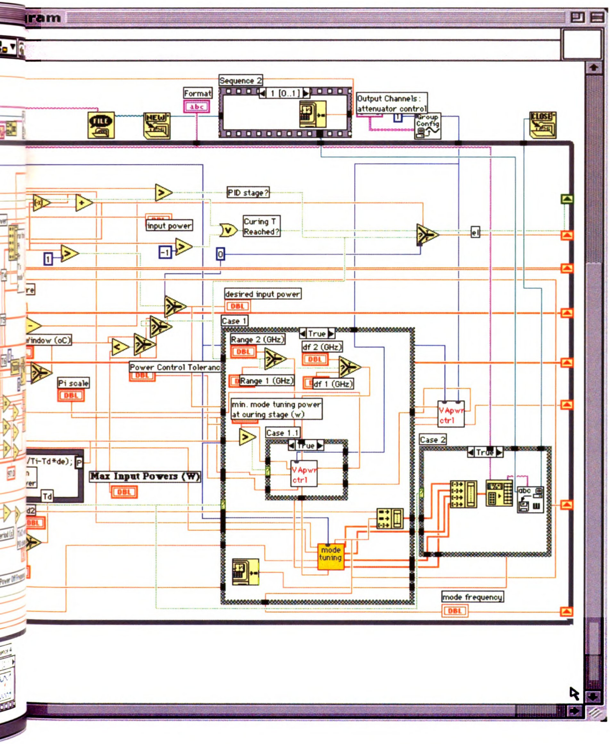
ram
Sequence 2
1 [0..1]
Format
abc
Output Channels :
attenuator control
Group
Config
FILE
NEW
CLOSE
PID stage?
input power
Curing T
Reached?
desired input power
DBL
Case 1
True
Range 2 (GHz)
df 2 (GHz)
Range 1 (GHz)
df 1 (GHz)
Window (oC)
Power Control Toleranc
Pi scale
min. mode tuning power
at curing stage (w)
Case 1.1
VApwr
ctrl
/Ti-Td*de);
Td
Max Input Powers (W)
mode
tuning
Case 2
mode frequency

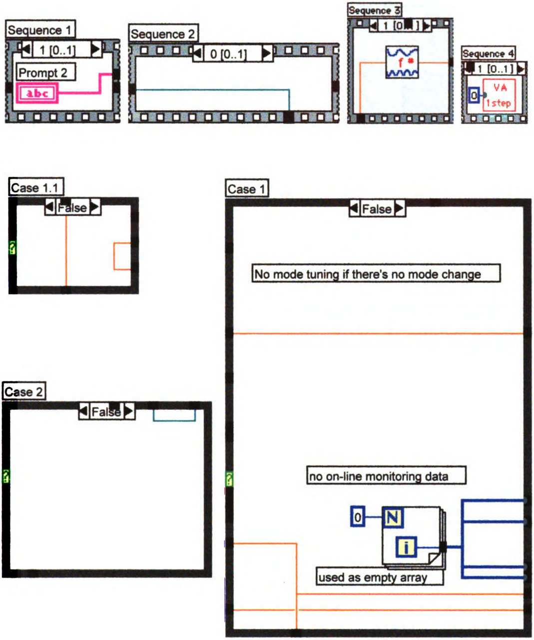

Figure D.3 Additional Elements of singlemode.vi Diagram

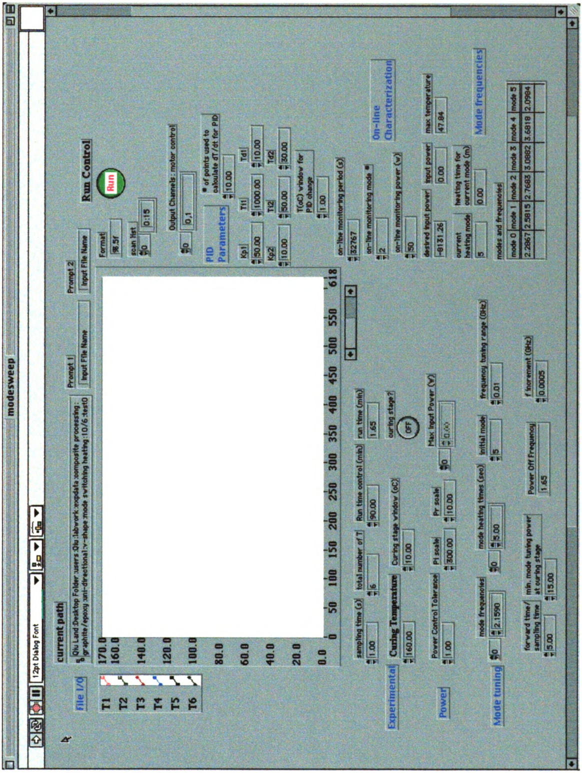

Figure D.4 LabVIEW Program of modesweep.vi - Front Panel

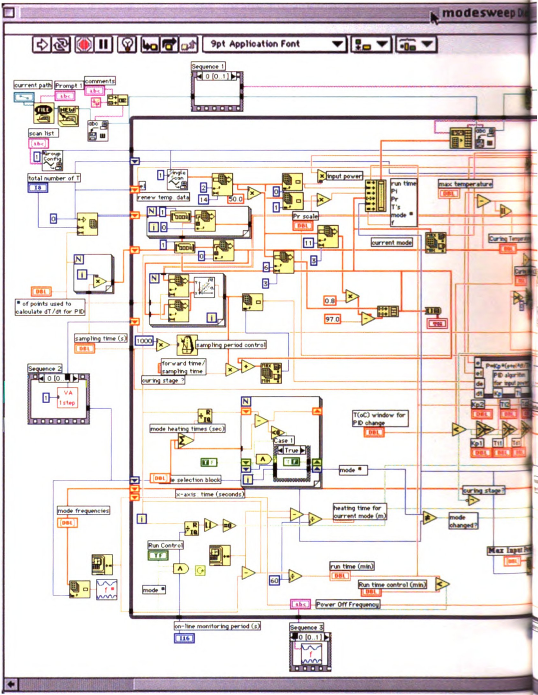

Figure D.5 LabVIEW Program of modesweep.vi - Diagram

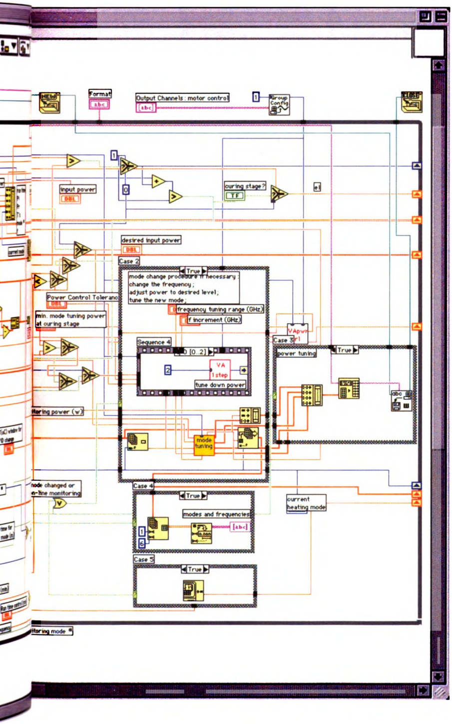
Format
Output Channels : motor control
Group Config
input power
curing stage?
desired input power
Case 2
True
mode change procedure if necessary ;
change the frequency ;
adjust power to desired level;
tune the new mode;
frequency tuning range (GHz)
f increment (GHz)
min. mode tuning power
at curing stage
Sequence 4
0 [0..2]
VA
1 step
tune down power
mode
tuning
Case 3
power tuning
Case 4
modes and frequencies
current
heating mode
Case 5

p.vi - Diagr

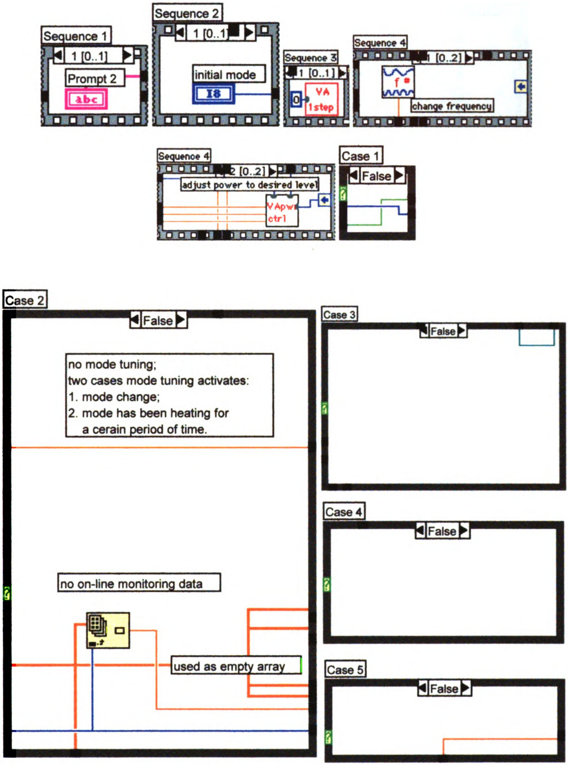

Figure D.6 Additional Elements of modesweep.vi Diagram

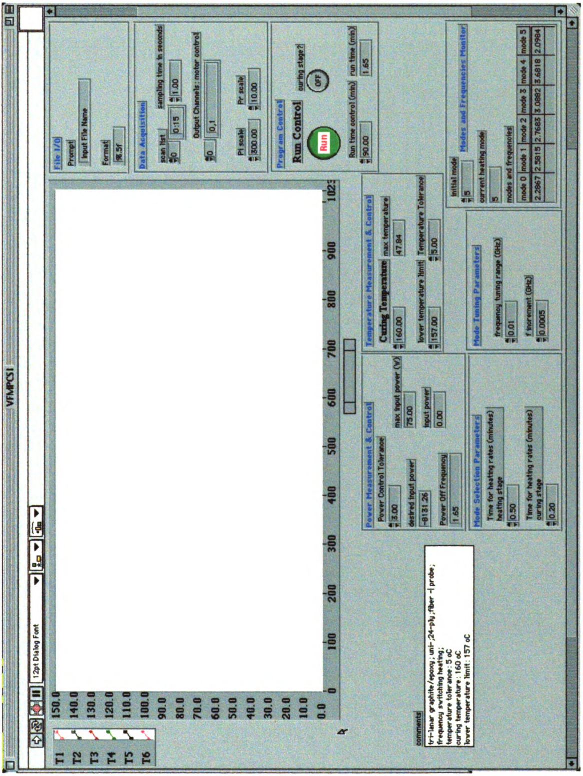

Figure D.7 LabVIEW Program of VFMPCSI.vi - Front Panel

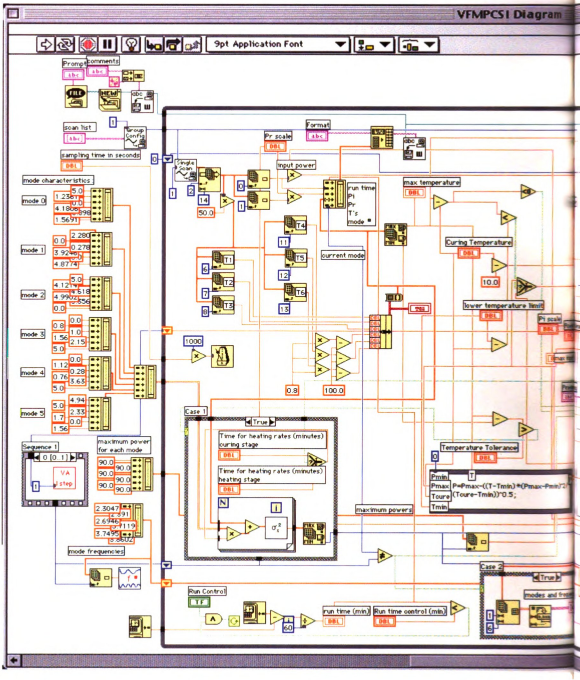

Figure D.8 LabVIEW Program of VFMPCSI.vi - Diagram

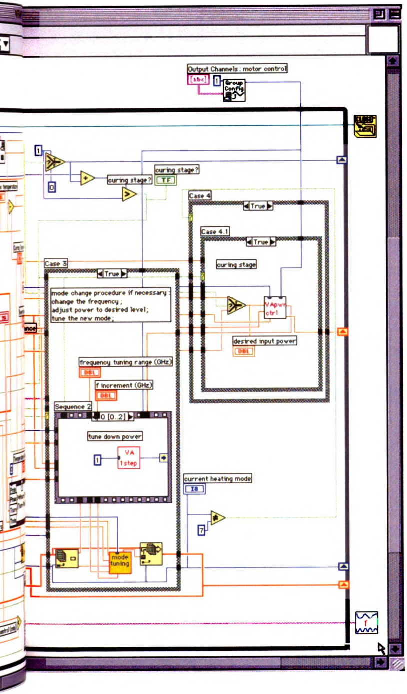
Output Channels: motor control
abc
1
Group Config
1
0
curing stage?
curing stage?
TF
Case 4
True
Case 4.1
True
curing stage
VApwr ctrl
desired input power
DBL
Case 3
True
mode change procedure if necessary:
change the frequency;
adjust power to desired level;
tune the new mode;
frequency tuning range (GHz)
DBL
f increment (GHz)
DBL
Sequence 2
0 [0..2]
tune down power
1
VA 1step
current heating mode
I8
7
mode tuning

SI.vi - Dia

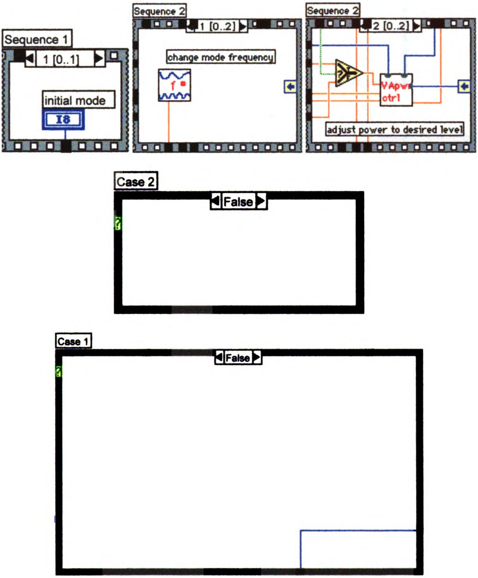

Figure D.9 Additional Elements of VFMPCSI.vi Diagram

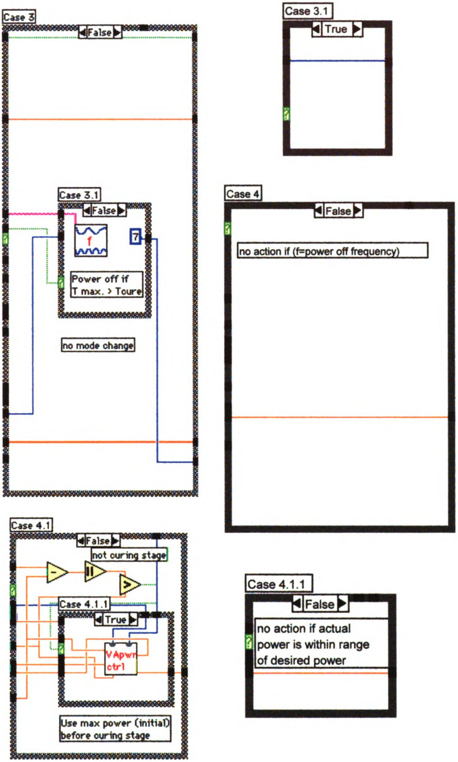

Figure D.9 (continued)

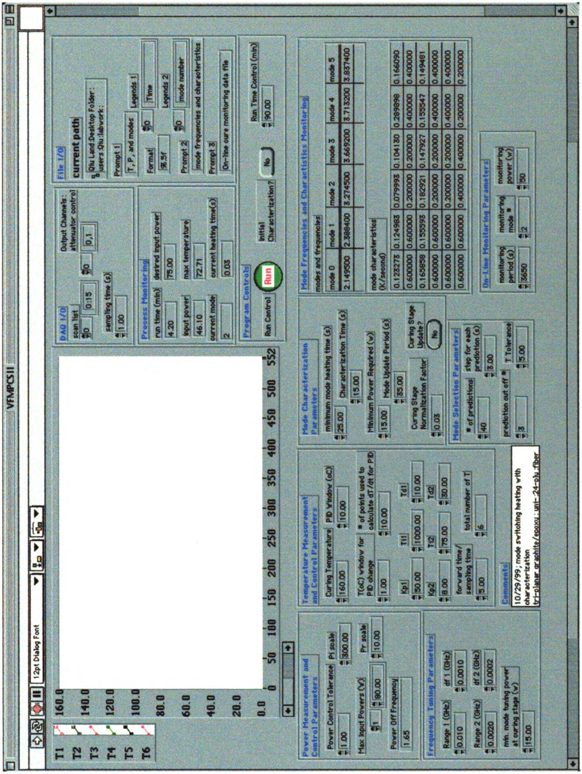

Figure D.10 LabVIEW Program of VFMPCSII.vi - Front Panel

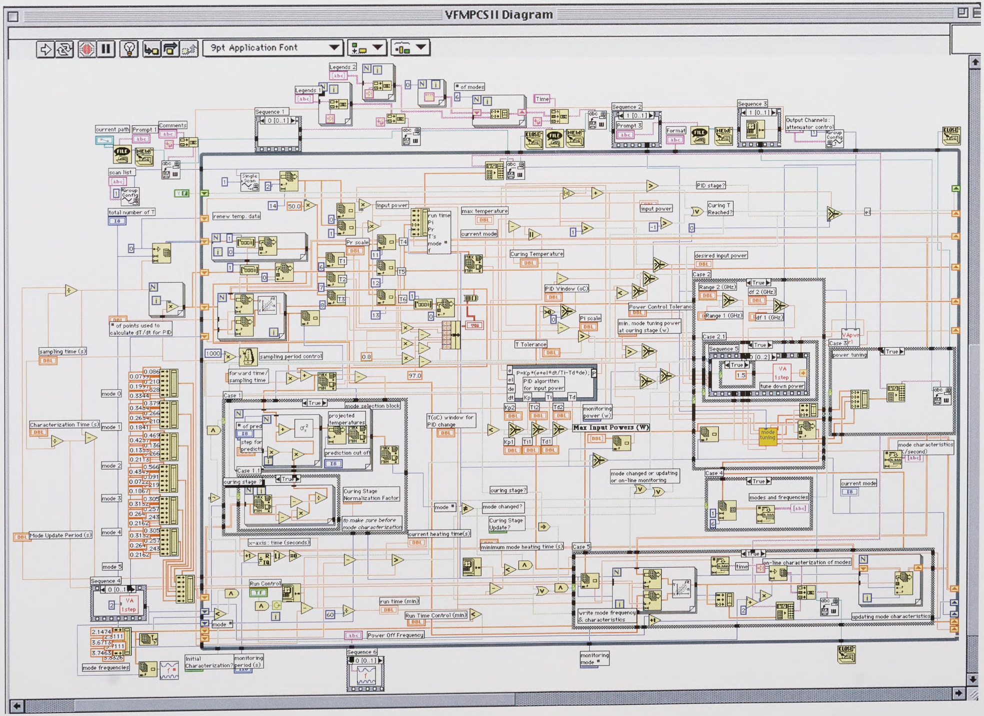

Figure D.11 LabVIEW Program of VFMPCSII.vi - Diagram

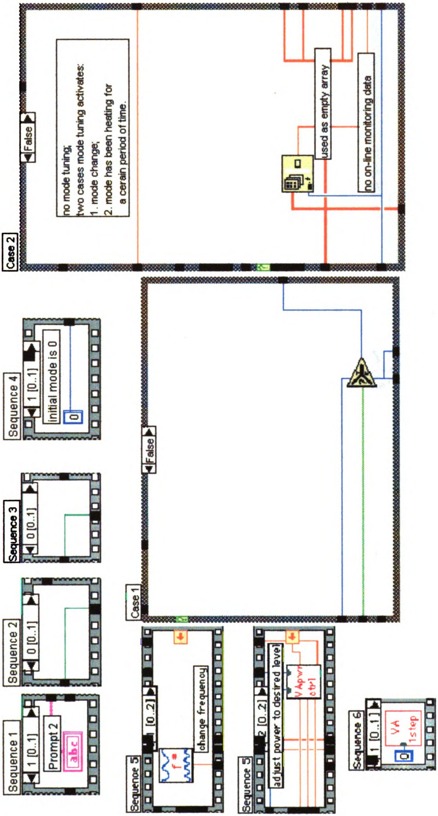

Figure D.12 Additional Elements of VFMPCSII.vi Diagram

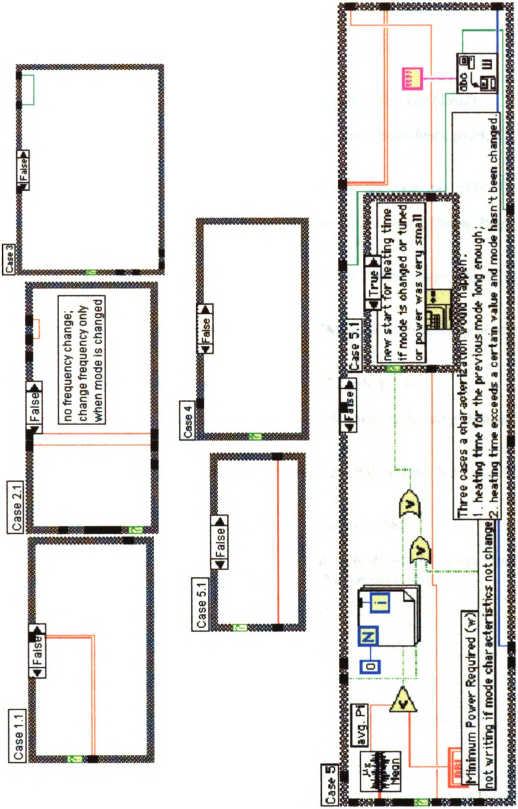

Figure D.12 (continued)

BIBLIOGRAPHY

1. White, W. C., *Proc. Inst. Radio Electron. Eng.*, August, p50, 1129 (1962)

2. Chabinsky, I. J., *Materials Research Society Symposium Proceedings*, p124, 17 (1988)

3. Krieger, B., *Proc. Am. Chem. Soc., Div. Polym. Mater.: Sci. Eng.*, 66, p339 (1992)

4. Gourdenne, A., A. H. Maassarani, P. Monchaux, and S. Aussudre, *Polym. Prepr.*, Am. Chem. Soc., Div. Polym. Chem., 20(2), p471 (1979)

5. Lewis, D., J. C. Hedric, T. C. Ward, and J. E. McGrath, *Polym. Prepr.*, Am. Chem. Soc., Div. Polym. Chem. 28(2), p330, (1987)

6. Lewis, D., *Mater. Res. Soc. Symp. Proc.*, 269, 21 [Microwave Processing of Materials III] (1992)

7. Jow, J., J. Delong, and M. C. Hawley, *SAMPE Q.*, 20, p46 (1989)

8. Methven, J.M. and S. R. Ghaffariyan, *Principles of Microwave Heating* (Binner, J.G.P., ed.), pp.56-77, Abington Publishing

9. Wei, J., J. D. Delong, M. DeMuse, and M. C. Hawley, *Polym. Eng. Sci.*, 33, p1132 (1993)

10. Beldjoudi, N. and A. Gourdenne, *Eur. Polym. J.*, 24, 265 (1988)

11. George, C. E., G. R. Lightsey, and A.G.Wehr, *Materials Research Society Symposium Proceedings*, 124, p189[Microwave Processing of Materials] (1988)

12. Agrawal, R. and L. T. Drzal, *J. Adhes.*, 29, 63 (1989)

13. Wei, J., *Ph.D. Dissertation*, Michigan State University (1992)

14. Asmussen, J., H. H.Lin, et al., *Rev. Sci. instrum.*, 1477-1486 (1987)

15. Chen, Y. F., and C. Y. C. Lee, *Polym. Mat. Sci. Eng.*, Am. Chem. Soc., 60, pp680-684 (1989)

16. Volgel, G. L., J. Jow, et al., *4th Technical conference of Composite Materials*, (1989)

17. Fellows, L. A., R. Delgado, and M. C. Hawley, *26th International SAMPE Technical Conf.*, Atlanta, GA, Oct. (1994)

18. Wei, J., J. Jow, J. D. Delong, and M.C. Hawley, *SAMPE J.*, 27(1), p.33 (1991)

19. Wei, J., and M.C. Hawley, *MRS Symposium Proceedings*, 269, 439 (1992)

20. Adegbite, V. O., *Ph.D. Dissertation*, Michigan State University (1995)

21. Harrington, R. F., *Time-Harmonic Electromagnetic Fields*, McGraw-Hill Book Company (1961)

22. Chen, Kun-Mu, *Electromagnetic Theory I*, Class Notes, Department of Electrical Engineering, Michigan State University (1995)

23. Tai, Chen-To, *Dyadic Green Functions in Electromagnetic Theory*, IEEE Press, New York, p.47 (1994)

24. Pozar, D. M., *Microwave Engineering*, Addison-Wesley Publishing Company, Inc. (1991)

25. Collin, R., *Foundations for Microwave Engineering*, McGraw-Hill (1966)

26. Ramo, S. and Whinnery, J. R., *Fields and Waves in Modern Radio*, John Wiley & Sons, New York (1944)

27. Ku, C.C. and R. Liepins, *Electrical Properties of Polymers: Chemical Principles*, Macmillan Publishing Company (1987)

28. Bruce, R.W., *Mat. Res. Soc. Symp. Proc.*, 124, 3 (1988)

29. Lee, W. I. and G. S. Springer, *J. Compos. Mater.*, 18(4), p.357 (1984)

30. Lewis, D. A., T. C. Ward, J. D. Summers, and J. E. McGrath, *Polymer Preprints*, 29(1), pp.174-175 (1988)

31. Lewis, D.A., T. C. Ward, J. D. Summers, and J. E. McGrath, *Journal of Polymer Science: Polymer Chemistry*, 30(8), pp.1647-1653 (1992)

32. Bush, S.F. and J. M. Methven, *Proceedings of the 39th International SAMPE Symposium*, Anaheim, April 11-14, pp.34-43 (1994)

33. National Materials Advisory Board Commission on Engineering and Technical Systems, (National Research Council), *Microwave Processing of Materials*, National Academy Press (1994)

34. Hottong, U., J. Wei, R. Dhulipala, and M. C. Hawley, *Ceram. Trans.*, 21, p587 (1991)

35. Mashida, T., S. Matsushita, and I. Ikegami, Japanese Patent 50 138 067 (1975)

36. Jullien, H. and H. Valot, *Polymer* 26, 505 (1985)

37. Gagliani, J., R. Lee, and A. L. Wilcoxson, US Patent 4 305 796 (1981)

38. Lewis, D., *Proceedings of the 39th International SAMPE Symposium and Exhibition*, pp.1-12, (1994)

39. DeMuse, M.T. and A. C. Johnson, *Proceedings of the 29th Mcirowave power Symposium*, pp. 168-171 (1994)

40. Thuillier, F.M. and H. Jullien, *Makromol. Chem.: Macromol. Symp.*, 25, p63 (1989)

41. Mijovic, J., A. Fishbain, and J. Wijaya, *Macromolecules*, 25, p.986 (1992)

42. Jow, J., *Ph.D. Dissertation*, Michigan State University (1988)

43. Lind, A.C., L. N. Medgyesi-Mitschang, J. E. Kurz, H. F. McKinney, and F.C. Wear, *Mater. Res. Soc. Symp. Proc.*, 189, p.461 [Microwave Processing of Materials II] (1991)

44. Ippen, J., *Rubber Chem. Technol.*, 44, p.294 (1971)

45. VanKoughnett, A.L. and J. G. Dunn, *J. Microwave Power*, 8, p.101 (1973)

46. Wang, C.S., *Rubber Chem. Technol.*, 57, p.134 (1984)

47. Methven, J.M., *Proceedings of the 39th International SAMPE Symposium and Exhibition*, pp. 25-33 (1994)

48. Wei, J., B. Thomas, and M. C. Hawley, *SPE Proc.: ANTEC '92* (Vol. 1), p. 1170 (1992)

49. Lin, M., and M. C. Hawley, *Proceedings of the 38th International SAMPE Symposium and Exhibition*, pp. 436-445 (1993)

50. Qiu, Y., A. Smith, J. Wei, M. Lin, and M.C. Hawley, *Composites in Manufacturing*, SME Quarterly, 1st Quarter, (2000)

51. Falconer-Flint, M.J., *Aust. Plast. Rubber J.*, 24(11), 33 (1973)

52. Clark, D.E., *Ceramic Engineering and Science Proceedings*, v14, n7-8, pt1, pp.3-21 Westville, OH (1993)

53. De',A.S., I. Ahmad, E. D. Whitney, and D. E. Clark, *Mater. Res. Soc. Symp. Proc.*, 189, 283-288, [Microwave processing of Materials II] (1991)

54. Patterson, M. C. L., P. S. Apte', R. M. Kimber, and R. Roy, *UIE Microwaves and Radio Frequency Conference Proceedings*, pp. 33-36, Nice, France (1991)

55. Patterson, M. C. L., P. S. Apte', R. M. Kimber, and R. Roy, *Mat. Res. Soc. Symp. Proc.*, [Microwave Processing of Materials III] (1992)

56. Acitally, M. A., R. B. Prime, and E. Sacher, *Polymer*, pp. 335-342 (1971)

57. Hagnauer, G. L., P. J. Pearce, B. R. LaLiberte, and M. E. Roylance, *Thermorheology of Thermosetting Polymers*, pp. 25-47 (1983)

58. Dutta, A. and M. E. Ryan, *Journal of Applied Polymer Science*, (24), p.635 (1979)

59. Mijovic, J., *Journal of Applied Polymer Science*, (31), p.1177 (1986)

60. Moroni, A., J. Mijovic, E. M. Pearce, and C. C. Foun, *Journal of Applied Polymer Science*, (32), p.3761 (1986)

61. Sichina, W.J., *Dupont Company Applications Brief*, No. TA-93

62. Gillham, J. K., *Developments in Polymer Characterization -3*, Dawkins, J.V., p.159, Applied Science, London (1982)

63. Sourour, S. and M. R. Kamal, *Thermochimic Acta*, (14), 41 (1976)

64. Lee, W.I., A. C. Loos, and G. S. Springer, *Journal of Composite Material*, (16), 510 (1982)

65. Jow, J., M. C. Hawley, M. Finzel, and T. Kern, *Polymer Engineering and Science*, 28(22), pp.1450-1454 (1988)

66. Delmotte, M., H. Jullien, and M. Ollivon, *Eur. Polym. J.*, Vol. 27, No. 4/5, pp.371-376 (1991)

67. Delmotte, M. and H. Jullien, *Makromolek. Chem.; Macromolec. Symp.*, 9, 185 (1987)

68. Marand, E., K. R. Baker, and J. D. Graybeal, *Radiation Effects on Polymers*, American Chemical Society, pp.385-400 (1991)

69. Livi, A., G. Levita, and P. A. Rolla, *Journal of Applied Polymer Science*, Vol. 50, pp.1583-1590 (1993)

70. Wei, J., Y. Chang, B. Thomas, and M. C. Hawley, *Proc. ICCM/VIII*, vol.I, 10-L Honolulu, Hawaii (1991)

71. Lin, M. and M. C. Hawley, *Proceedings of the 38th SAMPE International Symposium*, Anaheim, CA (1993)

72. Willams, N.H., *Journal of Microwave Power*, 2, pp.123-127 (1967)

73. Gourdenne, A. and V. Q. Le, *Eur. Polym. J.*, 23(10), pp.777-780 (1987)

74. Fellows, L.A. and M. C. Hawley, *Proceedings of the 29th Microwave Power Symposium*, p.91, Chicago, IL (1994)

75. Wei, J. et al., *SAMPE Journal*, 27 (1), 33 (1991)

76. Lee, W.I., and G.S. Springer, *J. Composite Materials*, 18(4), 357 (1984)

77. Kashyap, S.C., and W. Wyslouzil, *J. Microwave Power*, 12(3), pp. 223-230 (1977)

78. Espinosa, R.J., et al., *28th Microwave Symposium Proceedings*, Manassas, VA, pp.26-31 (1993)

79. Garard, R.S., *Mat. Tech.*, 9, pp.235-238 (1994)

80. Collins, R.E., *Flow of Fluids Through Porous Materials*, Reinhold, New York (1961)

81. Jow, J., M. C. Hawley, M. C. Finzel, and J. Asmussen, *Rev. Sci. Instrum.*, 60, 1, p.90 (1989)

82. Watanabe, M., M. Suzuki, and S. Ohkawa, *Journal of Microwave Power*, 13(2), pp.173-181 (1978)

83. Zhu, S. and H. Chen, *Journal of Microwave Power and Electromagnetic Energy*, 23(3), pp.139-143 (1988)

84. Paoloni, F., *Journal of Microwave Power and Electromagnetic Energy*, 24(1), pp.21-32 (1989)

85. Lin, H., *Ph.D. Dissertation*, Michigan State University (1989)

86. Manring, B., *Ph.D. Dissertation*, Michigan State University (1992)

87. de Pourcq, M., *IEE Proceedings*, Pt.H, 131(6), pp.411-419 (1984)

88. Jia, X. and P. Jolly, *Journal of Microwave Power and Electromagnetic Energy*, Vol.27, No.1, pp.11-22 (1992)

89. Volpe, V., *Journal of Composite Materials*, 14, p.189 (1980)

90. Morgan, M.A., D. L. Fisher, and E. A. Milne, *IEEE Transaction on Antennas and Propagation*, Ap-35(2), p.191 (1987)

91. Hashimoto, O. and Y. Shimizu, *IEEE Transactions on Microwave Theory and Techniques*, MTT-34(11), p.1202 (1986)

92. Wei, J., M. C. Hawley, and J. Asmussen, *Journal of Microwave Power and Electromagnetic Energy*, 28(4), p.234 (1993)

93. Hinrichs, R. J., *Composite Materials: Quality Assurance and Processing*, ASTM STP 797, pp. 29-37 (1983)

94. Alliouat, M., Y. Lecluse, J. Massieu, and L. Mazo, *Journal of Microwave Power and Electromagnetic Energy*, v25, n1, pp25-31 (1990)

95. Beale, G. O., F. J. Arteaga, and W. M. black, *IEEE Transactions on Industrial Electronics*, Vol. 39, No. 4, pp. 301-312, August (1992)

96. Sticklen, J., A. Kamel, M. C. Hawley, and V. Adegbite, *IEEE Expert*, pp. 43-53, April (1992)

97. Hawkins, R., M. C. Hawley, T. Lenz, J. McDowell, Y. Qiu, and J. Sticklen, *Proceedings of American Society of Composites 12th Technical Conferences*, Dearborn, MI (1997)

98. Hawkins, R., M. Hawley, J. Sticklen, Y. Qiu, and J. McDowell, *Proceedings of AICHE Annual Meeting*, Chicago, IL (1996)

99. National Instruments, DAQ - PCI E Series User Manual (1998)